

KU LEUVEN



***piggyBac* transposons for stem cell- based gene therapy of Duchenne muscular dystrophy**



Mariana Loperfido

Promoters (KUL and VUB):

Prof. Thierry VandenDriessche

Prof. Marinee K. L. Chuah

Co-promoter (KUL):

Prof. Maurilio Sampaolesi

Strandbeest loek van der Klis Umerus Silent beach.

Theo Jansen



KU Leuven
Biomedical Sciences Group
Department of Cardiovascular Science
Center of Molecular and Vascular Biology

VUB
Faculty of Medicine and Pharmacy
Department of Gene Therapy and
Regenerative Medicine

***piggyBac* transposons for stem cell- based gene therapy of Duchenne muscular dystrophy**

Mariana Loperfido

Joint PhD KUL and VUB

Promoters (KUL and VUB): Prof. Thierry VandenDriessche
Prof. Marinee K. L. Chuah
Co-promoter (KUL): Prof. Maurilio Sampaolesi

Chair: Prof. Roger Lijnen
Secretary: Prof. Mieke Dewerchin
Jury members: Prof. Gillian Butler-Browne
Prof. Patrick Midoux
Prof. Ron Kooijman
Prof. Frank Luyten

Leuven, 16th June 2016

Doctoral thesis submitted in partial fulfillment of the requirements for the joint Degree of
“Doctor in Biomedical Sciences” (KUL) and “Doctor in Medical Sciences” (VUB)

To Peppino

*Few things are impossible to diligence and skill.
Great works are performed not by strength, but perseverance.*

*Poche cose sono impossibili se si è diligenti e dotati di capacità.
Le grandi opere si compiono non con la forza, ma con la perseveranza.*

Samuel Johnson

Declaration of authorship

I, Mariana Loperfido, declare that the work presented in this thesis is my own.

I confirm that information derived from other sources or works performed in collaboration with other researchers has been clearly indicated in the thesis.

Summary

Duchenne muscular dystrophy (DMD) is a genetic disorder characterized by mutations in the dystrophin gene that cause the absence of the dystrophin protein at the muscle fiber membrane of the affected patients. This leads to myofiber degeneration and progressive muscle wasting, ultimately resulting in significant morbidity and mortality. Currently, there is no treatment that prevents or reverses the disease progression. Genetically corrected stem/progenitor cells could potentially provide an effective treatment. However, due to its large size, commonly used viral vector technologies preclude efficient gene transfer of the full-length dystrophin coding DNA sequence (*CDS*; size: 11.1 Kb).

In this study we validated a novel stem cell-based non-viral gene therapy approach for DMD with the use of *piggyBac* (*PB*) transposons. These plasmid-based non-viral vectors are able to stably integrate the gene of interest into the genome of the target cells leading to its sustained expression. Moreover, the large cargo capacity of these vectors could overcome one of the main bottlenecks in the field enabling gene therapy with full-length instead of truncated dystrophin. We have therefore generated *PB* transposons coding for either full-length or truncated versions of the human dystrophin *CDS*. We demonstrated that this system enables stable non-viral gene delivery, with sustained expression of both full-length and truncated versions of dystrophin into murine myoblasts. We subsequently transferred *PB* transposons containing the full-length human dystrophin *CDS* into dystrophic mesoangioblasts (MABs). These myogenic vessel associated stem/progenitor cells are capable of crossing the vessels and contribute to the regeneration of the dystrophic muscles upon intra-arterial transplantation. The use of MABs has resulted to be relatively safe in a recently completed phase I/II clinical trial based on intra-arterial infusions at escalating doses of HLA-matched donor-derived MABs in DMD patients under immunosuppressive regimen (EudraCTno. 2011-000176-33). In our study, MABs were isolated from the muscles of a large animal model for DMD, the Golden Retriever muscular dystrophy (GRMD) dog. The genetically corrected GRMD MABs showed stable transposition and expression of the full-length human

dystrophin. Since MABs have a limited proliferative capacity, we have also investigated the possible use of MABs generated from induced pluripotent stem cells (iPSCs) of patients suffering from DMD, as an alternative (designated as human iPSC-derived mesoangioblast-like cells or HIDE Ms). These cells can be expanded in culture to obtain a potentially unlimited supply of myogenic progenitors. HIDE Ms derived from patients affected by DMD were then genetically corrected with *PB* transposons resulting in stable expression of the full-length human dystrophin *CDS*. These cells successfully engrafted into the muscles of immunodeficient/dystrophic mice (*scid/mdx*) leading to the *in vivo* expression of the *PB*-mediated full-length human dystrophin in the myofiber membrane.

Taken together, these results showed for the first time the validity of a non-viral gene transfer approach based on *PB* transposons that allows for the sustained expression of the full-length human dystrophin in dystrophic MABs and DMD patient-specific iPSC-derived MABs. This study paves the way towards a novel stem/progenitor cell-based non-viral gene therapy for the treatment of DMD exploiting the potential of *PB* transposons to deliver large therapeutic genes.

Samenvatting

Duchenne spierdystrofie (DMD) is een genetische aandoening, die gekenmerkt wordt door mutaties in het dystrofine gen. Hierdoor ontbreekt het dystrofine eiwit in de membranen van de spiervezels in de getroffen patiënten. Dit leidt tot degeneratie van spiervezels en progressief spierverslies, uiteindelijk resulterend in aanzienlijke morbiditeit en mortaliteit. Momenteel is er geen behandeling beschikbaar die de ziekteprogressie voorkomt of om kan keren. Genetisch gecorrigeerde stam/progenitor cellen kunnen mogelijk een effectieve behandeling bieden. De veelgebruikte virale vector technologieën kunnen echter niet toegepast worden wegens de grootte van de complete dystrofine-coderende DNA sequentie (*CDS*; grootte: 11.1 Kb), waardoor er geen efficiënte genoverdracht plaatsvindt.

In deze studie valideerden we een nieuwe stamcel-gebaseerde niet-virale gentherapie aanpak voor DMD, met behulp van *piggyBac* (*PB*) transposons. Deze plasmide-gebaseerde niet-virale vectoren kunnen het betreffende gen stabiel integreren in het genoom van de target cellen en zo voor een langdurige expressie zorgen. Bovendien kan de relatief grote cargo-capaciteit van deze vectoren een mogelijke beperking van gentherapie met virale vectoren omzeilen. Daarom hebben we *PB* transposons gegenereerd die coderen voor de volledige en de getrunceerde versie van de humane dystrofine *CDS*. We hebben aangetoond dat dit systeem stabiele niet-virale genaflevering mogelijk maakt, met aanhoudende expressie van zowel de intacte als de getrunceerde versies van dystrofine in muis myoblasten. Vervolgens hebben we de *PB* transposons, met daarin de volledige dystrofine *CDS*, getransfecteerd in dystrofische mesoangioblasten (MABs). Deze stam/progenitor cellen geassocieerd met myogene bloedvaten zijn in staat om bloedvaten te doorkruisen en bij te dragen tot de regeneratie van de dystrofische spieren na intra-arteriële transplantatie. Het gebruik van MABs is relatief veilig, zoals aangetoond in een recent afgeronde fase I/II klinische studie, met intra-arteriële infusies van toenemende dosissen van HLA-gematchte donor-afgeleide MABs in DMD patiënten die met immunosuppressiva werden behandeld (EudraCTno. 2011-000176-33). In onze

studie werden MABs geïsoleerd uit de spieren van een groot diermodel voor DMD, het Golden Retriever musculaire dystrofie (GRMD) hondemodel. De genetisch gecorrigeerde GRMD MABs vertoonden stabiele transpositie en expressie van de intacte humane dystrofine *CDS*. Om de beperkte celdelingscapaciteit van MABs te omzeilen, hebben we ook de mogelijkheid onderzocht om gebruik te maken van MABs gegenereerd uit geïnduceerde pluripotente stam cellen (iPSCs), namelijk humane iPSC-afgeleide mesangioblast-achtige cellen (HIDEMs). Deze cellen kunnen geëxpandeerd worden in cultuur, om zo een potentieel ongelimiteerde voorraad van myogene progenitoren te bekomen. HIDEMs afkomstig van patiënten getroffen door DMD werden genetisch gecorrigeerd met *PB* transposons met de intacte humane dystrofine *CDS* wat tot stabiele expressie van het dystrofine eiwit leidde. Deze cellen konden succesvol getransplanteerd worden in de spieren van immunodeficiënte/dystrofische muizen (*scid/mdx*) en leidden tot de *in vivo* expressie van de *PB*-gemedieerde volledige humane dystrofine eiwit in het spiervezelmembraan.

Samengenomen tonen deze resultaten voor het eerst de validiteit van een niet-virale gentransfer aanpak, gebaseerd op *PB* transposons, die zorgt voor stabiele expressie van het intacte humane dystrofine in dystrofische MABs en DMD patiënt-specifieke iPSC-afgeleide MABs. Deze studie opent nieuwe mogelijkheden voor de behandeling van DMD op basis van niet-virale gentherapie met stam/progenitor cellen, waarbij het potentieel van *PB* transposons geëxploiteerd wordt om relatief grote therapeutische genen te transflecteren.

Acknowledgments

At the end of this unique journey...

I would like to express my deep gratitude to my promoters Prof. Marinee Chuah and Prof. Thierry VandenDriessche. I am grateful for your constant support and for giving me the opportunity to grow as a scientist and in my personal life. I am sure today is the beginning of a new prospective for our paths.

I would like to thank my co-promoter and friend Prof. Maurilio Sampaolesi who has accompanied me through the different steps of my professional life, from Pavia through Milan towards Leuven. I will be forever grateful to you for giving me the opportunity to meet people who will remain key points in my life.

I am thankful to our collaborator and friend Dr. Francesco Saverio Tedesco for his valuable contribution to this study and for having me in his laboratory in London everytime it was necessary to work together and achieve our goals. Working with you and your team in such a stimulating environment was a critical step in my professional and personal life, and for that I thank again also my promoters.

I would like to acknowledge the chairperson of the examining committee Prof. Johan Van Lint and the jury members Prof. Gillian Butler-Browne (Myology Center of Research, Inserm et Sorbonne Universités, France), Prof. Patrick Midoux (Centre de Biophysique Moléculaire, Inserm et Université d'Orléans, France), Prof. Ron Kooijman (Department of Pharmacology and Pharmacokinetics, Vrije Universiteit Brussel, Belgium), Prof. Mieke Dewerchin (Laboratory of Angiogenesis and Neurovascular link, Vesalius Research Center, KU Leuven, Belgium) and Prof. Frank Luyten (Skeletal Biology and Engineering Research Center, KU Leuven, Belgium) for their precious time in critical reviewing this thesis and attending my public defense. I would like to thank the

chairman of the department of Cardiovascular Sciences, Prof. Paul Herijgers and the director of the Center for Molecular and Vascular Biology, Prof. Roger Lijnen for the collaborative environment during the past years at the KU Leuven. I would also like to thank the director of the Doctoral School Biomedical Sciences (KU Leuven), Prof. Rik Lories and the director of the Doctoral School Medical Sciences (VUB), Prof. Chris van Schravendijk.

My acknowledgments also extend to the Flanders Fund for Scientific Research (Fonds Wetenschappelijk Onderzoek, FWO) for providing my personal PhD fellowship (2010-2014) and to the Scientific Fund Willy Gepts (Wetenschappelijk Fonds Willy Gepts, WFWG, VUB) for providing financial support for the last year of my PhD (2015). During my experiences abroad I was awarded an FWO travel grant (2014) and an EMBO travel grant (2015). Several funds made this work possible: FWO research project grant (2010-2014), Association Francaise contre les Myopathies (AFM), EU Framework Program 6 (Clini-Gene) and Walter Pyleman Fund (King Boudewijn Foundation).

At the end of this unique journey...

I find myself surrounded by people who will forever have a special place in my life. To all my friends and colleagues met in Leuven, Brussels and London during these years and to all my friends in Italy goes my sincere gratitude for their constant support and generosity. Each of you is part of an important moment of my professional and personal life. Thank you for the happy moments we have spent together, I hope we will cultivate our friendship day after day.

To Mattia, my best friend and colleague, my other half. I thank you for showing me a new way to live our work and our daily life together. I thank you for your constant and priceless help, and for taking me on our next adventure.

I am profoundly grateful to my parents, Betta and Gianni, for supporting me in all the choices of my life, and for facing with patience and love the difficulties that the distance brings with it. To my brother, Domenico, I miss you in every moment we spend far away. I will continue to be there for you every time you would need it. Our best time together has still to come.

Sono profondamente grata ai miei genitori, Betta e Gianni, per essermi stati di supporto in tutte le scelte della mia vita, e per aver affrontato con pazienza e amore le difficoltà dovute alla distanza. A mio fratello, Domenico, mi manchi in ogni momento non condiviso. Continuerò ad esserci ogni volta in cui ne avrai bisogno. I nostri momenti più belli insieme non sono ancora stati vissuti.

I would like to thank all the members of my family, my aunts and uncles, my cousins and in particular my grandmothers. Every time I was back home, you were there waiting for me with your smiles and open arms. A special thank also goes to my parents' friends, you have filled with joy every moment of sadness due to our distance. Growing up amongst with you taught me that the true friendship is timeless.

Vorrei ringraziare tutta la mia famiglia, le mie zie e i miei zii, i miei cugini e in particolare le mie nonne. Ogni volta in cui sono tornata a casa, voi eravate lì ad aspettarmi con i vostri sorrisi e a braccia aperte. Un ringraziamento speciale va agli amici dei miei genitori, avete riempito di gioia ogni momento di tristezza che la distanza ha potuto creare. Crescere con voi mi ha insegnato che la vera amicizia non ha né tempo né età.

Table of contents

Declaration of authorship	9
Summary	11
Samenvatting	13
Acknowledgments	15
Table of contents	21
List of abbreviations	25
List of figures	29
List of tables	31
Chapter 1	33
1. Introduction	33
1.1. Duchenne muscular dystrophy	33
1.2. Therapeutic approaches to treat Duchenne muscular dystrophy	36
1.2.1. Pharmacological therapy	38
1.2.2. Cell therapy	39
1.2.2.1. Mesoangioblasts	44
1.2.2.2. Human induced pluripotent stem cell-derived mesoangioblast-like cells	47
1.2.3. Gene therapy	52
1.2.3.1. Exon-skipping	53
1.2.3.2. Gene editing	55
1.2.3.3. Gene addition	57

1.3. Transposons	61
1.3.1. Transposons as gene therapy tools	63
1.3.1.1. <i>Sleeping Beauty</i>	63
1.3.1.2. <i>piggyBac</i>	65
1.3.1.3. Transposon delivery into target cells	69
1.3.2. Transposons for muscle disorders	71
Chapter 2.....	75
2. Objectives of the Research	75
2.1. General objective	75
2.2. Specific aims	76
Chapter 3.....	77
3. Methodology and Materials	77
3.1. Cells and culture conditions.....	77
3.2. Generation of PB transposon constructs for DMD.....	78
3.3. Cell electroporation	80
3.4. Flow cytometry and FACS.....	81
3.5. <i>In vitro</i> differentiation assays.....	81
3.6. RNA expression analysis	82
3.7. Immunohistochemistry	85
3.8. Western blot analysis	86
3.9. Transposon genome copy number quantification	87
3.10. Mice	87
3.11. Intra-muscular transplantation	88
3.12. Tumor formation assay.....	88

3.13. Statistical analysis.....	89
Chapter 4.....	91
4. Results.....	91
4.1. Genetic correction of dystrophic mesoangioblasts using <i>piggyBac</i>	
transposons expressing full-length human dystrophin <i>CDS</i>.....	91
4.1.1. Generation of <i>PB</i> transposons coding for human dystrophin <i>CDS</i>	91
4.1.2. Expression of human microdystrophins after <i>PB</i> -mediated transposition in C2C12 myoblasts	94
4.1.3. Increased transposition in C2C12 myoblasts with the hyperactive <i>PB</i> transposase and the <i>PB</i> transposon encoding the full-length human dystrophin <i>CDS</i> ..	98
4.1.4. Isolation and characterization of adult skeletal muscle pericyte-derived stem/progenitor cells from the Golden Retriever muscular dystrophy (GRMD) dog model	104
4.1.5. Genetic correction of dystrophic mesoangioblasts by delivery of the full-length human dystrophin <i>CDS</i> in <i>PB</i> transposon system	105
4.2. Genetic correction of DMD HIDEMs by <i>piggyBac</i> transposons expressing full- length dystrophin and transplantation in dystrophic mice	111
4.2.1. Generation and characterization of DMD patient-specific HIDEMs	111
4.2.2. Stable GFP expression after <i>PB</i> transposition in DMD HIDEM and DMD HIDEM ^{MYOD} cells.....	113
4.2.3. Correction of DMD HIDEM or DMD HIDEM ^{MYOD} cells mediated by <i>PB</i> transposons coding for full-length human dystrophin <i>CDS</i>	120
4.2.4. Transplantation of genetically corrected DMD HIDEM ^{MYOD} cells in scid/mdx mice and safety	124

Chapter 5.....	129
5. General conclusion	129
Chapter 6.....	131
6. Discussion.....	131
References	141
Appendix.....	167
Curriculum vitae.....	173
Publications and scientific communication	175

List of abbreviations

6MWT: 6-Minute walk test
AdVs: Adenoviral vectors
ANOVA: Analysis of variance
AON: Antisense oligonucleotides
AP: Alkaline phosphatase
APC: Allophycocyanine
BAC: bacterial artificial chromosome
BMD: Becker muscular dystrophy
BSA: Bovine serum albumin
CAR: chimeric antigen receptor
cDNA: complementary DNA
CDS: Coding DNA sequence
CPT2: Carnitine palmitoyltransferase 2
CRISPR: Clustered regularly interspaced short palindromic repeats
DAPC: Dystrophin-associated protein complex
DBD: DNA-binding domain
DMD: Duchenne muscular dystrophy
DMEM: Dulbecco's modified Eagle's media
DNA: Deoxyribonucleic acid
DRs: Direct repeats
DYS: Dystrophin
DYSF: Dysferlin
DYS-HAC: Human artificial chromosome containing the entire human dystrophin locus
EBV-CTLs: Epstein Barr virus-specific cytotoxic T lymphocytes
EDTA: Ethylenediaminetetraacetic acid
EP: Electroporation
ePB: enhanced piggyBac
ESCs: Embryonic stem cells
FACS: Fluorescent activated cell sorting
FBS: Fetal bovine serum
FGF-b: recombinant human fibroblast growth factor-basic
Flk-1 = Fetal liver kinase 1
GAPDH: Glyceraldehyde-3-phosphate dehydrogenase

GFP: Green fluorescent protein
GRMD: Golden Retriever muscular dystrophy
HAC: Human artificial chromosome
HD: Healthy donor
HAd: Helper-dependent adenoviral
HDR: Homology directed repair
HIDEMs: Human iPSC-derived mesoangioblast-like cells
HLA: Human leukocyte antigen
HLV: hydrodynamic limb vein
hyPB: hyperactive piggyBac
IDLV: Integrase-defective lentiviral
IF: Immunofluorescence
IGF-I: Insulin-like growth factor I
iPB: insect piggyBac
iPSCs: Induced pluripotent stem cells
IRs: Inverted repeats
LGMD2D: Limb girdle muscular dystrophy 2D
LV: Lentiviral vector
 μ UTRN: microutrophin
MABs: Mesoangioblasts
MD1: Microdystrophin 1
MD2: Microdystrophin 2
MGNs: Meganucleases
MM: Miyoshi myopathy
MOI: Multiplicities of infection
mPB: mouse piggyBac
mRNA: messenger RNA
MSC: Mesenchymal stem cell
Myf5: Myogenic factor 5
MyHC: Myosin heavy chain
MyoD: Myogenic differentiation 1
NLS: Nuclear localization signal
OPMD: Oculopharyngeal muscular dystrophy
pA: polyadenylation

PABPN1: Polyadenylate-binding protein nuclear 1
Pax3: Paired box 3
Pax7: Paired box 7
PB: piggyBac
PBS: Phosphate-buffered saline
PCR: Polymerase chain reaction
PDE5: Phosphodiesterase type 5
PDGFR β : Platelet derived grow factor receptor beta
PE: Phycoerythrine
PFA: Paraformaldehyde
Pgk: phosphoglycerate kinase 1
qPCR: Quantitative polymerase chain reaction
qRT-PCR: Quantitative reverse transcription polymerase chain reaction
rAAVs: recombinant adeno-associated virus
RNA: Ribonucleic acid
RT: Room temperature
RT-PCR: Reverse transcription polymerase chain reaction
SB: Sleeping Beauty
SCID: Severe combined immune deficiency
SDS: Sodium dodecyl sulfate
SD: Standard deviation
SEM: Standard error mean
Sgca: α -sarcoglycan
SKM: Skeletal muscle
SMA: Smooth muscle actin
snRNA: small nuclear RNA
SV40: Simian virus 40 late
TALEN: Transcription activator-like effector nucleases
UTRs: Untranslated regions
ZFN: Zinc-finger nucleases

List of figures

Figure 1. Schematic representation of dystrophin and the DAPC.

Figure 2. Schematic representation of the dystrophin exons and the corresponding functional domains

Figure 3. Potential autologous iPSC-based ex vivo gene therapies for muscle disorders

Figure 4. Schematic representation of the truncated mini- and microdystrophin versions.

Figure 5. Mechanism of PB transposition.

Figure 6. Schematic representation of PB transposon and PB transposase constructs.

Figure 7. PB-mediated expression of MD1 and MD2 in C2C12 myoblasts.

Figure 8. Validation of the use of hyPB transposase in C2C12 myoblasts.

Figure 9. Human full-length dystrophin expression in PB-transposed C2C12 myoblast-derived differentiated myotubes.

Figure 10. PB-mediated transposition of the full-length human dystrophin CDS in GRMD MABs.

Figure 11. Correction of GRMD MABs by the PB-mediated expression of the full-length human dystrophin.

Figure 12. Schematic representation of the two protocols used in this study to obtain stable transposition in HIDEs.

Figure 13. Stable GFP expression after transposition of the small size transposon PB-Pgk-GFP.

Figure 14. Stable GFP expression after transposition of the large size transposon PB-SPc-DYS-Pgk-GFP.

Figure 15. PB-mediated genetic correction of DMD HIDEs.

Figure 16. PB-mediated full-length dystrophin expression in scid/mdx mice upon transplantation of genetically corrected DMD HIDE^{MYOD} cells.

Figure 17. Tumor formation assay.

Figure S1. Isolation and characterization of GRMD MABs.

Figure S2. Optimization of the transfection protocol for GRMD MABs.

Figure S3. Immunostaining on differentiated GRMD MABs transposed with hyPB + PB-Pgk-GFP.

Figure S4. RT-PCR on full-length human dystrophin transcript in genetically corrected DMD HIDE^{MYOD} cells.

List of tables

Table 1. Summary of cell populations used in preclinical and clinical studies to treat muscular dystrophies.

Table 2. Summary of muscle differentiation protocols from ESCs and genetic correction.

Table 3. Summary of muscle differentiation protocols from iPSCs and genetic correction.

Table 4. List of primers utilized for RT-PCR.

Table 5. List of primers utilized for qRT-PCR.

Table 6. List of primers utilized for semi-quantitative RT-PCR.

Chapter 1

Published in part in:

Loperfido M*, Steele-Stallard HB*, Tedesco FS, VandenDriessche T. *Pluripotent Stem Cells for Gene Therapy of Degenerative Muscle Diseases*. *Current Gene Therapy* 2015;15(4):364-80.

* The authors declare joint first authorship.

1. Introduction

1.1. Duchenne muscular dystrophy

Duchenne muscular dystrophy (DMD; OMIM #310200) is amongst the most severe forms of muscular dystrophies, a heterogeneous group of inheritable pathologies characterized by the progressive weakening and degeneration of the skeletal muscle tissue (Mercuri and Muntoni, 2013; Emery, 2002). DMD is an X-linked disease affecting up to 1 in 5000 male newborns (Mendell and Lloyd-Puryear, 2013). It was first described by the English physician Edward Meryon in 1851 (Emery, 1993), who indicated its familial inheritance and significantly higher incidence in male subjects. This pathology owes its name to the French neurologist Duchenne de Boulogne who, a few years later, extensively detailed its symptoms, clinical features and pathological progression (Parent, 2005). Patients suffering from DMD generally experience difficulties running, standing and climbing stairs in early childhood. In this form of muscular dystrophy, muscle weakness is mainly proximal and progressive (Gower's sign). For this reason most of the patients are confined to a wheelchair by 12 years of age. The continuous impairment of the daily functional abilities drastically affects the patients' quality of life and causes a shortened life expectancy, mainly due to cardiac and respiratory complications.

DMD and its milder form Becker muscular dystrophy (BMD; OMIM #300376) are caused by mutations in the dystrophin gene (Hoffman et al., 1987). This is the

largest gene found in nature with a sequence of 2.4 Megabases (Mb) composed by 79 exons and coding for the dystrophin protein (427 kDa). This is a large protein that localizes in proximity of the myofiber membrane and is the main component of dystrophin-associated protein complex (DAPC; Figure 1; (McGreevy et al., 2015; Ervasti, 2007; Blake et al., 2002)). The complex functions as a mechanical link between the cytoskeletal components (actin and microtubules) and laminin in the extracellular matrix. Dystrophin presence is crucially required to give the stability of the complex and consequently to support the structural integrity of the myofibers (Petrof et al., 1993).

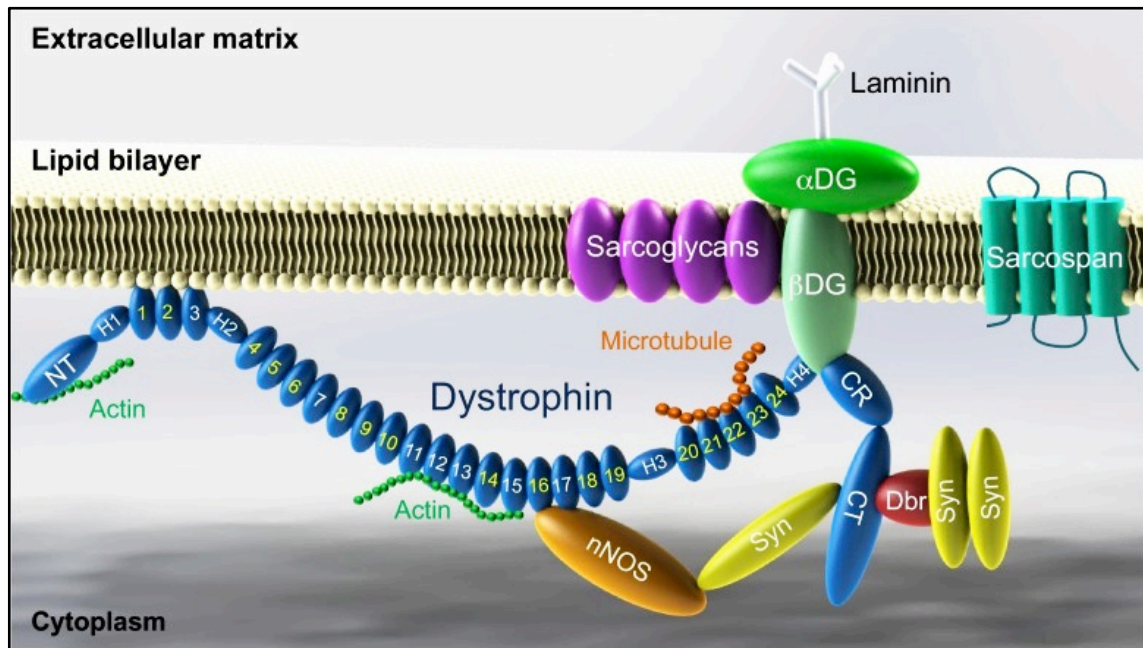


Figure 1. Schematic representation of the dystrophin and the DAPC. Dystrophin contains N-terminal (NT), middle rod, cysteine-rich (CR) and C-terminal (CT) domains. The middle rod domain is composed of 24 spectrin-like repeats and four hinges (H1, H2, H3 and H4). Dystrophin has two actin-binding domains located at NT and repeats 11-15, respectively. Repeats 1-3 interact with the lipid bilayer. Repeats 16 and 17 form the neuronal nitric oxide synthase (nNOS)-binding domain. Dystrophin interacts with microtubules through repeats 20-23. Part of H4 and the CR domain bind to the β -dystroglycan (β DG). The CT domain of dystrophin interacts with syntrophin (Syn) and

dystrobrevin (Dbr). Dystrophin links components of the cytoskeleton (actin and microtubule) to laminin in the extracellular matrix. Adapted from (McGreevy et al., 2015).

In DMD patients, lack of dystrophin makes the sarcolemma membrane vulnerable to damage, in response to muscle contractions. This leads to continuous cycles of degeneration and regeneration. Initially, resident stem cells increase their number, aiming to regenerate the afflicted myofibers (Kuang et al., 2008). However, this compensatory mechanism fails to sustain long-term tissue regeneration, producing damaged myofibers and necrotic tissue. This results in a chronic inflammation characterized by an increased number of resident monocytes combined with fibrotic and adipose infiltration that cause a permanent loss of muscular mass and function (Mann et al., 2011). The increased number of cell divisions causes a deleterious premature exhaustion of the stem cell pool to the extent that the regenerative process becomes impaired (Sacco et al., 2010; Decary et al., 2000). Nevertheless, a recent study provides new insights into the role of dystrophin, suggesting that in DMD it is not the depletion of muscle stem cells *per se*, but rather the absence of dystrophin that causes a dysfunction of these cells and consequently an impaired regeneration, due to a poor differentiation in myocytes (Dumont et al., 2015).

A first clinical diagnosis of DMD is based on the presence of impaired muscle function, delayed speech and elevated levels of muscle enzymes in the serum, like creatine kinase (Bushby et al., 2010a). The validation of the clinical diagnosis occurs via molecular biology techniques, including genetic analysis on the DMD gene, immunocytochemistry and Western blot analysis (Aartsma-Rus et al., 2016). Most of the DMD patients show deletions (~68%) or duplications (~11%) of one or several exons, and the remaining ~20% of patients is affected by small mutations. While the deletions are concentrated between exons 45–55, duplications occur more frequently between exons 2–10 (Bladen et al., 2015). In Figure 2, the functional domains of the dystrophin protein are indicated on the correspondent coding exons of the dystrophin gene (McGreevy et al., 2015).

In DMD, mutations that disrupt the reading frame or generate a premature stop codon lead to loss of protein function. However, revertant fibers expressing the dystrophin are found in DMD patients as a consequence of somatic mutations which restore the frameshift of the original mutations in the dystrophin gene (Klein et al., 1992). In BMD, mutations that maintain the open reading frame allow the production of a reduced amount or abnormal size of dystrophin proteins that are partially functional. Consequently, BMD patients show a milder phenotype compared to DMD patients, due to a later onset of the disease and a slower degenerative progression.

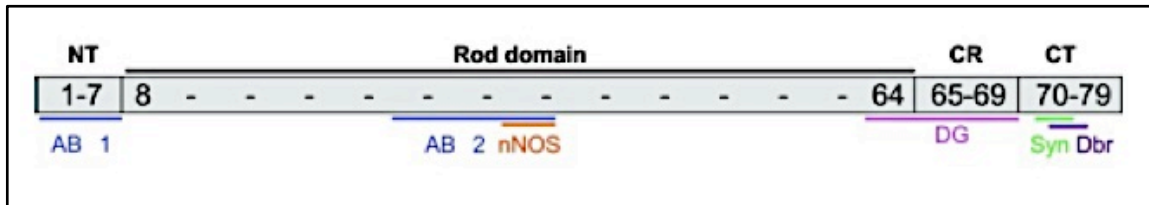


Figure 2. Schematic representation of the dystrophin exons and the corresponding functional domains. Most of the DMD mutations in patients are deletions concentrated between exons 45–55 or duplications that occur more frequently between exons 2–10. In the schematic representation of the dystrophin coding exons, the corresponding functional domains of the dystrophin protein are also reported. The features are indicated with the same terminology as that used in Figure 1. AB1 and AB2 correspond to the actin-binding domain 1 and 2. Adapted from (McGreevy et al., 2015).

1.2. Therapeutic approaches to treat Duchenne muscular dystrophy

In the last two decades, the life expectancy and the quality-of-life of DMD patients have significantly improved thanks to treatment with anti-inflammatory and immunosuppressive drugs and an advanced standard of care (Mercuri and Muntoni, 2015; Serra et al., 2012; Bushby et al., 2010a, 2010b). Nevertheless, to date no definitive treatment is available for DMD patients.

The design of novel therapeutic approaches to treat patients affected by DMD needs to take into account the various aspects related to the nature of the

disease (Boisgerault and Mingozi, 2015; Al-Zaidy et al., 2014; Maffioletti et al., 2014; Mercuri and Muntoni, 2013; Tedesco and Cossu, 2012; Arechavala-Gomez et al., 2010). An effective therapeutic strategy for DMD should ideally target different muscle districts, alleviate respiratory and cardiac complications, prevent or at least limit fibrotic tissue accumulation, prevent or suppress a potential immune response to dystrophin and have a sustainable long-term effect.

Numerous animal models of DMD, both naturally occurring and generated in laboratory, are available to study the pathogenic mechanisms of this muscle disorder and validate possible therapies for treating DMD, reviewed in (McGreevy et al., 2015). The most commonly used animal model is the *mdx* mouse with a nonsense point mutation C->T in exon 23 of the dystrophin gene that results in the absence of the full-length dystrophin expression (Sicinski et al., 1989). However, this model shows some limitations, such the development of dystrophin-positive revertant fibers and a mild clinical phenotype that could impair the assessment of a therapeutic approach based on the restoration of the dystrophin expression. Moreover, the lifespan of *mdx* mice is reduced only by ~25% in contrast to the lifespan of DMD patients that is reduced by ~75% (Chamberlain et al., 2007). Although the development of mouse strains with a more severe dystrophic phenotype, however the body size and immune response of these animal models remain significantly different compared to the human ones. To overcome these limitations, canine models for DMD have been established, such as the golden retriever muscular dystrophy (GRMD) dog (Cooper et al., 1988). This large size animal model carries a point mutation A->G in the intron 6 of the dystrophin gene that causes the skipping of exon 7 and a premature termination of translation. The severe phenotype of the GRMD dog resembles the clinical features of DMD patients with a lifespan reduced by ~75%. Moreover this animal model simulates the immune response observed in individuals affected by DMD thus representing an excellent model for this muscle disorder (Duan, 2015).

The complexity of this scenario has led to a number of different therapies for DMD currently under investigation, in preclinical and clinical studies. These can be classified in three main categories:

- Pharmacological therapy
- Cell therapy
- Gene therapy

1.2.1. Pharmacological therapy

Various pharmacological approaches have been used to directly restore the dystrophin expression in DMD patients. Gentamicin and Ataluren (PTC124) have been shown to induce a ribosomal read-through of the premature stop mutations in the defective gene, leading to the restored production of a functional full-length dystrophin (Welch et al., 2007; Barton-Davis et al., 1999). However, recent clinical trials based on gentamicin have demonstrated modest beneficial effects accompanied by significant side effects (Malik et al., 2010). Recently, hybrid liposomes-based drug-delivery systems have been developed to reduce the toxicity of gentamicin and increase its efficiency (Yukihara et al., 2011). On the other hand, encouraging results were observed in a Phase II clinical trial with Ataluren, where this drug seemed beneficial at low dose (Finkel et al., 2013). This led to a Phase III clinical trial aimed to assess the long-term safety and efficacy (Bushby et al., 2014). The European Medicines Agency granted conditional marketing authorization for this drug (Traslarna), making it the first drug approved for the treatment of DMD patients (Ryan, 2014).

Alternative pharmacological approaches are being explored that are based on the induction of a functional compensatory system. In particular, small molecule drugs can stimulate the transcription and increase the protein levels of the utrophin, the autosomal paralogue of the dystrophin (Tinsley et al., 2011; Tinsley and Davies, 1993). The increased levels of utrophin restore the assembly of the DAPC at the level of the sarcolemma and ameliorate the dystrophic phenotype. Since utrophin is naturally expressed in DMD patients and is not affected by

mutations in the dystrophin gene, no immunological response against this protein is expected as the immune system is tolerant to this “self” protein. This is in contrast with the induction of immune responses upon *de novo* expression of a functional dystrophin after gene therapy and/or after naturally occurring somatic reversion mutations (Mendell et al., 2010). Moreover this strategy is potentially effective for all DMD patients, regardless of the underlying gene defect. The utrophin modulators have been recently tested in a Phase I clinical trial to investigate safety, tolerability and pharmacokinetics, with encouraging results (Tinsley et al., 2015). However, compensatory methods do not correct the genetic defect that causes DMD.

Several other drugs are undergoing preclinical and clinical evaluation aiming to treat dystrophic patients such as insulin-like growth factor-I (IGF-I; (Barton et al., 2002)), nitric oxide-releasing drugs (Brunelli et al., 2007), myostatin inhibitors (Wagner et al., 2008), anti-inflammatory molecules (Serra et al., 2012), phosphodiesterase type 5 (PDE5) inhibitors aiming to reduce muscle ischemia (Nelson et al., 2014) and more recently anti-oxidant drugs (Buyse et al., 2015). The use of pharmacological methods is limited by the continuous need for drug administration and the potential undesirable toxic effects at therapeutic doses of a given drug.

1.2.2. Cell therapy

Cell therapy to treat muscular dystrophies is based on the transplantation of allogeneic or genetically corrected autologous stem/progenitor cells aiming to provide a correct functional copy of the mutated gene.

Satellite cells are the resident stem cells of skeletal muscle. These cells are considered the main player in skeletal muscle development, postnatal growth and regeneration of the damaged myofibers (Relaix and Zammit, 2012). First observed via transmission electron microscopy by Alexander Mauro in 1961, satellite cells are located in a peripheral position to the myofibers, with their niche underneath the myofiber basal lamina (Mauro, 1961). In the adult, satellite cells are mitotically quiescent and can be identified by the expression of the

transcription factor paired box 7 (Pax7, (Zammit et al., 2006)). In response to muscle injury, they become activated and asymmetric cell division takes place. These divisions generate committed cells, called myoblasts, and satellite cells that replenish the pool of quiescent stem cells (Rocheteau et al., 2012; Le Grand et al., 2009; Kuang et al., 2007; Shinin et al., 2006). Myoblasts can be identified for their positivity for both the markers Pax7 and myogenic differentiation 1 (MyoD). However, MyoD positivity is still debated as a defining criterium to identify activated satellite cells/myoblasts. Alternatively, a more relevant role for myogenic factor 5 (Myf5) has been suggested (Kuang et al., 2008; Rudnicki et al., 2008).

Because of their ability in regenerating skeletal muscle, myoblasts were the first cell type utilized for cell transplantation. After promising preclinical results obtained in dystrophic *mdx* mice (Partridge et al., 1989), several clinical trials have been carried out based on allogeneic myoblast transplantation in DMD patients. These trials showed very limited efficacy, probably as a result of poor survival, immune rejection and/or limited migration of transplanted cells (Tedesco and Cossu, 2012; Negroni et al., 2011). Consequently, further studies have been done to improve clinical trial protocols for allogeneic myoblast transplantation in DMD patients, implementing immunosuppressive regimens to enhance engraftment efficiency and performing high-density injections to treat large volumes of muscles (ClinicalTrials.gov NCT02196467 (Skuk and Tremblay, 2011; Skuk et al., 2007)). Nevertheless, this approach was not efficient for the treatment of DMD, where the body-wide treatment of the muscles would be required. A different scenario was observed in a phase I/IIa clinical trial for patients affected by oculopharyngeal muscular dystrophy (OPMD), treated with autologous intramuscular transplantation of myoblasts (ClinicalTrials.gov NCT00773227, (Périé et al., 2014)). In this particular pathology, caused by heterozygous mutation in the gene coding for polyadenylate-binding protein nuclear 1 (PABPN1), small muscles of the face and the neck are specifically affected by degeneration. Autologous myoblasts isolated from unaffected limb muscles were transplanted in the dystrophic pharyngeal muscles, leading to

clinical benefits to the patients with no adverse effects. These encouraging results support the use of autologous myoblast transplantation as a therapeutic strategy for limited muscle districts.

An ideal route to deliver cells through all the muscle districts of the body in DMD patients would be the circulatory system. Intravenous injection would be the simplest approach. However, cells administered through this route will be trapped in the filter organs before reaching the skeletal muscles (Sharma et al., 2014; Schrepfer et al., 2007). Alternatively, intra-arterial administration has been considered to target the muscle tissue. Myoblasts are unable to cross the blood vessel wall upon systemic delivery, thus limiting their use for the treatment of patients affected with systemic myopathies such as DMD (Dellavalle et al., 2007; Sampaolesi et al., 2006).

To overcome these limitations, other cell populations isolated from various tissues and capable of contributing to muscle regeneration have been investigated for the development of novel cell therapy strategies to treat DMD, such as mesoangioblasts (MABs; Table 1; (Costamagna et al., 2015; Benedetti et al., 2013). The use of these adult stem cells in clinical trials for DMD has proven relatively safe, though efficacy could still be improved (Cossu et al., 2015; Torrente et al., 2007).

However, the proliferative potential of these primary cells is not unlimited, thus affecting the large-scale production required to treat all of the skeletal muscles of patients with DMD (Holliday, 2014). Moreover, depletion or dysfunction of myogenic progenitors has been reported in different forms of muscular dystrophy, making their isolation more complex (Dumont et al., 2015; Kudryashova et al., 2012; Tedesco et al., 2012; Cassano et al., 2011; Sacco et al., 2010). This would affect also the investigation on these muscle disorders, being the patient-derived primary cells with myogenic potential considered the most common cell sources for assessing the disease phenotypes in *in vitro* studies.

To overcome these limitations, different protocols have been recently developed to generate transplantable skeletal muscle progenitors from pluripotent stem cells (Table 2 and Table 3; (Loperfido et al., 2015a)). These cells have the potential to be expanded indefinitely, allowing the production of the large numbers of cells required for cell-based therapies of skeletal muscle disorders. Notably, the possibility to derive patient-specific induced pluripotent stem cells (iPSCs) in combination with the current development of gene modification methods provides an attractive alternative for the treatment of genetic diseases by *ex vivo* gene therapy, moving closer to the prospect of an autologous and personalized cell therapy (Figure 3; (Loperfido et al., 2015a)). Moreover, skeletal muscle progenitors derived from patient-specific iPSCs can be used as an *in vitro* model to recapitulate the primary pathology, such as DMD, and for drug screening studies (Shoji et al., 2015; Abujarour et al., 2014).

Nevertheless, further studies are needed to ultimate the clinical translation.

In light of the results reported in this thesis, the next paragraphs will focus on MABs, vessel-associated progenitor cells, and their iPSC-derived counterpart, named HIDEMs (Human iPSC-derived mesoangioblast-like cells).

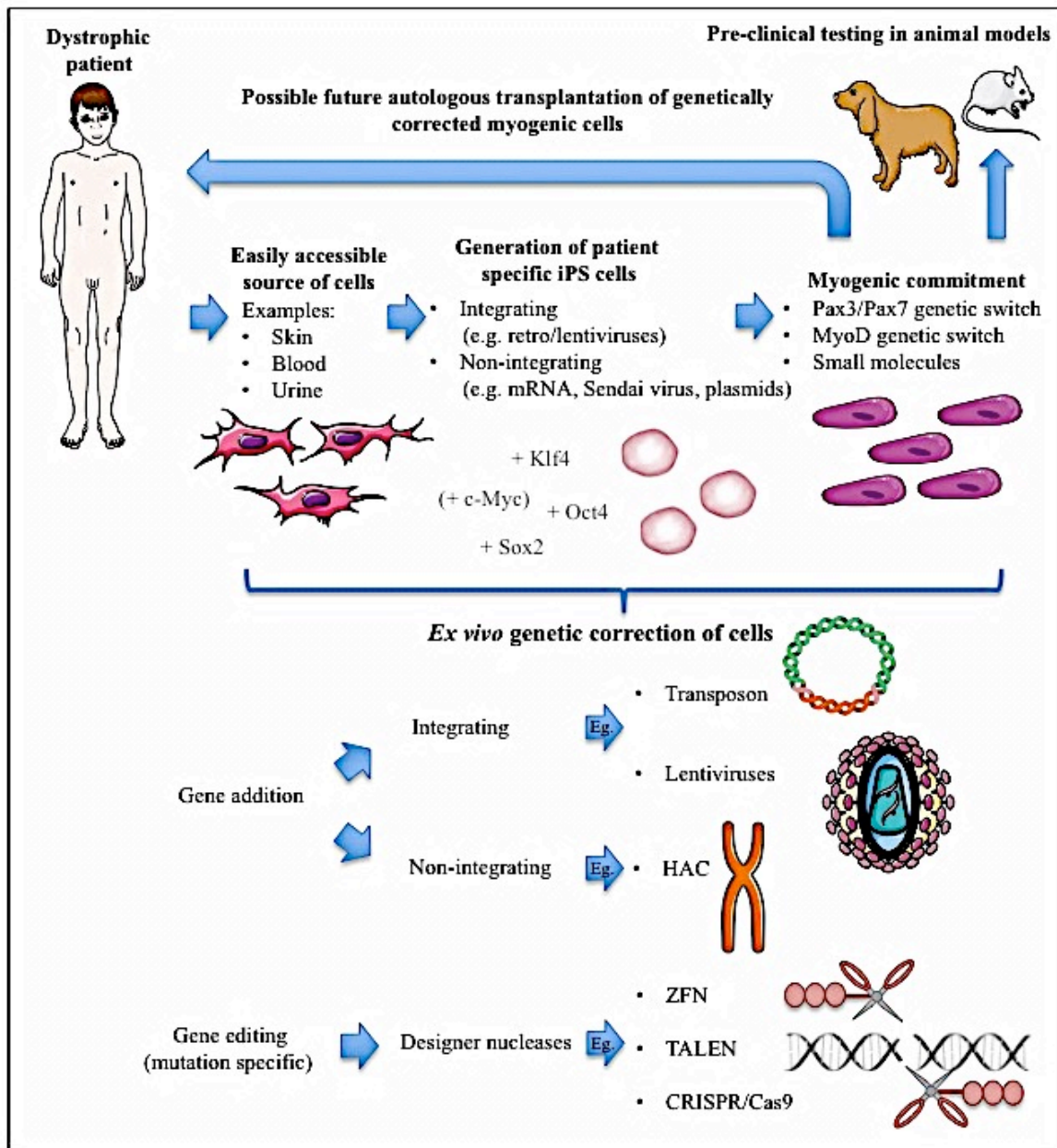


Figure 3. Potential autologous iPSC-based ex vivo gene therapies for muscle disorders. Cells from easily accessible sources can be obtained from patients affected by muscular dystrophies and reprogrammed into iPSCs by addition of reprogramming factors. The resulting iPSCs can then be committed into a potentially unlimited number of myogenic cells. Adapted from (Loperfido et al., 2015a)

1.2.2.1. Mesoangioblasts

Initially described by Bianco and Cossu's groups, mesoangioblasts (MABs) are defined as the *in vitro* counterpart of post-natal skeletal muscle pericytes (Cossu and Bianco, 2003). Isolated from the mouse embryonic dorsal aorta, these cells were assigned to the perivascular lineage and showed variable level of expression of the markers alkaline phosphatase (AP), fetal liver kinase 1 (Flk-1), smooth muscle actin (SMA), c-kit (CD117) and CD34. MABs are able to contribute to different mesodermal tissues *in vivo*, including skeletal muscle (Minasi et al., 2002). These cells have been subsequently isolated from adult mouse, dog and human skeletal muscle biopsies (Dellavalle et al., 2007; Tonlorenzi et al., 2007; Sampaolesi et al., 2006, 2003). More recently, lineage tracing experiments have shown that AP-positive pericytes and their progeny contribute to postnatal muscle development and are able to give rise to Pax7 positive satellite cells during growth and skeletal muscle regeneration (Dellavalle et al., 2011; Tedesco et al., 2011). Similarly to what was observed with mesenchymal stem cells (English and Mahon, 2011), adult mesoangioblasts have been reported to have an immunomodulatory potential, inhibiting T cell proliferation (English et al., 2013). Moreover, allogeneic mesoangioblasts can elicit an immune response only in presence of inflammatory cytokines (Noviello et al., 2014).

Since their discovery, MABs have been considered appealing candidate cells for cell therapy of muscular dystrophies as an alternative to myoblasts (Sampaolesi et al., 2005). In contrast to myoblasts, MABs have been shown able to cross the vessel wall upon intra-arterial delivery and colonize the downstream muscles, which is a major advantage for cell therapy (Dellavalle et al., 2007; Sampaolesi et al., 2006; Palumbo et al., 2004; Sampaolesi et al., 2003). Here, MABs actively contribute to muscle regeneration, thus leading to amelioration of the dystrophic phenotype of murine and canine models of muscular dystrophy (Sampaolesi et al., 2006, 2003). Moreover, MABs can be easily manipulated with viral and non-viral vectors, making them suitable for gene and cell therapy approaches (Tedesco et al., 2011; Dellavalle et al., 2007; Sampaolesi et al., 2006). Based

upon these findings, a series of studies investigated the possible applications of MABs to correct aged dystrophic muscles (Gargioli et al., 2008), cardiac defects (Galli et al., 2005) and different forms of muscular dystrophies (Domi et al., 2015; Díaz-Manera et al., 2010).

The encouraging results coming from these pre-clinical studies have led to a first-in-human phase I/II clinical trial based on intra-arterial transplantation of allogeneic MABs in five DMD patients, under immunosuppressive regimen (EudraCT N°2011–000176–33, (Cossu et al., 2015)). This trial, completed in 2015, met its primary endpoint providing insightful information on the safety of these cells to treat DMD patients. The administration at escalating doses of HLA-matched donor MABs in the limb arteries of the patients was possible without adverse events related to the procedure itself. Though the overall efficacy could still be improved, it sets the stage for future trials that may require enrollment of younger patients with less advanced muscle disease and/or increasing the MAB dose. Moreover, gene therapy approaches could be exploited to further amplify the therapeutic effect using genetically modified autologous MABs that over-express dystrophin upon myogenic differentiation. The use of such autologous MABs may obviate the need for immune suppression, in contrast to when allogeneic MABs are employed. Ultimately, whether these intrinsic immunosuppressive properties of MABs would suffice to prevent a dystrophin-specific immune response after transplantation of genetically modified, dystrophin-expressing MABs remains to be addressed in future clinical studies.

Cell type	Tissue of origin	Delivery	Animal model (disease)	Clinical Trials
Satellite cells and myoblasts	Skeletal muscle	Local	mdx mice (DMD) (Partridge et al., 1989); mdx nu/nu mice (DMD) (Montarras et al., 2005)	Phase I/II: Recruiting (DMD)* (Skuk and Tremblay, 2011); Phase I/IIa: completed (OPMD) (Périé et al., 2014)
Pericytes and Mesoangioblasts	Vessels / Skeletal muscle	Systemic / Local	scid/mdx mice (DMD) (Dellavalle et al., 2007; Tedesco et al., 2011); sgca-null mice (LMG2D) (Gargioli et al., 2008; Sampaolesi et al., 2003); scid/BIAJ mice (LMG2B) (Diaz-Manera et al., 2010); GRMD dogs (DMD) (Sampaolesi et al., 2006)	Phase I/II: completed (DMD) (Cossu et al., 2015)
Muscle derived stem cells	Skeletal muscle	Systemic / Local	mdx mice (DMD) (Cao et al., 2003; Qu-Petersen et al., 2002; Gussoni et al., 1999); mdx nude mice (DMD) (Meng et al., 2016; Meng et al. 2011); GRMD dogs (DMD) (Rouger et al., 2011)	N/A
CD133 positive cells	Blood / skeletal muscle	Systemic / Local	scid/mdx mice (DMD)(Benchaouir et al., 2007; Torrente et al., 2004); scid dysferlin null mice (MM) (Meregalli et al., 2013)	Phase I: completed (DMD) (Torrente et al., 2007); Phase II: Recruiting (DMD)
Pw1 positive Interstitial cells	Skeletal muscle	Local	Injured nude mice (Mitchell et al., 2010)	N/A
Mesenchymal stem cells	Bone marrow / vessels**	Systemic / Local	Injured rats and mdx nude mice (DMD) (Dezawa et al., 2005); injured NOD/scid and scid/mdx mice (Crisan et al., 2008); injured Rag2+ γ c+/C5 mice (Meng et al., 2010); injured nude mice (De Bari et al., 2003); mdx mice (DMD) (Gang et al., 2009; Wernig et al., 2005; De Bari et al., 2003)	N/A
Hematopoietic stem cells	Bone marrow / blood	Systemic / Local	mdx mice (DMD) (Gussoni et al., 1999); mdx4cv mice (Ferrari et al., 2001); injured scid/beige mice (Ferrari et al., 1998); injured mice (Corbel et al., 2003)	N/A

Amniotic fluid stem cells	Amniotic fluid	Systemic	HSA-Cre, SmnF7/F7 mice (Piccoli et al., 2012)	N/A
---------------------------	----------------	----------	---	-----

Table 1. Summary of cell populations used in preclinical and clinical studies to treat muscular dystrophies. * Past clinical trials on DMD have been reviewed in (Tedesco and Cossu, 2012). ** Cells have been isolated from other connective tissues that are also referred to as MSCs. This is in agreement with the criteria proposed by the Society for Cell Therapy for defining MSCs (Dominici et al., 2006). Adapted from (Benedetti et al., 2013).

1.2.2.2. Human induced pluripotent stem cell-derived mesoangioblast-like cells

In order to overcome the limited expansion potential of primary cells and their poor availability observed in the biopsies of the patients with limb-girdle muscular dystrophies 2D (LGMD2D), a method to derive MAB-like cells from human and mouse iPSCs was developed (Tedesco et al., 2012) that was further extended and optimized as a joint effort between Tedesco's group and ours (Maffioletti et al., 2015). In particular, this methodology was adapted to human embryonic stem cells (ESCs) and iPSCs cultured in feeder-free conditions and was validated based on iPSCs derived from several distinct genetic muscle disorders, including DMD.

Starting from a pluripotent stem cell culture, this optimized and novel technique allows robust differentiation towards the mesodermal lineage. The protocol entails a series of culture passages at different cell densities: in a first phase (early commitment) gently dissociated pluripotent cells are cultured at high density on matrigel coated dishes; the following steps (intermediate and late commitment) allow cells adaptation to a lower density, enzymatic dissociation and culture in proliferation media normally utilized to expand primary human MABs. Cells obtained with this protocol resemble MABs on the basis of their morphological characteristics, cell surface markers and gene expression profile and are characterized by a robust expansion potential. Terminal myogenic differentiation is then triggered upon tamoxifen-mediated conditional

overexpression of the transcription factor MyoD fused with the estrogen receptor for nuclear translocation (MyoD-ER(T), (Tedesco et al., 2012; Kimura et al., 2010)). This method allowed the derivation of the so-called human iPSC-derived mesoangioblast-like cells (HIDEMs) from healthy donors, LGMD2D patients and, relevant for this work, from DMD patients. LGMD2D HIDEMs were genetically corrected with a lentiviral vector coding for the human α -sarcoglycan gene (whose mutations cause LGMD2D) under a muscle specific promoter and then also transduced with another lentiviral vector coding for the MyoD-ER(T) transgene as a myogenic differentiation switch, as described above. Genetically corrected LGMD2D HIDEMs were successfully transplanted intramuscularly and intra-arterially into α -sarcoglycan-null immunodeficient (Sgca-null/scid/beige) mice, a preclinical model of LGDM2D, and produced α -sarcoglycan-positive muscle fibres that were detectable one-month post transplantation. Consequently, *de novo* expression of the missing α -sarcoglycan led to the reconstitution of the dystrophin-associated protein complex in host myofibers. Similarly, species-specific transplantation of mouse iPS cell-derived MAB-like progenitors in Sgca-null/scid/beige mice led to engraftment of large areas of host muscle, re-establishment of muscle pericytes *in vivo* and functional amelioration of the dystrophic phenotype. This proof of concept study established the validity of an autologous gene therapy approach for the treatment of LGMD2D, and possibly other forms of muscular dystrophy, based upon transplantable iPSC-derived myogenic cells. Indeed, the same protocol allowed the generation of HIDEMs also from DMD iPSCs, which were genetically corrected with the DYS-HAC (Loperfido et al., 2015a; Gerli et al., 2014; Tedesco et al., 2012) (see below). Interestingly, analysis of the interaction between HIDEMs and immune cells suggests a reduced risk of evoking potential immune responses. Indeed, HIDEMs suppress T cell proliferation through IDO and PGE-2 dependent pathways, consistent with the results from tissue-derived mesoangioblasts (Loperfido et al., 2015a; English et al., 2013; Li et al., 2013).

Overall, HIDEMs showed great proliferation potential and a strong myogenic differentiation ability. This aspect combined with the availability of patient-specific

DMD HIDEs made these cells an appealing candidate to test the transposon-based genetic correction strategy investigated in this thesis.

Pluripotent stem cell	Origin	Muscle differentiation method	Mouse model & genetic correction	<i>In vivo</i> results			Refs
				Engraftment/Differentiation	Systemic delivery	Functional test	
ESCs	mouse	EB cocultured with primary muscle cells	WT cells into mdx mouse, no genetic correction	✓	x	x	Bhagavati et al., 2005
		MyoD integration (IND)	WT cells into mdx mouse, no genetic correction	✓	x	x	Ozasa et al., 2007
		Pax3 integration (IND), EB, PDGF- α R ⁺ Flk-1 ⁻ cell sorting	WT cells into mdx mouse, no genetic correction	✓	✓	✓	Darabi et al., 2008
		Pax3 or Pax7 integration (IND), EB, PDGF- α R ⁺ Flk-1 ⁻ cell sorting	WT cells into mdx mouse, no genetic correction	✓	✓	✓	Darabi et al., 2011
		mesodermal commitment, PDGF- α R ⁺ cell sorting	WT cells into immunodeficient mouse, no genetic correction	✓	x	x	Sakurai et al., 2008
		EB and SM/C-2.6 cell sorting	WT cells into mdx mouse, no genetic correction	✓	x	x	Chang et al., 2009
		EB, GSK-3 inhibitor (CHIR99021), bFGF, N2	NA	x	x	x	Shelton et al., 2014
		Myf5 integration (IND), EB	NA	x	x	x	Iacovino et al., 2011
	human	mesenchymal commitment, CD73 ⁺ and NCAM ⁺ cell sorting	HD into immunodeficient mouse, no genetic correction	✓	x	x	Barberi et al., 2007
		Pax7 LV integration (IND), EB, purification by cell sorting	HD into immunodeficient/mdx mouse, no genetic correction	✓	x	✓	Darabi et al., 2012

		EB, mesenchymal commitment	HD into immunodeficient mouse, no genetic correction	✓	x	x	Awaya et al., 2012
		myogenic medium, MyoD AAV	Dys null cells into immunodeficient/mdx mouse, no genetic correction	✓	x	x	Goudeneg e et al., 2012
		BAF60C and MyoD LV integration	NA	x	x	x	Albini et al., 2013
		GSK-3 inhibitor (CHIR99021), bFGF, N2	NA	x	x	x	Shelton et al., 2014
		Myf5 integration (IND), EB	NA	x	x	x	Iacovino et al., 2011
		mesodermal commitment, MyoD-ER(T) LV integration (IND)	NA	x	x	x	Maffioletti et al., 2015

Table 2. Summary of muscle differentiation protocols from ESCs and genetic correction. NA: Not assessed (no disease, no genetic correction, in vitro only); ✓ Performed; x Not performed. Adapted from (Loperfido et al., 2015a).

Pluripotent stem cells	Origin	Muscle differentiation method	Mouse model & genetic correction	In vivo results			Refs
				Engraftment/Differentiation	Systemic delivery	Functional test	
iPSCs	mouse	Pax7 integration (IND), EB, PDGF- α R ⁺ Flk-1 ⁻ cell sorting	WT cells into mdx mouse, no genetic correction	✓	x	✓	Darabi et al., 2011
		Pax3 LV integration (IND), EB, PDGF- α R ⁺ Flk-1 ⁻ cell sorting	μ utrn-SB transposon corrected, dys null/ μ utrn positive cells into dys null/utrn null mouse	✓	✓	✓	Filareto et al., 2013
		mesodermal commitment, MyoD-ER(T) LV integration (IND)	WT cells into Sgca-null/immunodeficient mouse, no genetic correction	✓	✓	✓	Tedesco et al., 2012; Gerli et al., 2014
		EB and SM/C-2.6 cell sorting	WT cells into mdx mouse, no genetic correction	✓	x	x	Mizuno et al., 2010
		EB and SM/C-2.6 cell sorting	DMD: mdx iPSCs with full-length dys cDNA into scid/mdx	✓	x	x	Zhao et al., 2014
		Pax3 transposon integration and EB	NA	x	x	x	Belay et al., 2012
	human	Pax7 LV integration (IND), EB, purification by cell sorting	HD into immunodeficient or immunodeficient/mdx mouse, no genetic correction	✓	x	✓	Darabi et al., 2012
		EB, mesenchymal commitment	HD into immunodeficient mouse, no genetic correction	✓	x	x	Awaya et al., 2012
		treatment with GSK-3 inhibitor (CHIR99021) and bFGF, sorting for AChR ⁺ or CXCR4 ⁺ /C-MET ⁺	NA	x	x	x	Borchin et al., 2013

EB and treatment with GSK-3 inhibitor (BIO), bFGF and forskolin	HD into immunodeficient mouse, no genetic correction	✓	x	x	Xu et al., 2013
mesodermal commitment, MyoD-ER(T) LV integration (IND)	LGMD2D: HD and Sgca-LV corrected,(muscle specific promoter) cells into Sgca-null/immunodeficient mouse	✓	✓	x	Tedesco et al., 2012; Gerli et al., 2014; Maffioletti 2015
mesodermal commitment, MyoD-ER(T) LV integration (IND)	DMD: DYS-HAC corrected, <i>in vitro</i> only	x	x	x	Tedesco et al., 2012; Maffioletti 2015
myogenic medium, MyoD AAV	DMD cells into immunodeficient/mdx mouse, no genetic correction	✓	x	x	Goudenegge et al., 2012
MyoD (IND) PB-transposon integration	HD cells into immunodeficient/DMD mouse, no genetic correction	✓	x	x	Tanaka et al., 2013
MyoD (IND) PB-transposon integration	MM: <i>DYSF</i> -PB transposon corrected, <i>in vitro</i> only	x	x	x	Tanaka et al., 2013
MyoD (IND) PB-transposon integration	CPT II: <i>in vitro</i> only, no genetic correction	x	x	x	Yasuno et al., 2014
MyoD LV integration (IND)	HD, DMD, Becker, <i>in vitro</i> only, no genetic correction	x	x	x	Abujarour et al., 2014

Table 3. Summary of muscle differentiation protocols from iPSCs and genetic correction. NA: Not assessed (no disease, no genetic correction, *in vitro* only); ✓ Performed; x Not performed. Adapted from (Loperfido et al., 2015a).

1.2.3. Gene therapy

Gene therapy offers a unique scenario for the treatment of monogenic disorders. The use of advanced technologies tailored to correct the genetic defect underlying a disease has recently led to successful clinical trials (Hacein-Bey

Abina et al., 2015; Hacein-Bey-Abina et al., 2014; Nathwani et al., 2014; Aiuti et al., 2013; Biffi et al., 2013; Cavazzana-Calvo et al., 2010). The expression of the missing protein can be restored in the patients by direct correction of the mutated gene in the affected tissues (*in vivo* gene therapy) or alternatively by correction of the target cells isolated from the patient and subsequently re-administrated (*ex vivo* gene therapy). Despite early adverse events (Howe et al., 2008; Stein et al., 2010), the development of efficient, safe, non-immunogenic gene therapy procedures leading to long-term therapeutic effects have supported the market authorization of the first gene therapy product in the Western world (Glybera, (Kastelein et al., 2013)).

Different *in vivo* and *ex vivo* gene therapy strategies have been developed for DMD, aiming to restore the expression of the missing protein by modulation of the RNA processing (i.e. “exon-skipping”) or by gene repair mechanisms (i.e. “gene editing”), or in alternative to replace the defected gene by adding a functional copy (i.e. “gene addition” or “gene replacement”).

1.2.3.1. Exon-skipping

Exon-skipping is a gene correction approach based on short synthetic fragments of nucleic acids known as antisense oligonucleotides (AONs) that hybridize to the pre-mRNA causing the skipping of the exon carrying the mutation. As result, the dystrophin reading frame is restored and a functional slightly shorter dystrophin protein is produced, similar to the truncated version found in patients with BMD (Helderman-van den Enden et al., 2010). Therefore the aim of exon-skipping therapy is to convert the severe DMD symptoms towards the much milder symptoms observed in BMD. The efficacy of this approach has been successfully demonstrated in preclinical *in vivo* studies, leading to different clinical trials for DMD patients (Kole and Krieg, 2015). Two drugs are currently being evaluated: PRO051 (Drisapersen) by Prosensa and GSK, and AVI-4658 (Eteplirsen) by Sarepta Therapeutics. Both of them target and induce skipping of exon 51 that is applicable to the largest group of all DMD patients (13%) (Helderman-van den Enden et al., 2010). However, they differ in their chemical composition. Initially,

the phase II clinical trial on Drisapersen gave encouraging results, indicating a slight increase in dystrophin production and a better performance of the treated DMD patients in the 6-Minute walk test (6MWT) (Voit et al., 2014). This test is widely used as an outcome measure in DMD, as it integrates the measurement of endurance, ambulation and muscle function (McDonald et al., 2010). Nevertheless, the phase III clinical trial has been prematurely interrupted since it failed to meet the primary endpoint of a statistically significant improvement on the 6MWT, possibly due to rapid clearance of the compounds from the circulation. Moreover, controversial interpretation of the results coming from these studies (i.e. the non-correlation of amount of dystrophin positive fibres via immunohistochemistry and the level of protein detected via Western blot analysis), revealed the need to refine those analytical approaches (Lu et al., 2014). In a double-blind and open label treatment on Eteplirsen, the administration of the AONs led to dystrophin production in the muscles of DMD patients and a statistically significant advantage on 6MWT in comparison to historical controls, over 3 years of follow-up (Mendell et al., 2016). Moreover, a relative stability of respiratory muscle function and lack of toxicity were observed in this study, thus supporting further clinical investigations in larger cohorts of DMD patients.

One of the limits of the exon skipping approach is that repeated administrations of the AONs are required since the effects are expected to be short-term. In order to provide sustained levels of dystrophin protein for a long-term therapeutic efficacy, modified small nuclear RNAs (U1 and U7snRNA) have been designed to shuttle AONs via recombinant adeno-associated virus (rAAV) vectors (Kawecka et al., 2015; Benchaouir and Goyenvalle, 2012). The potential of this approach has been shown in preclinical *in vivo* studies. In dystrophic mice a single treatment of rAAV-snRNA-mediated exon skipping systemically delivered was able to restore dystrophin levels and improved muscle function body-wide (Goyenvalle et al., 2012a; Denti et al., 2006; Goyenvalle et al., 2004). Recurrent treatments were required in dystrophic dogs to reach a therapeutic dose of rAAV vector (Le Guiner et al., 2014; Vulin et al., 2012). Although no adverse events

were apparent in the dog model, the vector doses used may potentially evoke AAV capsid-specific immune responses in human subjects, that could potentially undermine the safety and efficacy, as shown in other gene therapy trials based on AAV (Nathwani et al., 2014; Mingozzi et al., 2009). Another limit of the exon skipping approach is that it is restricted to specific mutations, warranting a personalized mutation-dependent treatment for different patients with different genotypes. Therefore, multiexon-skipping approaches to target exons 45-55 at the mutation hotspot of the DMD gene have been developed aiming to rescue up to 63% of DMD patients with a deletion (Goyenvalle et al., 2012b; Bérout et al., 2007).

Further improvements are needed to improve the overall efficiency of the exon-skipping approach towards future clinical applications.

1.2.3.2. Gene editing

A recently developed and promising gene therapy strategy for the treatment of monogenic diseases, such as DMD, is based on the use of engineered endonucleases for site-specific correction of a mutated gene. Meganucleases (MGNs), zinc-finger nucleases (ZFNs), transcription activator-like effector nucleases (TALENs) and clustered regularly interspaced short palindromic repeats associated RNA-guided Cas9 (CRISPR/Cas9) nucleases are the classes of endonucleases that have been exploited for the editing of the dystrophin gene. The two different strategies validated for DMD are based on promoting the permanent removal of exon by non-homologous end joining (NHEJ) causing the disruption of the reading frame, thus leading to the production of a truncated dystrophin protein. Alternatively, full-length dystrophin expression could be restored by a homology-directed repair (HDR)-mediated insertion of correct gene sequence (Prakash et al., 2016). In primary myoblasts from DMD patients presenting the mutation in exon 51 locus (13% of patients), the dystrophin reading frame was restored by TALENs through the introduction of indels in the mutated exon (Ousterout et al., 2013) or by ZFNs that permanently excised exon 51 (Ousterout et al., 2015a). With a similar approach, a multiplex CRISPR/Cas9-

based system has been developed for the removal of exons 45-55 of DMD gene, a mutational hotspot which if targeted could be therapeutically applicable for 62% of patients (Ousterout et al., 2015b). These approaches resulted in a truncated but functional dystrophin protein. The mutational hotspot has also been targeted in immortalized myoblasts from DMD patients by MGN that mediated the homologous recombination knock-in of deleted exons 45-52 allowing the restoration of the full-length dystrophin (Poplewell et al., 2013).

Interestingly, TALEN and CRISPR/Cas9 approaches have been used to successfully correct the dystrophin gene in iPSCs derived from a patient with a deletion in exon 44 (Li et al., 2015). Three different correction methods were applied: exon skipping, frameshifting and exon knock-in; with the latter approach able to restore the full-length dystrophin expression.

Moreover, *in vivo* application of CRISPR/Cas9 has successfully shown the correction of the dystrophin gene in the germline of dystrophic mice. This led to dystrophin restoration and muscle phenotypic rescue in the progeny (Long et al., 2014). In order to target post-mitotic adult tissues, the use of CRISPR/Cas9 system was exploited in three different studies based on the delivery of gene editing components using AAV vectors *in vivo* in dystrophic mice (VandenDriessche and Chuah, 2016; Long et al., 2015; Nelson et al., 2015; Tabebordbar et al., 2015). These vectors could be delivered systemically and displayed high tropism for muscle. Results showed the expression of a truncated dystrophin upon excision of the mutated exon 23 and consequent rescue of the dystrophin reading frame. Although expression of dystrophin after gene correction was relatively low, a modest improvement in muscle function was reported which required high vector doses. In a recent study, CRISPR/Cas9 nucleases alone or together with TALENs have been combined with adenoviral vectors (AdVs) to rescue the dystrophic phenotype in mdx mice (Xu et al., 2015) or genetically correct immortalized DMD myoblasts (Maggio et al., 2016).

In contrast to transient methods based on AONs targeting the mRNA, endonucleases-based gene editing showed to permanently correct dystrophin mutations and therefore restore protein production, with the advantage of

obviating the need for continuous drug administration. However, optimization of these new gene-editing strategies to enhance safety (i.e. to minimize the risk of off-target sites) and protein expression levels is needed for potential clinical translation.

1.2.3.3. Gene addition

Gene addition strategies have successfully shown the possibility to provide an additional functional copy of the dystrophin gene that overcomes the genetic defect caused by a mutation in dystrophin. In this way, the expression of the missing protein is restored and the muscle function recovered, regardless of the type of mutation. Consequently, gene addition is potentially suitable for all the DMD patients. Nevertheless, achieving safety and demonstrating long-term efficiency by gene addition remains challenging. This is compounded by potential immune responses against the vector or the new protein expressed by the therapeutic gene. Another challenge relates to the abundance of the muscle tissues that need to be targeted in muscular dystrophies. Since the fibers are surrounded by connective and sometimes fibrotic tissue this may also affect the efficiency of delivering the therapeutic gene. The types of vectors currently in use for the treatment of muscular dystrophies can be divided in viral and non-viral vectors.

Viral vectors have the ability to relatively efficiently transduce different cell types and have been exploited as gene transfer vehicle for *in vivo* and *ex vivo* gene therapy approaches for DMD. Helper-dependent adenoviral (HDAd) vectors have a cargo up to 36 Kb and can easily accommodate the full-length dystrophin cDNA (14 Kb), resulting in its efficient expression (Guse et al., 2012; Kawano et al., 2008). Nevertheless, the applicability of this approach *in vivo* is limited by the need of multiple intramuscular administrations of HDAd vectors and the high risk of immune response, as previously showed in non-human primates (Brunetti-Pierri et al., 2004; Zoltick et al., 2001). Moreover, systemic administration of adenoviral vectors has been shown to result in acute inflammation and significant morbidity and mortality in clinical trials (Wilson, 2009).

Recombinant adeno-associated virus (rAAV) vectors overcome some of these hurdles, since they can be systemically delivered to efficiently target skeletal and cardiac muscles *in vivo* (Wang et al., 2005; Gregorevic et al., 2004) and exhibit low immunogenicity compared to HDAd vectors (Zaiss et al., 2002). However, the relatively limited packaging capacity of rAAV vectors (~4.5 Kb) precludes the incorporation of large transgenes such as the full-length dystrophin cDNA (14 Kb). Therefore, truncated but functional versions of the dystrophin cDNA have been generated that mimic the truncated, partially functional dystrophins characteristic in BMD patients (minidystrophins). Alternatively, only regions necessary for recruiting important dystrophin binding partners can be retained (microdystrophin) (Figure 4). Preclinical *in vivo* studies have shown that a single systemic administration of rAAV vectors coding for microdystrophin improves muscle function and rescues the dystrophic phenotype in mice (Koppanati et al., 2010; Wang et al., 2009; Gregorevic et al., 2006). Nevertheless, the translation to large size animal models for DMD and to patients is challenging, due to an immune response against the rAAV vectors and the transgene product itself (Bowles et al., 2012; Shin et al., 2012; Kornegay et al., 2010; Ohshima et al., 2009; Wang et al., 2007a, 2007b; Yuasa et al., 2007). These adverse events were responsible for the lack of long-term microdystrophin expression. Therefore, in order to increase the specificity towards the target cells and elicit an immune response to sustain high levels of expression of the protein, improvements on the design of gene delivery vectors have been reported. These consisted in the optimization of the transgene sequence (Athanasopoulos et al., 2011; Foster et al., 2008), the use of muscle-restricted promoters and enhancer transcriptional elements (Koo et al., 2011a, 2011b; Salva et al., 2007), the development of viral capsids with reduced immunogenic profile (Yue et al., 2015; Shin et al., 2013; Rodino-Klapac et al., 2010). The combination of these features, together with long-term studies on immunity in large animal models for DMD, would be required for ultimate clinical translation.

In contrast to rAAV, lentiviral vectors show a larger size capability (~ 9-10 Kb) and have been exploited to develop *ex vivo* gene therapy approaches for DMD.

However, vector titers dropped significantly with increased vector size. Muscle progenitors isolated from dystrophic animals and genetically corrected using lentiviral vectors coding for truncated forms of the dystrophin cDNA have been transplanted in dystrophic recipients. The dystrophin expression was successfully restored in the fibers of the treated muscles (Meng et al., 2016; Sampaolesi et al., 2006; Li et al., 2005a; Bachrach et al., 2004). Although this approach might represent a valid platform for the development of an autologous stem cell-based gene therapy, preclinical *in vivo* studies in dystrophic dogs have shown that microdystrophin does not replicate all of the essential functions of the full-length dystrophin (Sampaolesi et al., 2006). This strategy was effective to treat other muscular dystrophies where the smaller size of the therapeutic transgene facilitated gene delivery by lentiviral vectors (Meregalli et al., 2013; Tedesco et al., 2012; Sampaolesi et al., 2003). Although lentiviral vectors are efficient and relatively safe, as demonstrated by the successful on-going clinical trials for inherited diseases (Aiuti et al., 2013; Biffi et al., 2013), their use is hampered by the risk of insertional mutagenesis. To circumvent this problem, non-integrating integrase-defective lentiviral (IDLV) vectors have been recently generated (Vargas et al., 2004). Though IDLVs may enable gene transfer in post-mitotic tissues such as muscles (Kymäläinen et al., 2014), the levels of expression and the transduction efficiency are generally low. In this context, the use of non-viral vectors can be considered as a valid alternative for gene transfer-based therapies for muscular dystrophies.

Non-viral vectors evoke only limited or no adaptive immune responses and can transfer genetic material of various sizes. These features make them particularly attractive to treat diseases caused by mutations in large genes, such as DMD.

Naked plasmids coding for the full-length dystrophin have been employed for direct intramuscular injection in DMD patients (Romero et al., 2004). Although no adverse effects have been observed, this approach was limited to a defined area of the treated muscle and the expression of the protein was not sustained. Therefore new methods were considered to deliver the therapeutic gene

systemically, such as the hydrodynamic limb vein (HLV) injection (Herweijer and Wolff, 2007). Preclinical studies in dystrophic mice showed that the application of this method led to the restoration of the full-length dystrophin expression into the lower limbs and long-term protection of skeletal muscles (Zhang et al., 2010). Interestingly, studies on dose-response in rodents and nonhuman primates supported the use of HLV injection for possible therapeutic treatments of patients affected by DMD and other muscular dystrophies (Wooddell et al., 2011; Hegge et al., 2010). Alternatively, naked plasmids have been used in combination with a site-specific recombinase called phiC31 integrase to deliver the full-length murine dystrophin cDNA in mdx iPSCs (Zhao et al., 2014). The genetically corrected iPSCs were enriched for a common marker of murine muscle precursor cells (SM/C 2.6) and differentiated in myogenic precursors able to express the dystrophin *in vitro* and *in vivo*. However myogenic induction was relatively inefficient and further studies are necessary to make this approach applicable to human iPSCs.

The human artificial chromosome (HAC) is a non-integrating non-viral vector that can be stable maintained as an endogenous chromosome throughout subsequent cell divisions (Kouprina et al., 2014; Kazuki and Oshimura, 2011). DYS-HAC has been generated that contained the entire human dystrophin gene (2.4 Mb), including the regulatory elements (Hoshiya et al., 2009). Notably, in 2011, Cossu's group demonstrated the possibility of exploiting MABs for a cell-mediated non-viral gene replacement approach for DMD (Tedesco et al., 2011) based on DYS-HAC. Dystrophic murine MABs genetically corrected with DYS-HAC were transplanted in immunodeficient dystrophic (scid/mdx) mice. This resulted in human dystrophin expression in the muscle fibers of the recipient animals consistent with long-term functional amelioration of the dystrophic phenotype. In the next study from the same team, mesoangioblasts have been derived from iPSCs of a DMD patient genetically corrected with DYS-HAC, paving the way to future studies for autologous gene therapy approaches (Tedesco, 2015; Tedesco et al., 2012). However, the transfer of such a large size

vector into the target cells results quite challenging and efficiency is affected (approximately 1.2×10^{-5}). Moreover the production of such a complex vector makes it costly and time consuming. Therefore, further studies are needed in order to improve this technology and move towards a clinical application.

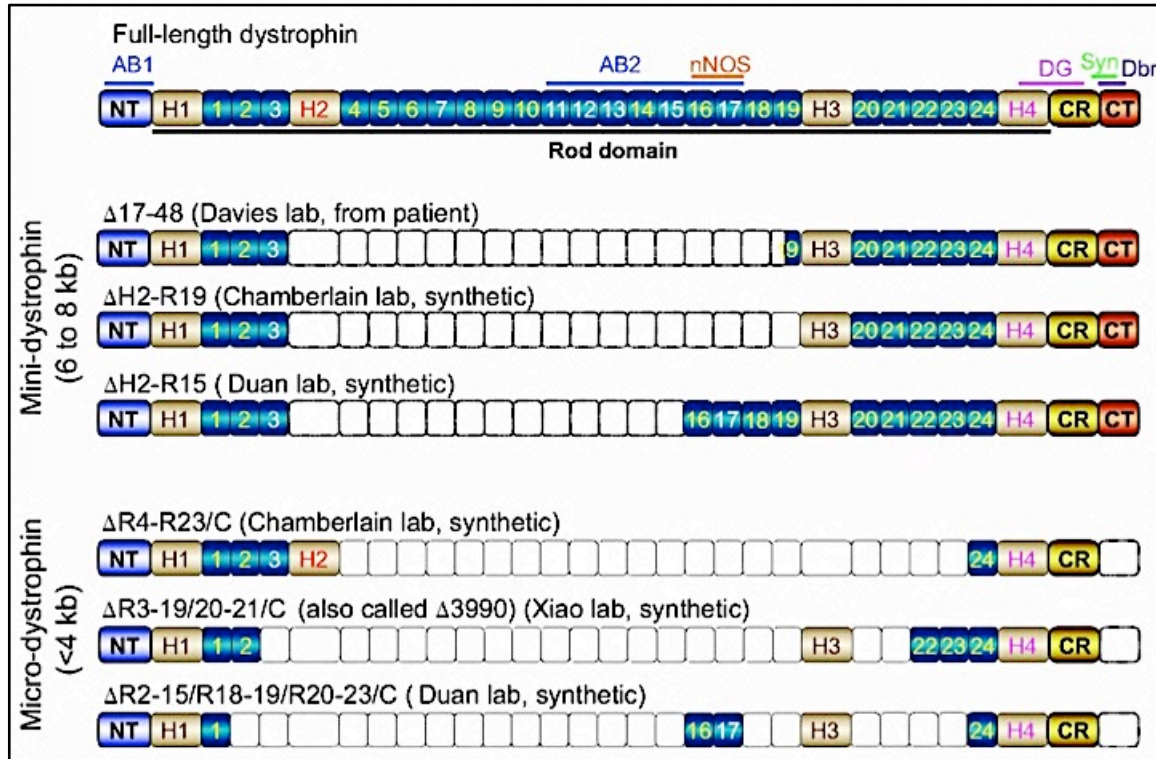


Figure 4. Schematic representation of the truncated mini- and microdystrophin versions. Examples of mini- and micro- dystrophin genes that have been developed by different groups for vector-mediated gene addition strategies for DMD. The full-length dystrophin structure is shown uppermost, and features the same terminology as that used in Figure 1. The two actin-binding domains of the dystrophin are indicated as AB1 and AB2. The name of the mini-dystrophin version from Davie’s lab indicates the deletion of exons corresponding to the sequence represented, at variance with the other mini- and microdystrophin versions where the name of the missing protein domains are indicated. In the microdystrophin mutants, ΔC indicates the deletion of the CT domain. Adapted from (McGreevy et al., 2015).

1.3. Transposons

Transposons represent a valid non-viral vector system alternative to the several methods currently under investigation, aimed at developing safe and efficient

gene therapy approaches for monogenic disorders. Transposons are plasmid-based non-viral vectors able to transfer the gene of interest into the genome of the target cells. The advantage of this gene delivery system is that it can stably integrate into the genome and achieve a prolonged expression of the transgene, while retaining the features of a non-viral vector system: low immunogenic profile, reduced risk of insertional mutagenesis, large cargo capability, easy manufacturing (Koonin and Krupovic, 2015; Loperfido et al., 2015a; Di Matteo et al., 2014a; Mátés et al., 2009; VandenDriessche et al., 2009).

In nature, DNA transposons are primitive genetic elements that have the ability to move within, and shape, the host genome (McClintock, 1950). On the other hand, transposons are regulated by host defensive mechanisms and self-inhibitory systems to reduce harm to the host genome (Biémont, 2009). Transposable elements present in the eukaryotic chromosomes are designated as class I (RNA-based) transposons when they encode for an intermediate mRNA transcript, followed by a “copy and paste” mechanism to move around. Whilst they are defined as class II (DNA-based) transposons when they jump from one site to another one by a “cut and paste” mechanism that is catalyzed by a transposase protein. This enzyme is encoded by the element itself. Indeed, class II transposons consist of a single gene coding for the transposase, flanked by terminal inverted repeats (IRs) that contain specific binding sites for the protein. When the transposase recognizes and binds the IRs, DNA mobilization occurs by recombinase activity. These features made transposable elements attractive as gene delivery tools: the transposase gene can be separated from the IRs and replaced by any other DNA sequence of interest. For mobilization, the new gene has to be supplied together with the transposase that is provided either as a plasmid or mRNA (Yant et al., 2000). To be effective and safe as gene delivery tools, transposon systems should show high transposition activity in the host cells and should be phylogenetically distant from the targeted host genome (Skipper et al., 2013). Indeed, endogenous copies of transposon should be absent in the target genome, in order to avoid remobilization of resident copies (Mátés et al., 2007).

1.3.1. Transposons as gene therapy tools

Numerous studies have enhanced the capacity of the transposons to efficiently transfer and stably express the gene of interest in mammalian cells, in order to obtain promising tools for human gene therapy (Meir and Wu, 2011). The most effective systems in mammalian cells to date are the salmonid transposon *Sleeping Beauty (SB)* and the insect-derived natural element *piggyBac (PB)*, thus representing the most promising transposons for gene therapy.

1.3.1.1. *Sleeping Beauty*

The salmonid transposon *Sleeping Beauty* is a member of the ancient Tc1/mariner-like elements that are prevalent in many fish genomes but not functional, due to accumulation of inactivating mutations (Plasterk et al., 1999). Based on phylogenetic studies, the salmonid transposase was “re-awakened” from its evolutionary dormancy through a series of mutagenesis steps, from which the name *Sleeping Beauty (SB)* (Ivics et al., 1997). In its natural configuration, the *SB* transposon is 1.6 Kb long and consists of a single gene coding for a transposase protein, flanked by two 230 bp terminal IRs. Each IR contains two 32 bp not identical direct repeats (DRs) that are the binding sites for the *SB* transposase (Cui et al., 2002). This protein is 360 amino acid-long and is composed of a N-terminal DNA-binding domain, a nuclear localization signal (NLS) and a C-terminal catalytic domain (Ivics et al., 1996). The NLS is located between the two domains and is important for nuclear import of the protein. Binding of a single transposase through the DNA-binding domain to each DRs into the terminal IRs results in the generation of a synaptic complex, in which the two ends of the transposon are held together by a tetramer of transposases (Izsvák et al., 2002). The transposon is excised from the donor locus by the catalytic domain and re-inserted into the TA-dinucleotide of the target sequences (Ivics et al., 1997). The aspartate-aspartate-glutamate (DDE) motif is an important conserved amino acid triad in the catalytic domain of the *SB* transposase, as well as in other recombinases (Plasterk et al., 1999). Deletions

in the DDE motif abrogate the catalytic activity. Upon transposition, the DNA repair machine by host enzymes creates a characteristic footprint at the excision site and a duplication of TA-dinucleotide at the integration site (Yant et al., 2005; Vigdal et al., 2002). Interestingly, *SB* transposons exhibit a nearly random integration profile with no preferential integration into active genes (~35% into RefSeqGenes; (Mátés et al., 2009; Yant et al., 2005; Huang et al., 2010)), thus representing a safer system for possible gene therapy applications compared to when integrating viral vectors are employed (Moldt et al., 2011; Hackett et al., 2007; Berry et al., 2006).

Transposition of *SB* is inhibited by elevated levels of transposase, a phenomenon called overproduction inhibition and indicating self-regulatory mechanisms developed during the evolution (Lohe and Hartl, 1996). Therefore in the engineered systems for gene delivery, the ratio of transposase DNA: transposon DNA would require optimization (Geurts et al., 2003). Moreover, *SB* transposase interacts with cellular cofactors such as HMGB1 and Miz-1, which might influence the overall transposition efficiency supporting the possible effect of a cell type on the *SB* transposition (Walisko et al., 2006; Zayed et al., 2003), The high activity of *SB* transposon system in mammalian cells has been exploited for non-viral vector gene therapy studies (Hackett et al., 2010; Izsvák et al., 2010; Ivics and Izsvák, 2006; Yant et al., 2004). The *SB* transposase and the *SB* transposon encoding the gene of interest have been used as gene delivery tools both *in vivo* in preclinical animal models (Hackett et al., 2011), as well as *ex vivo* in clinically relevant cells (Swierczek et al., 2012; Ivics and Izsvák, 2011). Initial studies showed a low efficiency in stable gene transposition, therefore the *SB* transposase has been engineered to produce hyperactive versions (Mátés et al., 2009; Baus et al., 2005; Yant et al., 2004). To date, the most hyperactive engineered *SB* transposase, called *SB100X*, has been first characterized by our team in collaboration with Izsvák's group (Mátés et al., 2009). *SB100X* transposase showed a robust 100-fold increase in transposition in human cell lines when compared to the first generation transposase *SB*. The superior gene transfer efficiency of *SB100X* transposase has been demonstrated in human

hematopoietic stem cells (Mátés et al., 2009; Xue et al., 2009), mesenchymal stem cells and muscle stem/progenitor cells (Filareto et al., 2015; Marg et al., 2014; Belay et al., 2010), T cells (Jin et al., 2011) and for reprogramming and targeted gene insertion in iPSCs (Filareto et al., 2013; Grabundzija et al., 2013; Belay et al., 2010). Moreover, the hyperactive *SB100X* transposase was exploited to obtain highly efficient germline transgenesis (Ivics et al., 2014a, 2014b, 2014c) and for *in vivo* transposition of therapeutically relevant genes (Hausl et al., 2010; Mátés et al., 2009). However, one of the limits of *SB* transposon system is the loss of transposition efficiency with large size inserts (> 5.6 Kb, (Karsi et al., 2001)). Therefore a "sandwich" *SB* transposon was generated, in which the DNA to be mobilized is flanked by two complete terminal IRs arranged in an inverted orientation. The sandwich *SB* transposon has superior ability to transfer >10 Kb transgenes, thereby extending the cloning capacity of the system (Turchiano et al., 2014; Zayed et al., 2004).

Remarkably, a first-in-human clinical trial has been recently approved utilizing the *SB* transposon system to treat patients with CD19⁺ B-lymphoid malignancies (Trial ID: US-0922; (Kebriaei et al., 2012; Williams, 2008)). Autologous T cells have been modified with *SB* vectors carrying chimeric antigen receptor (CAR) to make the T cells cytotoxic specifically toward CD19⁺ malignant cells and induce cancer regression. Although *SB* transposon system exhibits a nearly random integration pattern not associated with genotoxicity in T cells (Huang et al., 2010), however further studies to improve the transposition efficiency with minimal side effects need to be performed (Hackett et al., 2013; Meir and Wu, 2011).

1.3.1.2. *piggyBac*

PiggyBac (*PB*) transposon system is another efficient transposable element for gene transfer in mammalian cells. It was first discovered by mutational insertions within the Baculovirus genome present in the insect cell line TN-368, from the cabbage looper moth *Trichoplusia ni* of the order Lepidoptera (Fraser et al., 1985, 1983). In its natural configuration, the *PB* element is 2.4 Kb long and

consists of a single gene coding for a transposase protein flanked by two 13-bp terminal IRs and additional asymmetric 19-bp internal IRs (Fraser et al., 1995; Cary et al., 1989). The *PB* transposase enzyme is a 594 amino acid-long DNA-binding protein with a nuclear localization signal in the C-terminal region, necessary for its efficient translocation to the nucleus. The N-terminal sequence contains a highly conserved DDE/DDD catalytic domain with recombinase properties and necessary for DNA editing (Keith et al., 2008; Mitra et al., 2008). Catalytically inactive mutant transposases have been recently generated by introducing mutations in the DDD sequence (Burnight et al., 2012).

The *PB* transposase catalyzes transposition through a cut and paste mechanism. Differently from *SB* transposition, *PB* insertions into the target genome occur preferentially at TTAA nucleotide sequences without any deletion or duplication, thus bypassing DNA synthesis (Figure 5; (Mitra et al., 2008; Fraser et al., 1996, 1995; Cary et al., 1989)). Moreover, the genomic integration profile exhibits a slight tendency of *PB* to integrate in genes and their regulatory regions (~50% into RefSeqGenes) (Burnight et al., 2012; Doherty et al., 2012; Meir et al., 2011; Grabundzija et al., 2010; Huang et al., 2010; Galvan et al., 2009; Wilson et al., 2007). Nevertheless, most of the intergenic insertions (~90%) take place in intronic regions, followed by 3'UTRs, 5'UTRs and a minimal percentage in exonic regions (3%) (Meir et al., 2013; Ding et al., 2005). Interestingly, the nonrandom integration profile of *PB* in clinically relevant cells such as primary human T cells is not associated with genotoxicity and results to be safer compared to γ -retroviral and lentiviral vectors (Galvan et al., 2009). On the contrary, a recent study has shown a random integration pattern of *PB* in the genome of mesoangioblasts, another clinical relevant cell type (Ley et al., 2014). In order to direct the integration into specific "safe harbor" loci that virtually carry no risk of insertional mutagenesis (i.e. chemokine C-C motif receptor 5, CCR5), a heterologous DNA sequence-specific DNA-binding domain (DBD) was fused with the transposase enzyme (Voigt et al., 2008). In contrast to the *SB* transposase whose activity was compromised upon N-terminal or C-terminal fusions, *PB* transposase function was minimally perturbed when fused with different protein

domains. This enabled site-specific integration into the genome of human cells (Meir et al., 2013; Owens et al., 2013; Doherty et al., 2012; Owens et al., 2012; Kettlun et al., 2011; Wilson and George, 2010; Cadiñanos and Bradley, 2007). However, further studies are needed to improve the efficiency and specificity of this approach, as well as the exclusion of possible off-target effects.

The *PB* transposon system has been shown to enable efficient transposition in mice and in human cells (Wilson et al., 2007; Ding et al., 2005), thus emerging as an attractive vehicle for non-viral gene therapy studies. In contrast to the *SB* transposon system, *PB* transposition is not dependent on interaction with cellular co-factors and is not limited by overproduction inhibition (Wilson et al., 2007). In order to increase expression levels and enhance transposition activity, a new transposase designed as *mPB* has been generated for mammalian expression by a codon usage optimization of the original insect *PB* (*iPB*) transposase gene (Cadiñanos and Bradley, 2007). In addition, a hyperactive *PB* transposase named *hyPB* has been recently developed by introducing seven individual amino acid substitutions in the sequence of the *mPB* transposase (Yusa et al., 2011). The *hyPB* transposase has shown a protein level three times higher than *mPB* transposase, 17-fold increase in excision activity and 9-fold enhanced integration activity in mouse ESCs without significantly affecting the genomic integrity. The superior transposition activity of *hyPB* has been demonstrated also in human cells and *in vivo* in mice, in a head-to-head comparison with *SB100X* transposase (Doherty et al., 2012). Another strategy used to improve transposition consisted of modifying the *PB* transposon terminal IRs (Li et al., 2005b, 2001). *PB* transposons carrying mutant terminal IRs named enhanced piggyBac (*ePB*) led to a 90% increase in transposition efficiency in human ESCs compared to when the original IRs sequences were deployed (Lacoste et al., 2009). In addition, the *ePB* transposon system was able to boost the original *PB* cargo capacity of maximum 14.3 Kb insert size, allowing the delivery of inserts up to 18 Kb in size. However, transposition efficiency decreased significantly for inserts larger than 12 Kb. Alternatively, *PB* transposons lacking all the non-essential sequences in the terminal IRs, and therefore reduced in size, have

been shown to result in a a 1.5-fold increase in transposition activity when compared to the original version (Meir et al., 2011). Interestingly, when the terminal IRs sequences of the *PB* transposon were cloned into the bacterial artificial chromosome (BAC), the mobilization of a 100 Kb fragment was achieved in mouse ESCs (Li et al., 2011). This accomplishment made *PB* transposon system particularly attractive for the delivery of large therapeutic genes or multiple genes together, thus circumventing the size restrictions of viral vectors and other transposons.

The potential of *PB* transposon system as a gene therapy tool has been exploited in studies with preclinical animal models (Di Matteo et al., 2014a; Matsui et al., 2014) and clinically relevant cell types such as mesoangioblasts (Ley et al., 2014), mesenchymal stem cells (Wen et al., 2014), human hematopoietic stem cells (Grabundzija et al., 2010) and human primary T cells (Galvan et al., 2009; Nakazawa et al., 2009). The *iPB* transposon system has been used as an efficient alternative to *SB* to modify primary T cells for different purposes: to generate CD19-specific CAR T cells for the treatment of B-lineage malignancies (Saito et al., 2014; Manuri et al., 2010), to modify Epstein Barr virus-specific cytotoxic T lymphocytes (EBV-CTLs) and target HER2-positive cancer cells (Nakazawa et al., 2011), to render T cells resistant to rapamycin and direct them against B lymphomas (Huye et al., 2011). For future applications in cancer immunotherapy, the *hyPB* transposon system is a promising candidate. Although *iPB* has shown a similar efficiency in transposition when compared to *SB100X* (Huang et al., 2010), the latest *hyPB* is 2 to 3-fold more efficient than either the *iPB* or *SB100X* as a gene delivery system in primary T cells (Doherty et al., 2012).

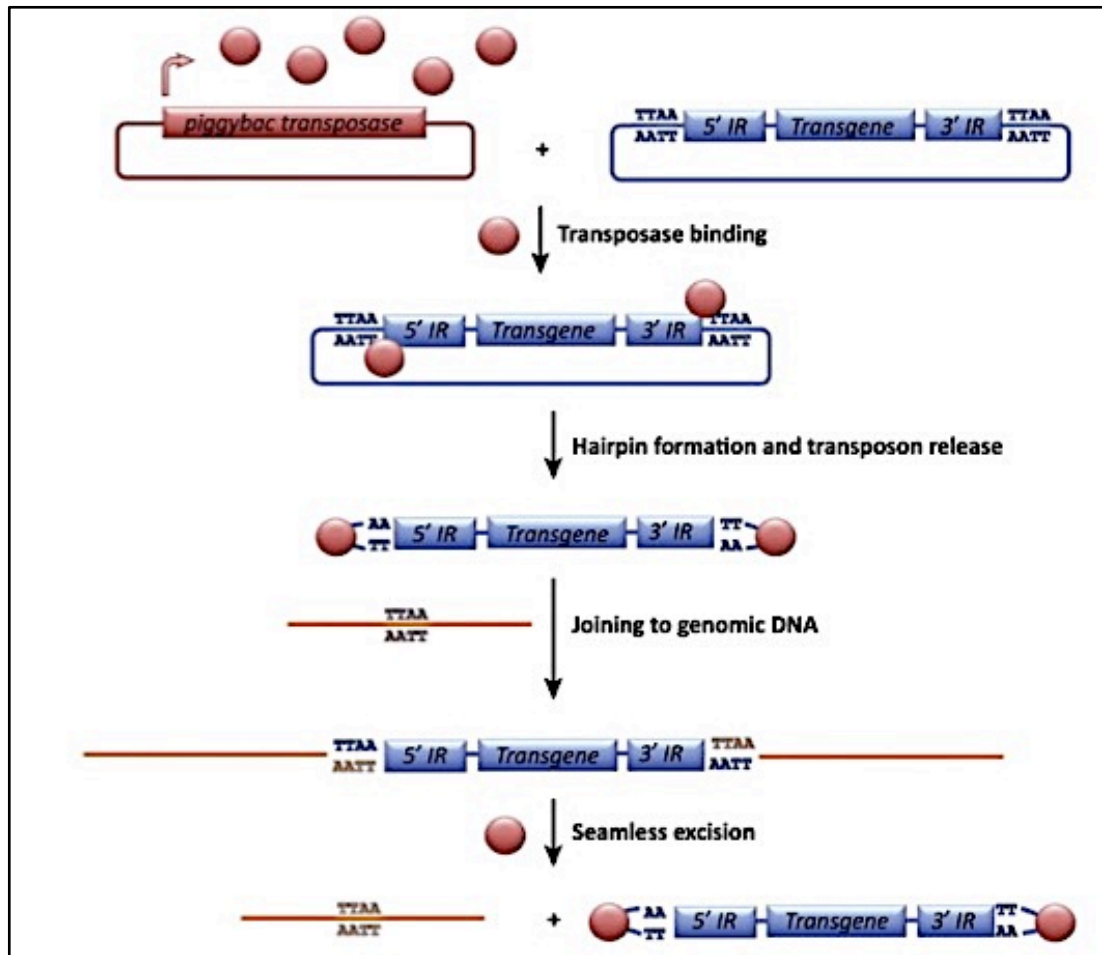


Figure 5. Mechanism of PB transposition. Once transposase is expressed (red circles), it binds to the piggyBac IRs and induces a hairpin formation. Transposon is excised and joined into the target genome at a TTAAs nucleotide sequence, resulting in TTAAs target site duplication at the genomic locus. If precise excision is desired, transposase can be re-expressed and the transposon can be excised, thereby recreating the original TTAAs target site at the original locus. Adapted from (Woodard and Wilson, 2015).

1.3.1.3. Transposon delivery into target cells

Unlike viral vectors that have developed efficient mechanisms to transfer their genetic material directly into the nucleus of the target cells, the transposon system requires efficient methods to permeate the cellular membranes. Consequently, gene delivery methods commonly used for non-viral vectors or alternatively viral/non-viral hybrid technologies have been exploited for the

transposon-based gene delivery. Hybrid technologies take advantage of the ability of the viral vector to transduce cells. In particular, IDLV (Cai et al., 2014; Moldt et al., 2011; Staunstrup et al., 2009; Vink et al., 2009), retroviral (Galla et al., 2011), herpes simplex (de Silva et al., 2010; Bowers et al., 2006) and adenoviral vectors (Hausl et al., 2010; Yant et al., 2002) have been used to transfer the transposon system into the target cells either *in vitro* or *in vivo*. Nevertheless, these hybrid technologies are characterized by some of the intrinsic disadvantages of viral vectors, outlined above, such as manufacturing hurdles and possible immune reactions.

Non-viral vector delivery methods are simpler and potentially safer than viral vectors, although achieving high transfection efficiencies, prolonged gene expression and low toxicity is challenging. Transposase and transposon plasmids can be delivered through physical methods such as electroporation (Hollis et al., 2006), hydrodynamic injection (Yant et al., 2000), sonoporation (Chen et al., 2012) or chemical carriers such as nanoparticles (Kren et al., 2009) and polycation-based DNA complexes (i.e. lipofectamine and polyethylenamine, (Li et al., 2011; Podetz-Pedersen et al., 2010)).

Electroporation is a delivery technology that consists in exposing cells to high-voltage pulses of electricity that creates transient pores in the cell membrane, promoting DNA transfer. Although some cells die in the process, this approach is applicable to almost all types of cells. Nucleofection technology is an electroporation-based method effective even in “hard-to-transfect” primary and pluripotent stem cells. It combines electrical parameters and cell type-specific buffer solutions to directly deliver the DNA into the cell nucleus. In contrast to other non-viral vector delivery methods that rely on cell division for the DNA transfer into the nucleus, the transfection of the target cells by nucleofection occurs independent from the cell cycle status. Nevertheless, nucleofection technology also adversely affects cell viability. Therefore optimization of the transfection reactions is necessary for each cell type and is generally achieved by varying the ratio of the two plasmids transposase DNA: transposon DNA (Izsvák et al., 2009).

The host lab and other groups established proof-of-concept that nucleofection of transposons is effective in hard-to-transfect primary cells. In particular, delivery of the transposon system by nucleofection in clinically relevant cells yielded a stable expression of the genes of interest corresponding to 35-50% in human hematopoietic stem/progenitor cells (Mátés et al., 2009), 40-50% in T cells (Manuri et al., 2010; Nakazawa et al., 2009), 30-40% in mesenchymal stem/progenitor cells and muscle stem/progenitor cells (Belay et al., 2010) and 25% in pluripotent stem cells (Belay et al., 2010). Therefore, nucleofection represents a promising technology for transposon-mediated delivery of large therapeutic genes.

1.3.2. Transposons for muscle disorders

Recent studies have explored the use of *SB* and *PB* transposon systems to develop therapeutic strategies for muscular dystrophies. Muscle stem/progenitor cells (satellite cells/myoblasts) are relevant targets for muscle regeneration and for gene therapy in muscle disorders. The host lab was the first to demonstrate that primary human myoblasts can be manipulated *in vitro* with the *SB* transposon system without affecting their myogenic potential (Belay et al., 2010). In order to overcome the limited proliferation capacity of these primary cells, conditionally immortal myoblast cell lines were generated (Escobar et al., 2016; Muses et al., 2011a). *SB* transposons have been shown to efficiently integrate into immortalized myoblasts and stably express the green fluorescent protein (GFP) reporter transgene (Muses et al., 2011a) as well as therapeutic genes such as microdystrophin (size: 3.6 Kb; (Muses et al., 2011b)) and full-length dysferlin (DYSF; size: 6.2 Kb; (Escobar et al., 2016)). Genetically corrected immortal myoblast cell lines retained their myogenic potential *in vitro* and *in vivo*. Although these immortalized myoblasts represent a reliable model to investigate stem cell based therapies for muscle disease, they cannot be deployed clinically. Consequently, different studies have focused on the development of tools for the enrichment and the expansion of satellite cells in culture, while maintaining their stem cell regenerative properties (Filareto et al., 2015; Marg et al., 2014). In

these studies, *SB*-mediated gene transfer was applied successfully to cultured satellite cells allowing a stable expression of the GFP reporter or the microdystrophin transgene (size: 3.6 Kb) upon cell transplantation, and contribution to muscle regeneration *in vivo*. As an alternative, other cell types with myogenic potential and clinically relevant for the treatment of muscle disorders such as mesoangioblasts (Cossu et al., 2015) have been investigated for a possible application of *PB* transposon vectors (Ley et al., 2014). In this study, it has been shown that the *PB* enables sustained expression of the GFP reporter gene in cultured mesoangioblasts and upon their differentiation into muscle fibers following transplantation. Moreover, the *PB* integration profile resulted to be nearly random (73 % of the recovered integration events were found in intergenic regions) and therefore relatively safe, supporting the use of *PB* transposon system in stem cell-based gene therapy studies for muscle disorders.

However, the regenerative potential of these genetically modified adult stem/progenitor cells is not unlimited and exhaustion/dysfunction of muscle stem/progenitor cells has been reported in several muscular dystrophies and/or after expansion *in vitro*. Different protocols have been developed to obtain an efficient directed differentiation of the pluripotent stem cells into myogenic cells (see above, Table 2 and Table 3; reviewed in (Loperfido et al., 2015a)). Transposon technology has been used to genetically modify ESCs and iPSCs. In the work of (Belay et al., 2010), the host lab has showed that *SB*-mediated Pax3 gene transfer in murine iPSCs coaxed their differentiation into multinucleated MyoD⁺MyHC⁺ myotubes. Alternatively, a *PB*-mediated MyoD inducible system was used for myogenic differentiation of human iPSC from patients with Miyoshi myopathy (MM), an inherited muscular dystrophy caused by DYSF mutations, and for carnitine palmitoyltransferase II deficiency, an inherited myopathy caused by mutations in CPT2 (Yasuno et al., 2014; Tanaka et al., 2013). The resulting human MyoD-iPSCs were able to undergo direct myogenic differentiation without a mesodermal transition step (10 days).

Nevertheless, the *in vivo* regenerative potential of the myogenic cells derived using this method remains to be determined.

In the work of Filareto *et al.* the dystrophic phenotype of dystrophin/utrophin null mouse iPSCs was corrected by expressing micro-utrophin (μ UTRN; size: 3.5 Kb) with the *SB* transposon system (Filareto *et al.*, 2013). Upon myogenic differentiation, the genetically corrected cells were transplanted in dystrophin/utrophin null mice and contributed to muscle regeneration and improvement in contractility. This study does not represent dystrophin/DMD gene correction *sensu stricto*, as the defective dystrophin is replaced by utrophin, which may not replicate all of the essential functions of dystrophin. Importantly, this strategy is so far limited to mouse iPSCs and data supporting its validity using DMD iPSCs will be necessary in order to consider potential clinical translation (Loperfido *et al.*, 2015a). Using the *PB* transposon system expressing the full-length DYSF transgene, correction of human iPSCs derived from patients affected by MM was achieved (Tanaka *et al.*, 2013). In particular, restoration of expression of the missing protein has been detected *in vitro* on the membrane of genetically corrected MM human iPSC-derived myotubes. Moreover the expression of full-length DYSF by the therapeutic transgene rescued the MM phenotype, as demonstrated by an improvement in the defective membrane repair phenotype of MM myotubes during *in vitro* functional tests such as two-photon laser-induced injury of the sarcolemma. Transplantation in MM animal models is expected to move this strategy forward. Though these previously mentioned studies demonstrated the validity of using transposons as a tool to genetically correct iPSCs derived from patients with muscular dystrophies, it has not yet been shown that they can be used for the delivery of the full-length dystrophin transgene into patient iPSCs or their myogenic progeny or into mesoangioblasts *sensu stricto*.

Chapter 2

2. Objectives of the Research

2.1. General objective

Gene therapy for DMD is particularly challenging given the large size of the dystrophin gene (2.4 Mb) and its corresponding coding DNA sequence (*CDS*, 11.1 Kb). Consequently, the dystrophin *CDS* cannot readily be accommodated into most of the commonly used viral vectors. This is compounded by the immune challenges associated with the use of viral vectors as opposed to when non-viral gene delivery systems are used. To overcome these limitations, a non-viral vector based *ex vivo* gene therapy strategy will be developed based on the stable genetic modification of dystrophic myogenic stem/progenitor cells with transposons encoding the full-length dystrophin *CDS*.

The **main objective** of my PhD thesis was to address this unmet need and to develop and validate a novel stem cell-based non-viral vector gene therapy approach for DMD using the latest-generation *piggyBac* (*PB*) transposons encoding the full-length human dystrophin *CDS*. The main advantage of using *PB* transposons as gene delivery tools over the commonly used vector systems is attributed to their large cargo capability, a low immunogenic profile, easy manufacturing and the ability to achieve long-term transgene expression upon their stable integration in the target genome. In order to accomplish this, we genetically modified distinct myogenic stem/progenitor cells including vessel-associated pericyte-like mesoangioblasts (MABs) and human iPSC-derived mesoangioblasts (HIDEMs). The peculiarity of these types of cells is based on their ability to extravasate from the circulation and differentiate into functional differentiated muscle fibers. We therefore wish to address the following specific hypotheses.

2.2. Specific aims

- 1) *Does the latest-generation hyperactive PB platform result in stable reporter gene expression in normal murine myoblast cells (i.e. C2C12), dystrophic MABs isolated from the skeletal muscle of a large animal model of DMD (i.e. Golden Retriever muscular dystrophy dog, GRMD) and DMD patient-specific HIDEs?*

- 2) *Can sustained expression of truncated or full-length human dystrophin be achieved in vitro after stable transposition in dystrophic GRMD MABs or DMD patient-specific HIDEs after induction of myogenic differentiation?*

- 3) *Can we detect dystrophin expression in vivo after transplantation of DMD patient-specific HIDEs engineered with the PB transposon encoding the full-length human dystrophin in dystrophic immunodeficient scid/mdx mice?*

If successful, this would establish the first proof of concept study of a gene therapy approach for DMD based on *PB* transposon-mediated expression of a functional full-length dystrophin, paving the way towards the development of new protocols for autologous cell therapy.

Chapter 3

3. Methodology and Materials

3.1. Cells and culture conditions

Biopsies from Golden Retriever muscular dystrophy (GRMD) dogs were kindly provided by Dr. Richard and Dr. Hubert-Martrou from Le Centre de Boisbonne-ONIRIS (Nantes-Atlantique, France). This colony of GRMD dogs presents a A->G mutation in the acceptor splice site of intron 6 of the dystrophin gene that causes the skipping of exon 7 and a premature termination of translation.

Canine mesoangioblasts (MABs) were isolated from the limb muscles of the GRMD dogs and maintained in culture, as described previously (Sampaolesi et al., 2006; Tonlorenzi et al., 2007). Briefly, a biopsy from the *Vastus lateralis* muscle of a 10-month-old male dog was minced in 1mm² pieces. These fragments were transferred onto collagen type I-coated dishes (C8919, Sigma-Aldrich) and incubated in growth medium composed of MegaCell DMEM (Dulbecco's modified Eagle's medium, M3942, Sigma-Aldrich) containing 5% fetal bovine serum (FBS, 10270-106, Gibco), 0.1 mM β -mercaptoethanol (31350-010, Gibco), 1% MEM non-essential amino acids (Gibco), 1% penicillin/streptomycin (P/S, 15140122, Gibco), 1% L-glutamine (25030024, Gibco), 5 ng/ml recombinant human fibroblast growth factor-basic (FGF-b, PHG0261, Gibco) at 37 °C in a 5% CO₂, 3% O₂ cell culture incubator. After 5 to 7 days, small, round, refractile cells that adhered weakly to the initial cell outgrowth were identified. This cell population was collected and maintained in growth medium on collagen-coated flasks. In order to confirm that the identified population was composed of *bona fide* MABs, cells were characterized for the typical markers of adult dog MABs, after five and ten passages. The alkaline phosphatase (AP) expression was detected by enzymatic activity using the NBT/BCIP kit (11697471001, Roche). The staining was performed on fixed cells in order to allow the formation of a black/purple precipitate in the cells expressing the enzyme. Moreover, their capacity to differentiate into mesodermal lineages was

analyzed by assessing their intrinsic differentiation potential into multinucleated skeletal myotubes or, under appropriated stimuli, into smooth muscle cells (See the specific section “*In vitro* differentiation assays”).

Human skeletal muscle cells (SKM, C-12530, Promocell) were used as positive control and cultured in the same condition of GRMD MABs.

Human iPSC-derived mesoangioblast-like cells (HIDEMs) utilized in this study were kindly provided by our collaborator in this study Dr. Tedesco from the University College of London (London, United Kingdom). HIDEMs were generated from DMD patients and healthy donors (HD) induced pluripotent stem cells (Kazuki et al., 2010; Tedesco et al., 2012) and maintained in culture as previously described (Tedesco et al., 2012; Gerli et al., 2014; Maffioletti et al., 2015). The DMD patient-derived HIDEMs presented a deletion of exons 4–43 in the dystrophin gene, thus representing a valid candidate for the *PB*-mediated transfer of the full-length human dystrophin *CDS*. Using the same protocol, we also independently confirmed the generation of HIDEMs from another DMD patient-specific iPSC line that we generated in-house.

C2C12 myoblasts ((91031101, Sigma-Aldrich, (Yaffe and Saxel, 1977)) were cultured, as previously described (Tonlorenzi et al., 2007), in D20 medium composed of high glucose DMEM (41965062, Gibco) supplemented with 20% FBS, 1% P/S, 1% L-glutamine at 37 °C in a 5% CO₂ cell culture incubator.

HeLa cells, a human cervical cancer cell line (Scherer et al., 1953), were used as positive control for a tumor formation assay as described below. The cells were cultured in D10 medium composed of high glucose DMEM (41965062, Gibco) supplemented with 10% FBS, 1% P/S, 1% L-glutamine at 37 °C in a 5% CO₂ cell culture incubator.

3.2. Generation of *PB* transposon constructs for DMD

The *piggyBac* (*PB*) transposase constructs encoding the non-hyperactive *PB* transposase (*mPB*) or the hyperactive *PB* transposase (*hyPB*) were described previously (Di Matteo et al., 2014a). An identical expression plasmid devoid of the *PB* transposase gene (denoted as empty) was used as control. The *PB*

transposon constructs were generated after synthesis of the wild type sequences of the *PB* terminal inverted repeats (*IRs*; Gene Synthesis, Canada) and cloning into the *pBluescript II SK (+)* plasmid upon digestion with *BssHII* restriction enzyme (Li et al., 2001, 2005b). To produce the transposons *PB-SPc-MD1* and *PB-SPc-MD2*, the muscle-specific synthetic promoter SPc5-12 (Li et al., 1999) was amplified with primers (forward: 5'-ATAGCTAGCCAGATCGAGCTCCACCGCGGT-3'; reverse: 5'-ATAACGCGTGAATTCCTGCAGCCCGGGG-3') adding flanking *NheI* and *MluI* restriction sites, and ligated between the 5' and 3' *IRs*. This intermediate plasmid, designated as *PB-SPc5-12*, was used to insert the codon-usage optimized coding DNA sequence (*CDS*) of human microdystrophin *MD1* or *MD2* (Koo et al., 2011b; Athanasopoulos et al., 2011), together with the simian virus 40 (SV40) late polyadenylation (pA) signal, after amplification with primers (forward: 5'-ATAACGCGTGCCACCATGCTGTGGTGGGAG-3'; reverse: 5'-ATACTCGAGGTTTATTGCAGCTTATAATGGTTACAAATAAAGCAATAGCATCA-3') and digestion with *MluI* and *XhoI* restriction enzymes. To generate the transposon *PB-SPc-GFP*, the SV40 pA sequence was amplified with primers (forward: 5'-ATAACGCGTCAGACATGATAAGATACATTGATG-3'; reverse: 5'-ATACTCGAGGTTTATTGCAGCTTATAATGGTT-3') adding flanking *MluI* and *XhoI* restriction sites, and ligated into the intermediate plasmid *PB-SPc5-12*. Then the transgene copepod green fluorescence protein (GFP, Lonza) was PCR-amplified (forward: 5'-ATAACTAGTAGCGCTACCGGTCGCCACC-3'; reverse: 5'-ATAACGCGTAGATCTGGCGAAGGCGATGGG-3') flanked by *SpeI* and *MluI* restriction sites and cloned between the SPc5-12 promoter and the SV40 pA signal. To produce the transposon *PB-Pgk-GFP*, the PCR primers (forward: 5'-GTACGGCTAGCGTTAACAATTCTACCGGGTAGG-3', reverse: 5'-GACGTAGCGCTATGCAGGTCGAAAGGC-3') containing *NheI* and *Eco47III* restriction sites were used to amplify the constitutive phosphoglycerate kinase 1 (*Pgk*, Addgene) promoter and cloned it into the correspondent sites of *PB-SPc5-12*, in order to replace SPc5-12 promoter. For the construction of the large size transposon *PB-SPc-DYS-Pgk-GFP*, the following fragment SPc5-12 promoter-

KpnI-NheI-SgsI-SV40 pA signal has been synthesized (DNA cloning, Germany) adding flanking restriction sites *NotI* and *XhoI*, and inserted between the 5' and 3' *PB IRs* of the *pBluescript II SK (+)* plasmid. This allowed the ligation of the codon usage optimized full-length human dystrophin *CDS* (Jarmin et al, unpublished) upon digestion first with *KpnI* and *NheI*, and then with *NheI* and *SgsI* restriction enzymes. The GFP reporter gene was then inserted together with the *Pgk* promoter and the SV40 pA signal downstream the full-length human dystrophin expression cassette using *HpaI* and *XhoI* restriction sites. The entire expression cassette of all the *PB* transposons was flanked with *loxP* sites allowing for a possible subsequent excision by CRE recombinase (Di Matteo et al., 2012; VandenDriessche et al., 2009). The sequences of the constructs involving PCR-based cloning were confirmed by DNA sequencing.

3.3. Cell electroporation

Cells were electroporated with the Amaxa Nucleofector II (Lonza). For GRMD MABs and DMD HIDEMs, the Human MSC Nucleofector Kit was used with respectively the program U-23 and C-17. For C2C12 myoblasts, the Cell Line Nucleofector Kit V and the program B-32 were applied.

Transfections were optimized to obtain good efficiency with low levels of toxicity, modifying the amount of plasmids used and the transposase DNA: transposon DNA ratio. Briefly, cells were trypsinized (Trypsin-EDTA 1X, 25300-054, Gibco), washed in phosphate-buffered saline (PBS, 14190169, Gibco) and counted. One million cells were electroporated with the indicated concentration of transposase DNA: transposon DNA and subsequently seeded in a single well of a 6-well multidish (Nunc). The day after, the medium was refreshed. When the cells were transfected with *PB* transposons coding for the GFP, the expression of the reporter was monitored at different time point post-electroporation (post-EP) by live cell imaging using fluorescence microscopy (IX81,Olympus; DMI6000B, Leica).

3.4. Flow cytometry and FACS

Expression of CD44, CD34 and CD45 markers on GRMD MABs was assessed after the cells were trypsinized, washed in PBS and incubated with specific anti-dog fluorochrome-conjugated monoclonal antibodies for 1 hour at 4 °C: anti-CD44-APC (FAB5449A, R&D Systems), anti-CD34-PE (559369, BD Biosciences), anti-CD45-RPE (MCA1042PE, AbD Serotec). Cells were subsequently washed with PBS, fixed in 2% paraformaldehyde (PFA, Sigma-Aldrich) and resuspended in PBS supplemented with 1% FBS and 2mM EDTA (15575020, Invitrogen). Cytofluorimetric analysis was performed using a FACSCanto flow cytometer (Becton Dickinson).

When GRMD MABs, DMD HIDEMs and C2C12 were transfected with *PB* transposons coding for the GFP, the transfection efficiency was assessed by the detection of the percentage of GFP positive cells post-EP by flow cytometer (FACSCanto, Becton Dickinson; CyAn ADP, Beckman Coulter). Transfected cells were monitored at different time points for 30 to 45 days post-EP to assess transposition efficiency. Where indicated, the GFP positive populations were enriched by cell sorting using a BD FACSAria III cell sorter (Becton Dickinson). Briefly, cells were trypsinized, washed in PBS, counted and resuspended in PBS supplemented with 1% FBS and 2mM EDTA (15575020, Invitrogen). Analysis of the acquired data was performed with Summit (Beckman Coulter) or BD FACSDiva (Becton Dickinson).

3.5. *In vitro* differentiation assays

The ability of MABs, HIDEMs, SKM cells and C2C12 cells to differentiate into skeletal muscle was assessed *in vitro* by exposing the cells, upon reaching 80% of confluence, to a specific differentiation medium composed of DMEM supplemented with 2% horse serum (ECS0090L, Euroclone), 1% P/S, 1% L-glutamine for 4 to 10 days (Tonlorenzi et al., 2007). For this assay MABs, HIDEMs and SKM cells were seeded onto matrigel (356230, Becton Dickinson) coated dishes while C2C12 cells were induced to differentiate on a 6-well multidish (Nunc). To induce myogenic differentiation of MABs at late passages

(i.e. passage P15-18) and of HIDEs, cells were transduced with lentiviral vectors containing a tamoxifen-inducible MyoD-ER (MyoD-ER(T) LV vector) (Kimura et al., 2010; Tedesco et al., 2012; Maffioletti et al., 2015). Lentiviral vector titration was calculated using the p24 assay (QuickTiter Lentivirus Quantitation Kit, Cellbiolabs). Briefly, 0.14×10^6 cells were transduced with 10 or 50 multiplicities of infection (MOI) of MyoD-ER(T) LV vector in 1 ml of growth medium and incubated for 12 hours at 37 °C in a 5% CO₂, 3% O₂ cell culture incubator. The medium was subsequently changed and cells were maintained in culture for 2 to 3 passages. The *in vitro* myogenic differentiation assay was performed seeding the cells onto matrigel (BD Biosciences) coated dishes, followed by the exposure to 1 μ M 4-hydroxy-tamoxifen (Sigma-Aldrich) in the growth medium for 24 hours, upon confluence. This was replaced by differentiation medium supplemented with 1 μ M 4-hydroxy-tamoxifen for additional 24 hours. Half of the medium was replaced with fresh differentiation medium every other day for 5-7 days. Immunofluorescence (IF) staining for myosin heavy chain (MyHC) was performed to confirm terminal myogenic differentiation (see specific section for “Immunohistochemistry”).

Differentiation of GRMD MABs in smooth muscle-like cells was induced by treating the cells for 10 days with differentiation medium supplemented with 5 ng/ml transforming growth factor β 1 (TGF- β 1, 100-21, Peprotech) (Ross et al., 2006). Smooth muscle differentiation was confirmed by IF staining for α -smooth muscle actin (see specific section for “Immunohistochemistry”).

3.6. RNA expression analysis

Total RNA from cells was extracted (RNeasy Mini Kit, QIAGEN) and reverse transcribed using a cDNA synthesis kit (SuperScript I I I First-Strand synthesis system for RT-PCR kit, Invitrogen). For Reverse transcription-PCR (RT-PCR), cDNA was amplified on a PCR thermocycler (Biorad) with GoTaq DNA Polymerase (M3005, Promega). Amplifications were performed using the primers listed Table 4, at the annealing temperature of 60 °C for 29 cycles on

GRMD MABs, 25-28 cycles on DMD HIDEMs and 25 cycles on C2C12 cells. The amplified fragments were resolved by electrophoresis on a 2% agarose gel. For quantitative RT-PCR (qRT-PCR), cDNA was amplified on a Step-One Real-Time PCR System (Applied Biosystems) with SYBR green PCR Master mix (4309155, Applied Biosystem). The mRNA levels of the transgene of interest were determined by qRT-PCR using the primers described in Table 5. The semi-quantitative RT-PCR for the characterization of GRMD MABs was performed by using the primers listed in Table 6 at the annealing temperature of 60 °C for 33 cycles. Amplicons were then resolved by electrophoresis on a 2% agarose gel. Data were normalized to the Glyceraldehyde-3-phosphate dehydrogenase (GAPDH) housekeeping gene or to the MyHC gene specific for the skeletal muscle differentiation, as specified. The expression levels of the selected transgene was calculated using a standard $\Delta \Delta$ Ct method (Livak and Schmittgen, 2001).

Primer	Sequence	Amplicon size
<i>N-terminus</i>		221 bp
<i>huDys_co seq 1</i>	5'-GGGCCTGATCTGGAACATCATC-3'	
<i>huDys_SO f1 R2</i>	5'-CGAACAGGTCGGGTCTGTGGC-3'	
<i>Central domain</i>		222 bp
<i>huDys_SO f5 F</i>	5'-CTTCGAGGATCTGTTCAAGCAGG-3'	
<i>huDysSO.f5 R</i>	5'-CTGTCGAATCTGCCCTGCCGG-3'	
<i>C-terminus</i>		228 bp
<i>huDys_SO f5 F2</i>	5'-CCGAGTACGACAGACTGAAG-3'	
<i>huDys_SO f7 R2</i>	5'-CCAGCAGCTGTCTGAGTCTG-3'	

Table 4. List of primers utilized for RT-PCR. Listed in the table the RT-PCR primers used for this study with the corresponding expected size of the amplicons.

Primer	Sequence	Amplicon size
<i>huMD1co/ huMD2co</i>	5'-GTGCCCTACTACATCAA-3' 5'-AGGTTGTGCTGGTCCA-3'	174 bp
<i>huDYSco</i>	5'-GGGCGACAACATGGAGACCGA-3' 5'-AGGGCGTGCACTCTGGTGCT-3'	263 bp
<i>DYS</i>	5'-GCAAGAGCAACAAAGTGGCCTA-3' 5'-AGCTTCTTCCAGCGTCCCTCA-3'	128 bp
<i>GFP</i>	5'-GAGCACCAAAGGCGCCCTGA-3' 5'-CGGGTGTTGGTGTAGCCGCC-3'	143 bp
<i>MyHC</i>	5'-GCATCGAGCTCATCGAGAAG-3' 5'-CATACAGCTTGTTCCTTGAAGGAGG-3'	102 bp
<i>GAPDH</i>	5'-TCAAGAAGGTGGTGAAGCAGG-3' 5'-ACCAGGAAATGAGCTTGACAAA-3'	168 bp

Table 5. List of primers utilized for qRT-PCR. Listed in the table the qRT-PCR primers used for this study with the corresponding expected size of the amplicons.

Primer	Sequence	Amplicon size
<i>PAX7</i>	5'-CAGGCCGACTTCTCCATCTC-3' 5'-GAGTCCCAGCACAGCAGAAT-3'	288 bp
<i>MYF5</i>	5'-TCCGAGTACTTCTACGACGG-3' 5'-AGGCTCTCGATGTAGCGGAT-3'	368 bp
<i>CD56</i>	5'-TCTCTCCCACCGACCATCAT-3' 5'-GTTCCCCCTCCTTTGTCCAG-3'	328 bp
Desmin	5'-ATGAGCCAGGCCTACTCGTC-3' 5'-GCCCACCTTCTCGATGTAGT-3'	378 bp
<i>NG2</i>	5'-GTCCGACGGGCGGCACCAGG-3' 5'-CACAGGCCCTGCCTCCACGG-3'	340 bp
<i>PDGFRβ</i>	5'-GCCAGCTCCTGTCTCAAAG-3' 5'-GAGTTCCTCAGGGTCAACCG-3'	385 bp
<i>GAPDH</i>	5'-TCAAGAAGGTGGTGAAGCAGG-3' 5'-ACCAGGAAATGAGCTTGACAAA-3'	168 bp

Table 6. List of primers utilized for semi-quantitative RT-PCR. Listed in the table the primers for semi-quantitative RT-PCR utilized in this study for the characterization of the GRMD MABs.

3.7. Immunohistochemistry

Immunofluorescence (IF) assays were performed on cells fixed with 4% paraformaldehyde (Sigma-Aldrich) at room temperature (RT) for 10 minutes or directly on sections from processed tissues. After permeabilization in PBS containing 0.2% Triton X-100 (T9284, Sigma-Aldrich) and 1% bovine serum albumin (BSA, A8022, Sigma-Aldrich) at RT for 30 minutes, the non-specific binding sites were blocked using 10% donkey serum (D9663, Sigma-Aldrich) at RT for 30 minutes. Samples were subsequently incubated overnight at 4 °C with the following primary antibodies: rabbit anti-turboGFP (AB513; Evrogen), mouse anti-dystrophin (NCL-DYS1, NCL-DYS2, NCL-DYS3; Novocastra), mouse anti-myosin heavy chain (MyHC MF20; Developmental Studies Hybridoma Bank,

USA), rabbit anti-myosin (476126; Calbiochem), rabbit anti-human lamin A/C (ab108595, Abcam), rat anti-laminin (sc33709; Santa Cruz Biotechnology), mouse anti-myogenin (F5D; Developmental Studies Hybridoma Bank, USA), rabbit anti-MyoD (M-318; Santa Cruz), mouse anti-sarcomeric α -actinin (ab9465; Abcam), mouse anti- α -smooth muscle actin (A2547; Sigma-Aldrich). After incubation, samples were washed with PBS and incubated with the appropriate 488, 546, 594 or 647 fluorochrome-conjugated secondary antibodies (Life Technologies) together with Hoechst 33342 for nucleic acid staining (B2261; Sigma-Aldrich) for 1 hour at RT in PBS containing 0.2% Triton X-100. After washing with PBS, slides were mounted using fluorescent mounting medium (Dako) and examined by fluorescence microscopy (DMI6000B, Leica; Eclipse80i, Nikon). Images were analyzed using ImageJ software (NIH; <http://rsbweb.nih.gov/ij/download.html>).

3.8. Western blot analysis

The expression of the full-length human dystrophin protein mediated by the PB transposon was assessed by Western Blot analysis. Upon myogenic differentiation in vitro, cells were washed 2 times with cold PBS and lysed in RIPA buffer (50 mM Tris pH 8, 150 mM NaCl, 1% Triton X - 100, 0.5% sodium deoxycholate, and 0.1% sodium dodecyl sulfate (SDS)) supplemented with a protease inhibitor cocktail (11836145001, Roche) for 30 minutes on ice. Clear cell lysates were obtained by centrifugation at 13200 rpm for 15 minutes at 4 °C and total proteins were quantified by BCA protein assay kit (23227, ThermoFisher). Equal amounts of total proteins per sample were separated by SDS-PAGE on 3-8% Tris-Acetate Gel (EA0378BOX, Invitrogen). After electrophoresis, the gel was transferred to a 0,2 μ m nitrocellulose membrane using the Trans-Blot turbo transfer system (Bio-Rad). To prevent the nonspecific binding of the antibodies, the membrane was incubated in TBST buffer 5% milk for 1 hour. The membrane was then probed with the following non-conjugated primary antibodies and incubated overnight: mouse anti-dystrophin DYS1 and

DYS2 (NCL-DYS1 and NCL-DYS2, mouse anti-dystrophin, Novocastra), mouse anti-human dystrophin (NCL-DYS3, Novocastra) and mouse anti-myosin heavy chain (MyHC MF20, Developmental Studies Hybridoma Bank, USA). An HRP-conjugated goat anti-mouse (sc-2005, Santa Cruz) was used as secondary antibody. To detect a housekeeping protein, the HRP-conjugated anti-beta tubulin (ab21058, Abcam) was used. The acquisition of the signal was performed by Enhanced Chemiluminescent Reagents (ECL, Invitrogen) or West Femto (Thermo Scientific), according to the manufacturer's instructions. SKM cells differentiated into skeletal muscle *in vitro* were used as positive control.

3.9. Transposon genome copy number quantification

The number of copies of *PB* transposons integrated per cell (diploid genome) was calculated by performing a qPCR analysis on genomic DNA extracted from the cells (DNeasy Blood & Tissue Kit, Qiagen). Primers specific for the 5' inverted repeat region (5'IR) of the *PB* transposon were used, as previously described (Di Matteo et al., 2014a). The standard curve was determined by a known copy number of the corresponding *PB* transposon plasmid.

3.10. Mice

Immunodeficient dystrophic scid/mdx mice were kindly provided by Dr. Torrente from the University of Milan (Milan, Italy; (Farini et al., 2007)). Nude mice (CrI:NU-Foxn1^{nu} strain) were purchased from Charles Rivers. All the animals used for this study were housed in specific pathogen free (SPF) condition at the KU Leuven facility (Leuven, Belgium) or at UCL facility (London, United Kingdom). The experimental procedures were approved by the Institutional Animal Care and Research Advisory Committee of KU Leuven as well as by the UCL ethical committee, in accordance to the Home Office regulations (ASPA 1986). The use of animals has been rationalized by implementing the 3Rs (Reduction, Refinement, Replacement).

3.11. Intra-muscular transplantation

Adult age matched scid/mdx mice were used for the intra-muscular transplantation experiments (n= 6). As previously reported (Tedesco et al., 2012; Gerli et al., 2014; Maffioletti et al., 2015), mice were treated with 3.5 μ l/g of 10 mg/ml tamoxifen (liposoluble formulation, T5648, Sigma-Aldrich) via intra-peritoneal injection during the three days prior to- and post-transplantation, once a day. The cells were pre-treated with 1 μ M 4-hydroxy-tamoxifen (aqueous formulation, H7904, Sigma-Aldrich) in the growth medium overnight prior to the transplantation. The cells were then trypsinized, washed in PBS, filtered with a 40 μ m cell strainer to avoid possible clusters (352340, Corning), centrifuged at 232 x g for 5 min and resuspended in PBS at the concentration of 1×10^6 cells/30 μ l. Injection of 30 μ l of cell suspension was performed into the *tibialis anterior* and the *gastrocnemius* muscles with a 30G needle syringe. Muscles injected with 30 μ l of PBS were used as negative controls. Animals were sacrificed 1 and 3 weeks after the intra-muscular transplantation. Treated and control muscles were harvested, dehydrated in liquid nitrogen-cooled isopentane for one minute, snap-frozen in liquid nitrogen for two additional minutes and stored at -80 °C. The tissue samples were processed with the cryostat (CM1850, Leica) to obtain 7 μ m thick sections for immunofluorescence staining. Serial sections were also collected into a 1.5 ml tubes to perform molecular biology assays.

3.12. Tumor formation assay

To assess the safety of the cell lines used in this study for *in vivo* applications, a tumor formation assay was performed. DMD HIDEMs co-transfected with *hyPB* transposase and *PB-SPc-DYS-Pgk-GFP* transposon (n= 8) or *PB-Pgk-GFP* transposon (n= 8) and transduced with MyoD-ER(T) LV vector were injected subcutaneously in immunodeficient nude mice (CrI:NU-Foxn1^{nu} strain). As controls, untransfected DMD HIDEMs with and without MyoD-ER(T) LV vector infection (n= 3 and n= 2, respectively) were utilized. HeLa cells, a tumorigenic human cell line, were injected as a positive control (n= 2). Briefly, the cells were

trypsinized, washed in PBS, filtered with a 40 μ m cell strainer, centrifuged at 232 x g for 5 min and resuspended in PBS at the concentration of 2×10^6 cells/100 μ l. After the subcutaneous injection, the mice were then inspected biweekly for 4 months. At the end of the assay, animals were sacrificed and necropsy was operated to confirm the absence of tumor masses.

3.13. Statistical analysis

Data were presented as mean \pm standard deviation (SD) or standard error of the mean (SEM). Comparison between groups was performed by using two-tailed unpaired Student's t-test or two-way ANOVA (Bonferroni's multiple comparison test).

Chapter 4

4. Results

The data of the following section 4.1 are published in:

Loperfido M, Jarmin S, Dastidar S, Di Matteo M, Perini I, Moore M, Nair N, Samara-Kuko E, Athanasopoulos T, Tedesco FS, Dickson G[#], Sampaolesi M[#], VandenDriessche T[#], Chuah MK^{#,*}. *piggyBac transposons expressing full-length human dystrophin enable genetic correction of dystrophic mesoangioblasts*. Nucleic Acids Research 2016 Jan 29;44(2):744-60. doi: 10.1093/nar/gkv1464. Epub 2015 Dec 17.

[#] These authors share joint senior authorship; *Corresponding author.

4.1. Genetic correction of dystrophic mesoangioblasts using *piggyBac* transposons expressing full-length human dystrophin CDS

4.1.1. Generation of *PB* transposons coding for human dystrophin CDS

We generated *PB* transposons designed to express the full-length or truncated versions of a codon-optimized human dystrophin CDS (Athanasopoulos et al., 2011) from the muscle-specific synthetic promoter SPc5-12 (346 bp) (Li et al., 1999; Koo et al., 2011b; Rincon et al., 2014) (Figure 6). The simian virus 40 (SV40) late polyadenylation (pA) signal was incorporated as transcription terminator in all the expression cassettes. Given the large cargo that *PB* transposons could accommodate (Ding et al., 2005; Li et al., 2011), we generated a large-size transposon named *PB-SPc-DYS-Pgk-GFP* coding for the full-length human dystrophin CDS (*huDYSco*; size: 11.1 Kb) driven by the synthetic SPc5-12 promoter, and a GFP reporter transgene driven by the constitutive phosphoglycerate kinase 1 (*Pgk*) promoter (transposon size: 17 Kb) (Figure 6A). *PB-SPc-MD1* (Figure 6B) and *PB-SPc-MD2* (Figure 6C)

transposons encoded respectively for two different codon usage-optimized microdystrophin CDS: *huMD1co* (size: 3.6 Kb) and *huMD2co* (size: 4 Kb) whereby the C-terminal domain was deleted in *huMD1co* (Koo et al., 2011b) (transposon size: 8.2 Kb and 8.6 Kb, respectively). As controls, *PB-SPc-GFP* (Figure 6D) and *PB-Pgk-GFP* (Figure 6E) transposons carried only the copepod GFP sequence under the control of the SPc5-12 or the constitutive *Pgk* promoter (transposon size: 5.2 Kb and 5.4 Kb, respectively). The transposase plasmids included the *mPB* expression plasmid encoding the murine codon-optimized non-hyperactive *PB* transposase (Figure 6F; (Cadiñanos and Bradley, 2007)) and the *hyPB* expression plasmid encoding the murine codon-optimized hyperactive *PB* transposase (Figure 6G; (Yusa et al., 2011)). The transposases were driven by the cytomegalovirus (CMV) promoter cloned upstream of a β -globin intron (β GI) sequence, and were followed by a bovine growth hormone polyA (*bghpA*) signal. An empty plasmid that contained an identical expression cassette, but devoid of transposase (Figure 6H), was employed as control (Di Matteo et al., 2014a).

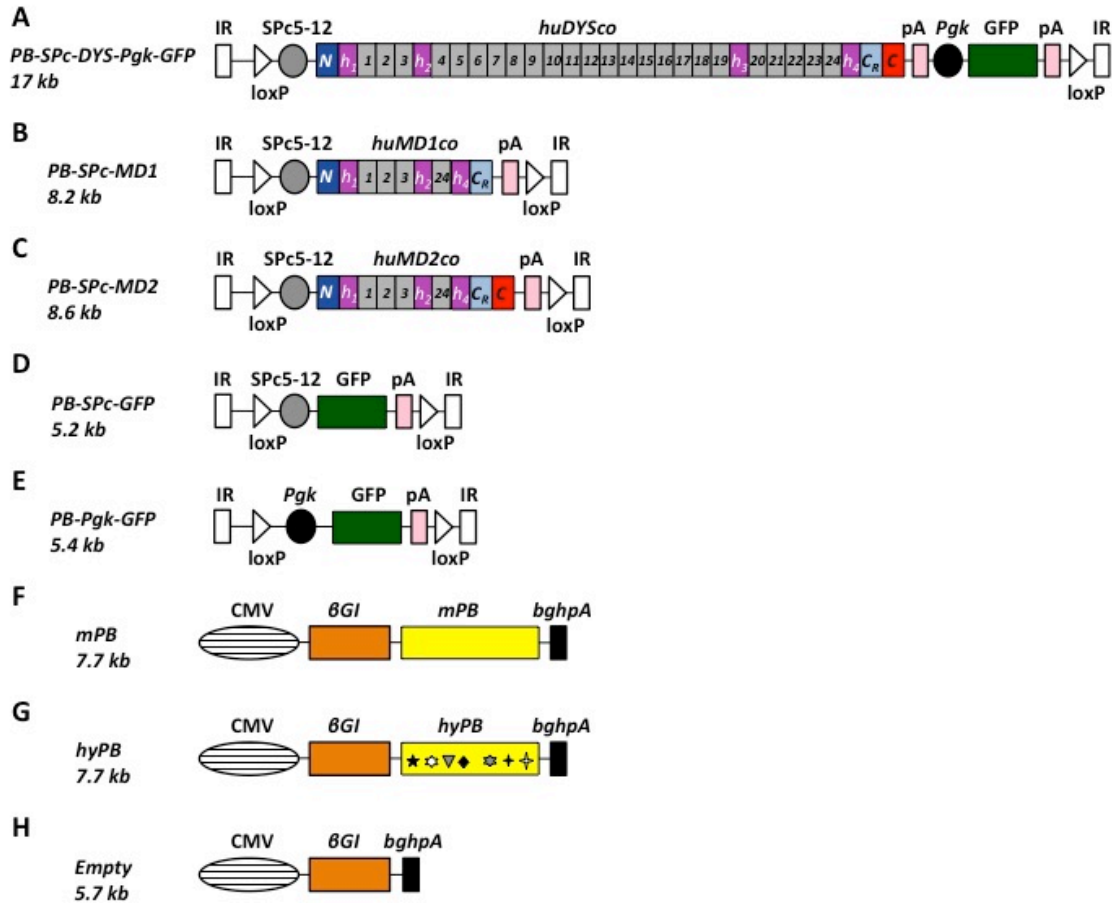


Figure 6. Schematic representation of PB transposon and PB transposase constructs. (A) PB-SPc-DYS-Pgk-GFP transposon encoding the codon optimized full-length human dystrophin CDS (*huDYSco*; (Athanasopoulos et al., 2011)) is represented as in its four major structural domains: N-terminal domain (N), a central rod domain, a cysteine-rich (CR) domain and a distal C-terminal domain (C). The central rod domain contains 24 triple-helix rod repeats and four hinges (H1–H4). The full-length human dystrophin CDS is driven by the muscle-specific synthetic promoter SPC5-12 (Li et al., 1999). Downstream, the sequence of a copepod GFP has been cloned as a reporter driven by the *Pgk* promoter. (B) PB-SPc-MD1 transposon and (C) PB-SPc-MD2 transposon encode respectively for *huMD1co* and *huMD2co* CDS; these are two different codon optimized human microdystrophins that lack the original sequence of rod repeats 4-23 and differ for the presence of the C-terminal domain sequence in MD2 (Athanasopoulos et al., 2011). This extra sequence has been shown to improve the efficiency on restoring muscle function in dystrophic mdx mice (Koo et al., 2011a). Both the microdystrophins are driven by SPC5-12 promoter. (D) PB-SPc-GFP and (E) PB-

Pgk-GFP are transposons that accommodate the GFP sequence respectively under the *SPc5-12* or the *Pgk* promoter. All the transposon constructs are flanked by wild-type inverted repeats (*IR*) and *loxP* sites (*loxP*). All the transgenes in the transposon constructs are followed by the simian virus 40 late polyadenylation signal (*pA*). **(F)** The *mPB* transposase and **(G)** the *hyPB* transposase are driven by the cytomegalovirus (*CMV*) promoter cloned upstream of a β -globin intron (β *GI*). The seven hyperactive mutations that differ the *hyPB* transposase sequence from the *mPB* are indicated as seven different symbols in the *hyPB* construct. A bovine growth hormone polyA (*bghpA*) signal is cloned downstream of the transposase sequences. **(H)** The empty control plasmid contains a multiple cloning site (*MCS*) between the *CMV* promoter and the *bghpA*.

4.1.2. Expression of human microdystrophins after *PB*-mediated transposition in C2C12 myoblasts

We first tested the functionality of the *PB-SPc-GFP*, *PB-SPc-MD1* and *PB-SPc-MD2* transposons since they are smaller in size and therefore easier to transfer into the target cells. C2C12 cells, a murine myoblast cell line (Yaffe and Saxel, 1977), were co-transfected by electroporation with the *PB-SPc-GFP* transposon and the *mPB* transposase-encoding construct (ratio of 1.26 pmol transposase DNA: 3.48 pmol transposon DNA). In parallel, *PB-SPc-MD1* and *PB-SPc-MD2* transposons were electroporated under the same conditions. To determine the transfection efficiency of *mPB* transposase and *PB-SPc-GFP* transposon, FACS analysis was performed 48 hours post-electroporation (EP), showing 26 \pm 4% GFP+ cells which remained relatively stable (24 \pm 4% GFP+ cells at 72 hours post-EP; not statistically significant) (Figure 7A, left panel). As control, the empty expression plasmid- devoid of *mPB* transposase gene- was electroporated with the *PB-SPc-GFP* transposon resulting initially in comparable transfection efficiencies at 48 hours (17 \pm 1% GFP+ cells). However, in contrast to when the *mPB* expression vector was employed, the percentage of GFP+ transfected cells gradually declined at 72 hours post-EP, consistent with the loss of non-integrated *PB-SPc-GFP* plasmids in the rapidly dividing C2C12 cells (9 \pm 1% GFP+ cells; $p \leq 0.01$). Similarly, the mean fluorescent intensity (MFI) was sustained when the

PB-SPc-GFP transposon was co-transfected with *mPB* and significantly different from the controls ($p \leq 0.001$) (Figure 7A, right panel). These FACS data were confirmed by live cell imaging (Figure 7B).

Subsequently, we assessed whether C2C12 cells transposed with the *PB* transposons retained their ability to differentiate into skeletal muscle and whether expression of the GFP and microdystrophins MD1 and MD2, encoded by the transposons, was sustained upon differentiation. Four days after incubation with the differentiation medium (corresponding to 10 days post-EP), multinucleated myotubes were observed. The transcription levels of GFP (Figure 7C) and the human microdystrophins *MD1* and *MD2* (Figure 7D) were detectable by qRT-PCR and showed a significantly increased expression upon differentiation ($p \leq 0.01$ for GFP, $p \leq 0.001$ for the microdystrophins). This confirmed the muscle-specificity of the synthetic SPc5-12 promoter, consistent with its up-regulation upon myogenic differentiation. The transcript levels of the microdystrophins *MD1* and *MD2* in the differentiated C2C12 cells were comparable to the level of human dystrophin transcripts in differentiated human skeletal muscle (SKM) cells (Figure 7D). In contrast, we were not able to detect any GFP expression from differentiated C2C12 cells that were co-transfected with the empty plasmid and the *PB-SPc-GFP* transposon (Figure 7C). This indicates that transposition was a prerequisite to ensure stable GFP transcript levels. Immunofluorescence (IF) staining independently confirmed GFP (Figure 7E) and human microdystrophin MD1 and MD2 expression (Figure 7F) respectively in the myosin heavy chain (MyHC) and myosin positive myotubes, derived from the transposed C2C12 cells. The percentage of myotubes positive for GFP, MD1 or MD2 was determined by counting the nuclei within these myotubes divided by the total number of nuclei within the MyHC positive myotubes ($68 \pm 6\%$ for GFP; $65 \pm 2\%$ for MD1 and $66 \pm 2\%$ for MD2, respectively). Collectively, these results demonstrate that the *PB* transposon system is well suited to achieve sustained muscle-specific expression of human microdystrophins upon transposition in differentiated myogenic cells. The validation of the *PB* transposon system for the

delivery of the truncated human dystrophins paves the way towards the use of the full-length human dystrophin.

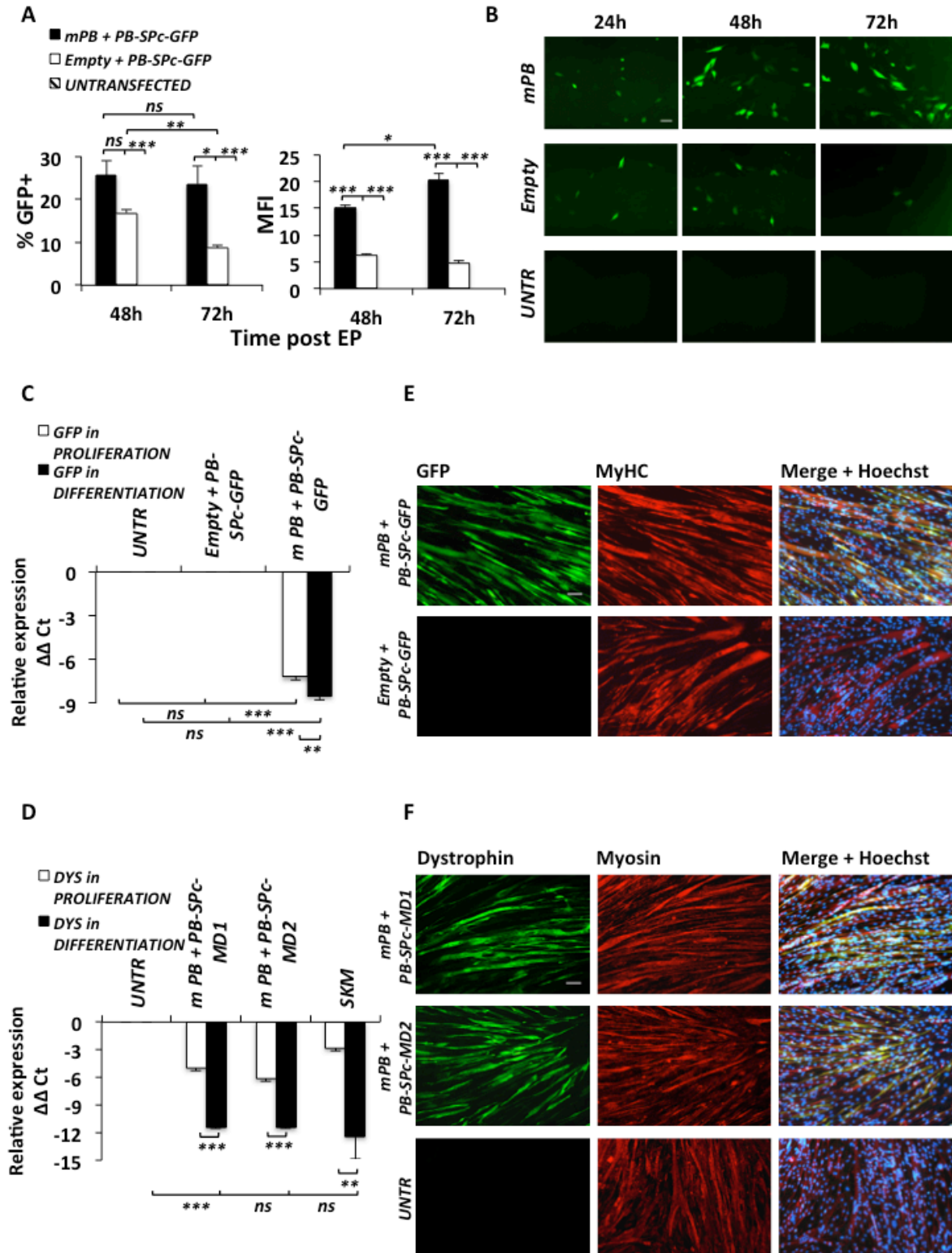


Figure 7. PB-mediated expression of MD1 and MD2 in C2C12 myoblasts. (A) The bar graphs show respectively the percentage of GFP+ (left) and the mean fluorescence intensity (MFI; right) of C2C12 cells at 48 and 72 h post-electroporation (EP) with the PB-SPc-GFP transposon when co-transfected with the mPB transposase or the empty plasmid (ratio of 1.26 pmol transposase DNA: 3.48 pmol transposon DNA). Untransfected cells are also shown. Shown are mean±SEM of three independent biological replicates; two-tailed unpaired Student's t-test (** $P \leq 0.001$; ** $P \leq 0.01$; * $P \leq 0.05$; ns: not significant). (B) Live cell imaging showing the GFP expression of the conditions described in (A) at 24, 48 and 72 h post-EP (UNTR: untransfected; scale bar 100 μm). (C) The bar graph depicts the GFP transcript levels detected by qRT-PCR in PB-transposed C2C12 myoblasts in proliferation (white bars) and myotubes in differentiation (black bars). (D) The bar graph depicts the MD1 and MD2 transcript levels detected by qRT-PCR in PB-transposed C2C12 myoblasts in proliferation (white bars) and myotubes in differentiation (black bars). (C,D) In both the graphs, the transcript levels of the human dystrophin from the human skeletal muscle (SKM) cells and myotubes were used as positive control. Values were normalized for the myosin heavy chain (MyHC) and shown as relative expression. Shown are mean±SEM of triplicate qRT-PCR analyses performed for three independent biological replicates; two-tailed unpaired Student's t-test (** $P \leq 0.001$; ** $P \leq 0.01$; ns: not significant). (E) Immunofluorescence staining to detect the co-localized expression of the GFP (in green) and the MyHC (in red) in C2C12 cells differentiated in skeletal muscle in vitro upon transposition with hyPB transposase and PB-SPc-GFP transposon. The condition empty plasmid + PB-SPc-GFP is shown as negative control. (F) Immunofluorescence staining to detect the co-localized expression of the human microdystrophin MD1 or MD2 (in green) and the myosin (in red) in C2C12 cells differentiated in skeletal muscle in vitro upon transposition with hyPB transposase and PB-SPc-MD1 or PB-SPc-MD2 transposon. Untransfected cells are also shown as negative controls. The mouse anti-human dystrophin NCL-DYS3 antibody was used. The nuclei were stained with Hoechst (Scale bar 100 μm).

4.1.3. Increased transposition in C2C12 myoblasts with the hyperactive *PB* transposase and the *PB* transposon encoding the full-length human dystrophin *CDS*

Different research groups, including ours, have shown that the *hyPB* transposase resulted in increased transposition as compared to the *mPB* transposase (Di Matteo et al., 2014a; Burnight et al., 2012; Doherty et al., 2012; Yusa et al., 2011). In line with these results, we therefore assessed the transposition efficiency of *hyPB* transposase in a head-to-head comparison with the *mPB* transposase, along with the large-size transposon *PB-SPc-DYS-Pgk-GFP* (17 Kb) in C2C12 myoblasts. This represents the first attempt in delivering the full-length dystrophin *CDS* by the *PB* transposon system. The *mPB* or *hyPB*-encoding expression constructs were electroporated together with *PB-SPc-DYS-Pgk-GFP* transposon in C2C12 myoblasts (ratio of 0.32 pmol transposase DNA: 0.87 pmol transposon DNA). Controls were transfected with the empty expression plasmid devoid of any *PB* transposase and with the *PB-SPc-DYS-Pgk-GFP* transposon. Due to the large size transposon, the percentage of GFP positive C2C12 myoblasts at 4 days post-EP resulted to be $4\pm 0.5\%$ after co-transfection with the *hyPB* transposase and $2\pm 0.5\%$ after co-transfection with the *mPB* transposase. The GFP positive populations were then enriched by FACS sorting and monitored at different time points by FACS analysis and fluorescence microscopy (Figure 8A, 8B). At 30 days post sorting, $78\pm 3\%$ of the cells transfected with the *hyPB* transposase were GFP positive, showing a statistically significant ($p\leq 0.01$) higher percentage compared to when the *mPB* was employed ($63\pm 3\%$ GFP positive cells). Consistently, a statistically significant difference in MFI ($p\leq 0.001$) was detected by FACS when the *hyPB* was used compared to the *mPB* (Figure 8B).

We subsequently assessed whether C2C12 cells transposed with the *hyPB* transposase and the large-size transposon *PB-SPc-DYS-Pgk-GFP* expressed the human full-length dystrophin and retained their ability to differentiate into skeletal muscle. Four days after incubation with the differentiation medium (corresponding to 24 days post-EP), multinucleated myotubes were observed.

The transcription levels of the full-length human dystrophin were detectable by qRT-PCR and showed a significant increase in expression in C2C12 cells differentiated in myotubes compared to when the cells were retained in a proliferative, non-differentiated state ($p \leq 0.001$; Figure 9A). This is consistent with our previous results (Figures 6C, 6D) and confirms the muscle-specificity of the synthetic SPc5-12 promoter and its up-regulation upon myogenic differentiation. To demonstrate that the full-length human dystrophin *CDS* expresses a full-length transcript, a reverse transcriptase PCR (RT-PCR) was first performed using three different primer pairs that respectively amplify three different regions of the full-length dystrophin transcript, including the N-terminal, central and C-terminal sequences (Table 4). The three bands corresponding to these respective amplified regions were detected in differentiated C2C12 myoblasts that had undergone transposition after transfection with the *hyPB* transposase and the *PB-SPc-DYS-Pgk-GFP* transposon constructs (Figure 9B). In contrast, these specific PCR bands were absent in the untreated differentiated C2C12 cells or in differentiated C2C12 cells co-transfected with the *PB-SPc-DYS-Pgk-GFP* transposon and an empty expression plasmid without transposase (Figure 9B).

Western blot analysis subsequently confirmed expression of the full-length human dystrophin protein (427 kDa) in myotubes derived from C2C12 cells that had undergone transposition after transfection with the *hyPB* transposase and the *PB-SPc-DYS-Pgk-GFP* transposon constructs (Figure 9C). Dystrophin expression in these myotubes coincided with GFP and myosin expression, as confirmed by immunofluorescence assay (Figure 9D, 9E). Similarly, Western blot analysis demonstrated expression of the full-length human dystrophin protein (427 kDa) in differentiated normal human skeletal muscle cells (SKM, Figure 9C), whereas no dystrophin expression was apparent in non-transfected differentiated C2C12 cells or differentiated C2C12 cells co-transfected with the *PB-SPc-DYS-Pgk-GFP* transposon and an empty expression plasmid without transposase (Figure 9C).

Collectively, these results justify the use of hyperactive *PB* transposase to achieve a stable integration of the *PB* transposon coding for the full-length human dystrophin and a sustained expression of the protein in differentiated myogenic cells.

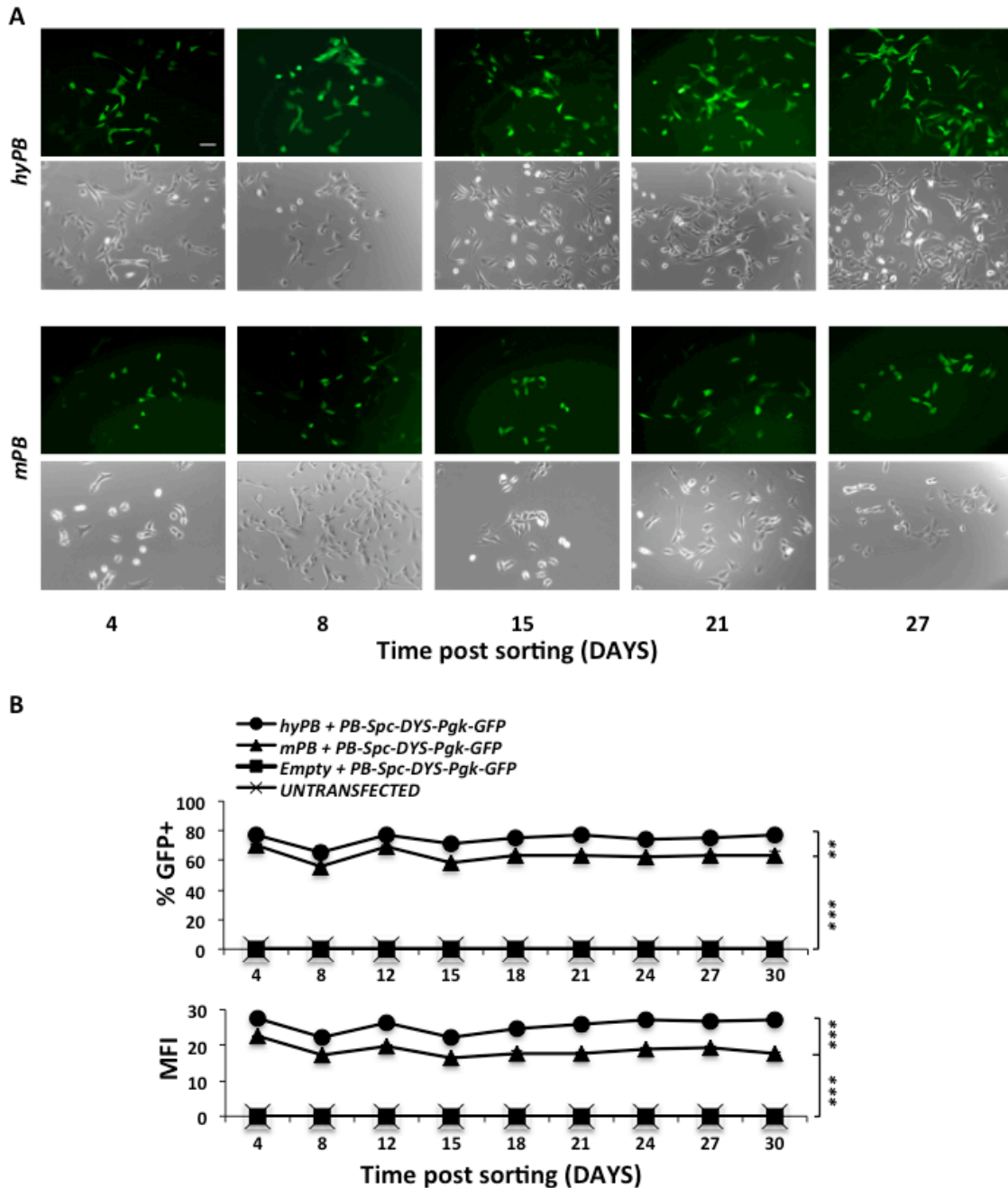


Figure 8. Validation of the use of *hyPB* transposase in C2C12 myoblasts. (A) Live cell imaging depicting the GFP expression in C2C12 myoblasts at different time points

after sorting, when the large-size transposon PB-SPc-DYS-Pgk-GFP is co-transfected with hyPB or mPB transposase (Scale bar 100 μ m). **(B)** Graphs representing the comparison between hyPB and mPB transposases in terms of percentage of GFP+ population (graph above) and mean fluorescence intensity (MFI, graph below). The GFP+ populations were enriched by FACS at 4 days post-EP and monitored for the GFP expression in the next 30 days after the sorting. The higher efficiency of the hyPB transposase over the mPB transposase was assessed at the concentration of 0.32 pmol transposase DNA: 0.87 pmol transposon DNA. Results were presented as mean \pm SD of three independent biological replicates; two-way ANOVA (Bonferroni's multiple comparison test); *** $P \leq 0.001$; ** $P \leq 0.01$.

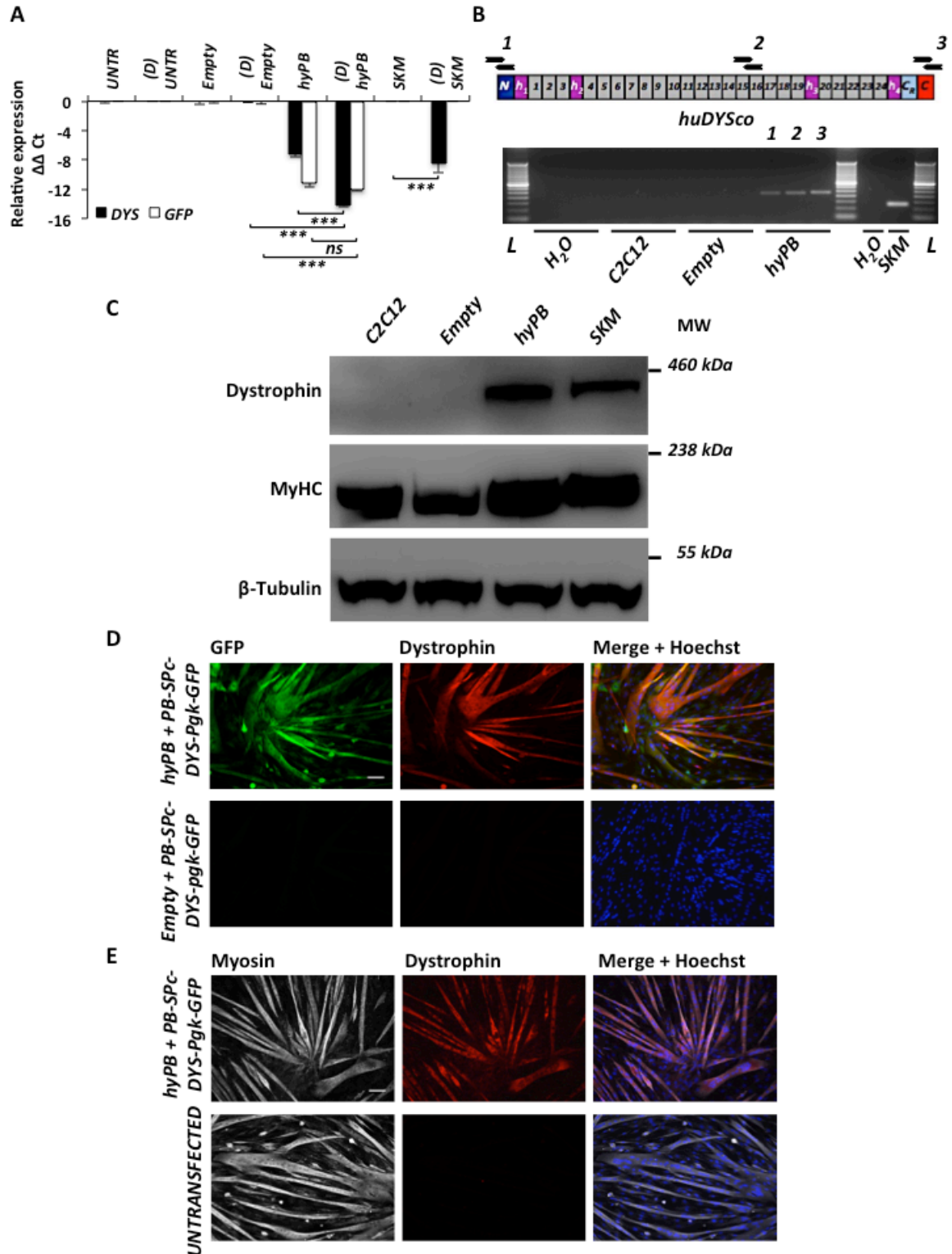


Figure 9. Human full-length dystrophin expression in PB-transposed C2C12 myoblast-derived differentiated myotubes. (A) The transcript levels of the full-length human dystrophin (black bars) and the GFP (white bars) were detected by qRT-PCR in

C2C12 cells transposed with *hyPB + PB-SPc-DYSPgk-GFP*, while in proliferation or in differentiated myotubes (D: differentiated sample). Results were presented as mean±SEM of triplicate qRT-PCR analyses performed for three independent biological replicates; two-tailed unpaired Student's t-test (** $P \leq 0.001$; ns: not significant). **(B)** RT-PCR showing expression of full-length human dystrophin transcript in myotubes derived from C2C12 cells that had undergone transposition after co-transfection with *hyPB* and *PB-SPc-DYS-Pgk-GFP*. Three different primer pairs were used that recognize respectively (1) the N-terminal, (2) a central region and (3) the C-terminal sequences, yielding amplicons of 221 bp, 222 bp and 228 bp, respectively. A schematic representation of the PCR primers relative to the different regions of the dystrophin transcript is depicted. Human skeletal muscle cells (SKM) differentiated in myotubes were used as a positive control; the primer pairs *DYS* listed in Table 5 have been used for this sample. Negative controls included untreated differentiated C2C12 cells (designated as C2C12) or differentiated C2C12 cells co-transfected with the *PB-SPc-DYS-Pgk-GFP* transposon and an empty expression plasmid without transposase (designated as Empty). L: 50 bp ladder. **(C)** Western blot analysis demonstrating expression of the full-length human dystrophin protein (427 kDa) in myotubes derived from C2C12 cells that had undergone transposition after cotransfection with *hyPB* and *PB-SPc-DYS-Pgk-GFP*. The antibody NCL-DYS3 was used to detect the human dystrophin. Non-transfected differentiated C2C12 cells or differentiated C2C12 cells co-transfected with the *PB-SPc-DYS-Pgk-GFP* transposon and an empty expression plasmid without transposase were included as negative controls. Normal human skeletal muscle cells were used as positive control. In vitro skeletal muscle differentiation was confirmed for all the samples by the expression of the MyHC protein (223 kDa). β -Tubulin (50 kDa) was used to normalize the amount of loaded proteins. **(D)** Immunofluorescence staining on C2C12 cells transposed with *hyPB + PB-SPc-DYS-Pgk-GFP* and differentiated in skeletal muscle in vitro upon 4 days in conditioning medium (24 days post-EP) showing a co-localized expression of the GFP (in green) and the full-length human dystrophin (in red). The condition empty plasmid + *PB-SPc-DYS-Pgk-GFP* is shown as negative control. **(E)** Immunofluorescence staining on the cells described in (D) and showing a co-localized expression of the myosin (in white) and the full-length human dystrophin (in red) when differentiated in myotubes. Untransfected cells are also shown as negative controls. The Ab mouse anti-human dystrophin NCL-DYS3 was used. The nuclei were stained with Hoechst (Scale bar 100 μ m).

4.1.4. Isolation and characterization of adult skeletal muscle pericyte-derived stem/progenitor cells from the Golden Retriever muscular dystrophy (GRMD) dog model

Adult pericyte-derived stem/progenitor cells or mesoangioblasts (MABs) were isolated from the skeletal muscle of a Golden Retriever Muscular Dystrophy dog, as previously described (Sampaolesi et al., 2006; Tonlorenzi et al., 2007). Small, round, refractile and poorly adherent cells were visible with the initial outgrowth of adherent cells (Figure S1A). This population of cells was collected, kept in culture and characterized for the typical markers of adult skeletal muscle MABs (Tonlorenzi et al., 2007; Dellavalle et al., 2011). Alkaline phosphatase (AP) positive cells were detected in the cultured cell population (Figure S1B). The presence of the CD44 marker and the absence of CD34 and CD45 markers were assessed by FACS analyses, showing the typical profile of this subset of adult pericytes (Figure S1C). Further markers were subsequently analyzed by semi-quantitative RT-PCR at different time points (passage P5 and P10), using as a positive control a heterogeneous bulk cell population directly derived from the GRMD muscle biopsy (passage P1). As expected, the transcript levels of *PAX7*, *MYF5*, *CD56* and desmin, typically associated with satellite cells, decreased significantly after the first passage ($p \leq 0.01$, $p \leq 0.001$; Figures S1D, S1E). In contrast, the transcript levels of *NG2* and *PDGFR β* , typical markers of pericytes, remained stable over time. Finally, the isolated cell population was capable to spontaneously differentiate *in vitro* into skeletal myotubes or into mesodermal lineages upon appropriated stimulation (Figures S1F, S1G). Collectively, this gene expression profile and functional analyses confirmed that the GRMD cell isolated were bona fide mesoangioblasts.

4.1.5. Genetic correction of dystrophic mesoangioblasts by delivery of the full-length human dystrophin CDS in *PB* transposon system

We subsequently optimized the transfection conditions of the dystrophic GRMD MABs. These were transfected by electroporation with the *hyPB* transposase-encoding construct and the *PB-Pgk-GFP* transposon (ratio of 0.32 pmol transposase DNA: 0.87 pmol transposon DNA) showing a transfection efficiency of $44\pm 1\%$ GFP+ cells at 7 days post-EP (Figure 10A). The transfected cells were sorted and the GFP expression was maintained, resulting in $88\pm 3\%$ GFP+ cells at 28 days post sorting ($p\leq 0.001$; Figure 10B). In contrast, in the absence of the *hyPB* transposase, the percentage of GFP+ cells gradually declined resulting in only background levels of GFP, indistinguishable from untransfected control GRMD MABs. This indicates that the sustained GFP expression in the transfected MABs could be ascribed to and is dependent on *bona fide* transposition. Based on these encouraging results, we subsequently transfected the GRMD MABs by electroporation with the same molar ratios of *hyPB* transposase expression construct and the large-size transposon *PB-SPc-DYS-Pgk-GFP* (ratio of 0.32 pmol transposase DNA: 0.87 pmol transposon DNA), encoding both full-length human dystrophin and GFP. This resulted in a transfection efficiency of $3\pm 1\%$ GFP+ cells at 7 days post-EP (Figure 10A). The difference in transfection efficiency between the equimolar doses of *PB-SPc-DYS-Pgk-GFP* and *PB-Pgk-GFP* transposons reflected the different sizes of the plasmids, as previously reported ($p\leq 0.001$, Figure 10A) (Sharma et al., 2013). Though doubling the *hyPB* transposase and transposon doses, while maintaining the transposase: transposon ratio, further increased the percentage of GFP+ cells (Figure S2), the viability of the transfected cells concomitantly declined ($p\leq 0.001$). GRMD MABs transfected with *hyPB* transposase and *PB-SPc-DYS-Pgk-GFP* transposon were sorted at 7 days post-EP, and the GFP expression was monitored by FACS analysis and fluorescence microscopy during the 28 days post sorting (Figure 10B, 10C). The transfected cells exhibited stable expression of $50\pm 5\%$ GFP+ cells, consistent with stable transposition ($p\leq 0.001$). The

transposon copies per diploid genome quantified by qPCR corresponded to 0.5 ± 0.03 copies for the condition *hyPB + PB-SPc-DYS-Pgk-GFP* and 1.7 ± 0.04 copies for *hyPB + PB-PgkGFP* (Figure 10D). GRMD MABs that were transfected with the transposon and without the transposase did not show any detectable integrated transposons ($p \leq 0.001$), indistinguishable from non-transfected control cells.

To assess if the integrated *PB-SPc-DYS-Pgk-GFP* transposon could result in sustained expression of the full-length human dystrophin, transposed GRMD MABs were subsequently differentiated in vitro into myocytes/myotubes after tamoxifen-induced overexpression of MyoD-ER (Kimura et al., 2008). This approach allowed to rescue myogenic differentiation of adult canine MABs at late passages (i.e. passage P15-18). The transcript levels of the full-length human dystrophin were detected by qRT-PCR ($p \leq 0.001$; Figure 11A). Moreover, the three different regions including the N-terminal, the central region and the C-terminal region of the full-length human dystrophin transcript were detected by RT-PCR in the differentiated GRMD MABs that had undergone transposition after transfection with the *hyPB* transposase and the *PB-SPc-DYS-Pgk-GFP* transposon constructs (Figure 11B). The expression of the full-length human dystrophin protein was confirmed by immunofluorescence staining in differentiated GRMD MABs, where it co-localized with the expression of GFP (Figure 11C) and myosin (Figure 11D) in genetically corrected myocytes/myotubes. In contrast, dystrophin and GFP were not detectable in untransfected cells nor in the control GRMD MABs co-transfected with the *PB-SPc-DYS-Pgk-GFP* transposon and the empty expression plasmid without transposase (Figure 11C, 11D). This was consistent with the lack of dystrophin mRNA in these controls (Figure 11A, 11B). Similarly, sustained GFP transcript levels were detected by qRT-PCR in GRMD MABs that had undergone transposition after co-transfection with *hyPB* transposase and *PB-Pgk-GFP* transposon ($p \leq 0.001$; Figure 11A). The GFP expression was confirmed by IF in differentiated cells (Figure S3). In the absence of the *hyPB* transposase, GFP

transcript and protein were absent, confirming the need for transposition to enable stable integration and transgene expression (Figures 10A, S3).

Taken together, these findings demonstrate that it is possible to genetically correct dystrophic adult mesoangioblasts by using a *PB*-transposon based platform to deliver the full-length human dystrophin *CDS*.

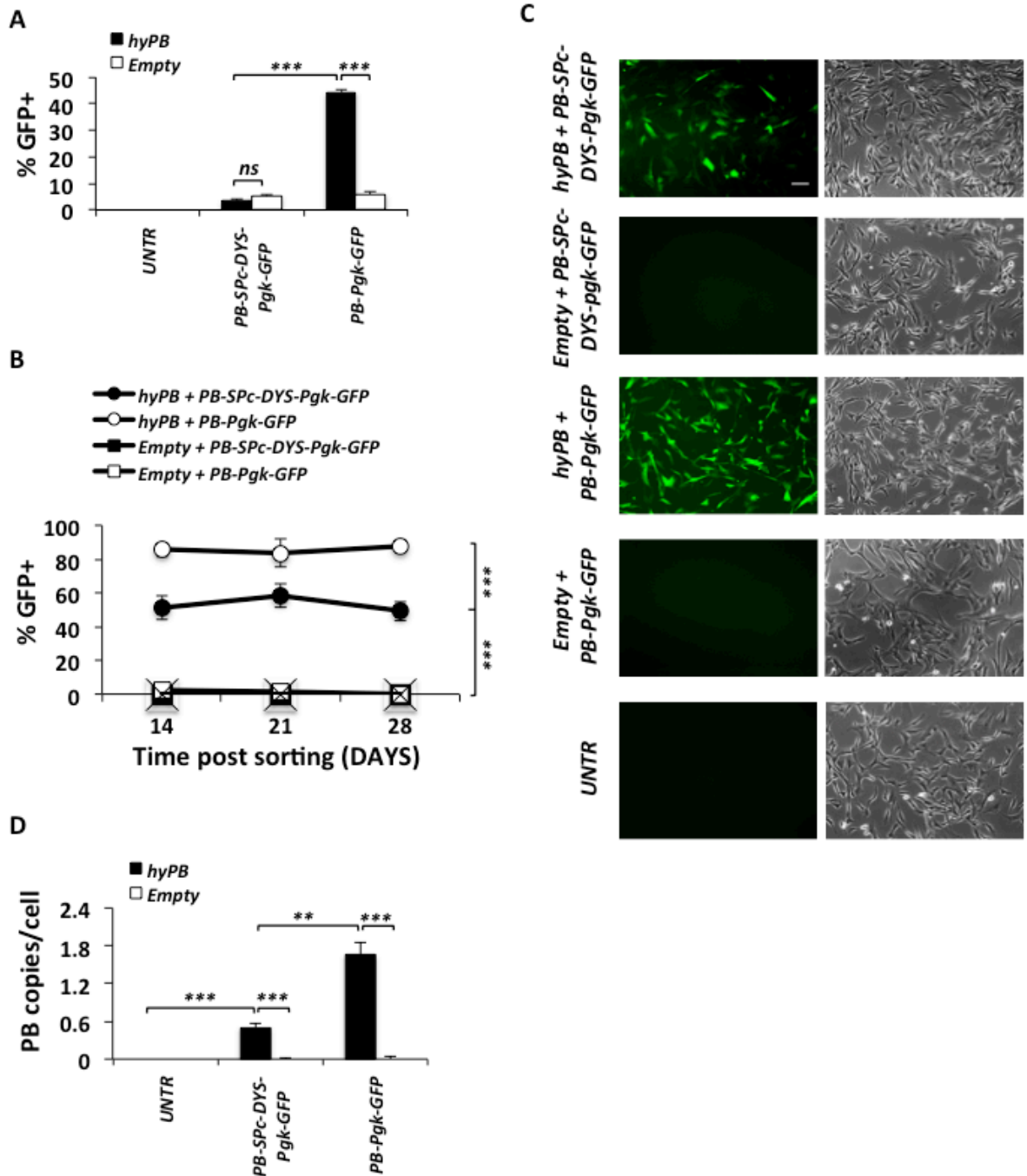


Figure 10. PB-mediated transposition of the full-length human dystrophin CDS in GRMD MABs. (A) The bar graph shows the percentage of GFP+ GRMD MABs at the day of the sorting performed at 7 days post-EP. Optimized and equimolar doses have been used in the different conditions. The statistically significant difference in transfection efficiency detected when PB-SPc-DYS-Pgk-GFP or PB-Pgk-GFP transposon are deployed reflects the different sizes of the plasmids. Results were presented as mean±SEM of three independent biological replicates; two-tailed unpaired Student's t-test (***P ≤ 0.001; ns: not significant). (B) The GFP+ populations were monitored at different time points for 28 days post sorting. GRMD MABs co-transfected with the empty plasmid and the same transposons, and untransfected cells were used as controls. Shown are mean±SD on a biological replicate; two-way ANOVA (Bonferroni's multiple comparison test); ***P ≤ 0.001. (C) Live cell imaging showing the GFP expression of the different conditions at day 21 post sorting (Scale bar 100 μm). (D) Bar graph representing the transposon copies per diploid genome detected by qPCR in transposed GRMD MABs (PB-SPc-DYS-Pgk-GFP 0.5 ± 0.03 copies/cell; PB-Pgk-GFP 1.7 ± 0.04 copies/cell). Shown is mean±SEM, n=3 technical repeats, of one experiment, representative of 3 biological repeats; two-tailed unpaired Student's t-test (*** P ≤ 0.001; **P ≤ 0.01).

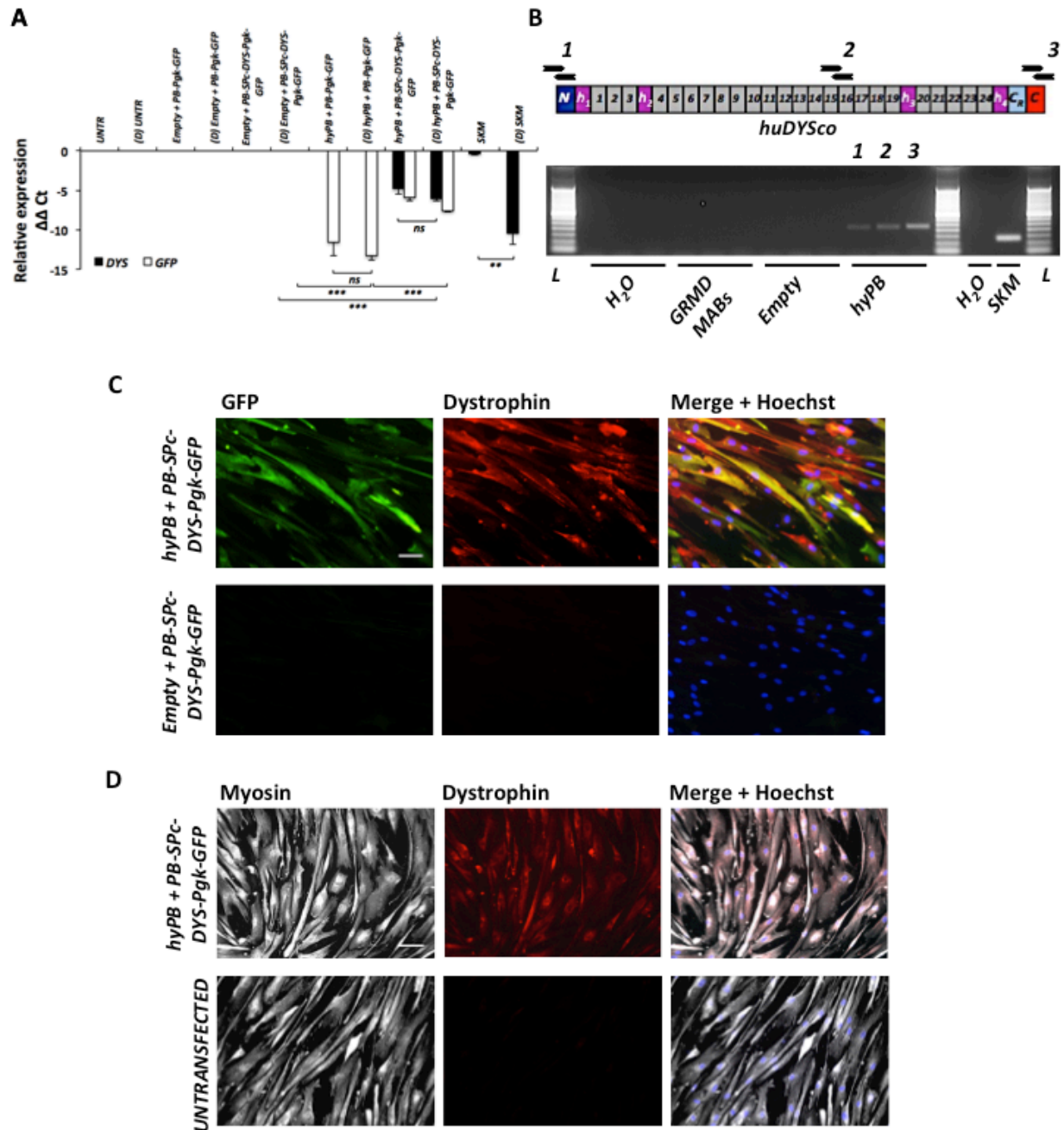


Figure 11. Correction of GRMD MABs by the PB-mediated expression of the full-length human dystrophin. (A) The transcript levels of the full-length human dystrophin (black bars) and GFP (white bars) were detected by qRT-PCR analysis in GRMD MABs transposed with hyPB + PB-SPC-DYS-Pgk-GFP or PB-Pgk-GFP. SKM cells have been used as positive control. Samples are indicated with (D) when differentiated in myocytes/myotubes. Shown is mean \pm SEM, $n=3$ technical repeats, of one experiment, representative of 3 biological repeats; two-tailed unpaired Student's t -test ($***P \leq 0.001$;

****P** ≤ 0.01; ns: not significant; D: differentiated sample). **(B)** RT-PCR demonstrating expression of full-length human dystrophin transcript in differentiated GRMD MABs that had undergone transposition after co-transfection with hyPB and PB-SPc-DYS-Pgk-GFP. Three different primer pairs were used that recognize respectively (1) the N-terminal, (2) a central region and (3) the C-terminal sequences, yielding amplicons of 221 bp, 222 bp and 228 bp, respectively. A schematic representation of the PCR primers relative to the different regions of the dystrophin transcript is depicted. Controls included differentiated human SKM, untreated differentiated MABs (designated as GRMD MABs) and differentiated GRMD MABs co-transfected with the PBSPc-DYS-Pgk-GFP transposon and an empty expression plasmid without transposase (designated as Empty). The primer pairs *DYS* listed in Table 5 have been used for the positive control. L: 50 bp ladder. **(C)** Immunofluorescence analysis showing the expression and the co-localization of the full-length human dystrophin (in red) and the GFP (in green) of GRMD MABs corrected with hyPB + PB-SPc-DYS-Pgk-GFP and induced to differentiate in skeletal muscle *in vitro* upon MyoD-ER(T) overexpression after 6 days in conditioning medium (21 days post-EP). The condition empty plasmid + PB-SPc-DYS-Pgk-GFP is shown as negative control. **(D)** Immunofluorescence analysis of the cells described in (C) showing the expression and co-localization of the full-length human dystrophin (in red) and the myosin (in white). Untransfected cells are also shown as negative controls. The mouse anti-dystrophin NCL-DYS1 and NCL-DYS2 antibodies were used. The nuclei were stained with Hoechst (Scale bar 100 μm).

The data of the following section 4.2.1 are published in:

Maffioletti SM[#], Gerli MFM[#], Ragazzi M, Dastidar S, Benedetti S, **Loperfido M**, VandenDriessche T, Chuah MK, Tedesco FS*. *Efficient derivation and inducible differentiation of expandable skeletal myogenic cells from human ES and patient-specific iPSC cells*. Nature Protocols 2015 Jul;10(7):941-58. doi: 10.1038/nprot.2015.057. Epub 2015 Jun 4. (Article awarded as cover story of the issue).

[#]The authors declare joint first authorship; *Corresponding author.

The data of the following section 4.2, but section 4.2.1 are included in the submitted manuscript:

Loperfido M, Dastidar S, Gerli MFM, Ragazzi M, Di Matteo M, Nair N, Jarmin S, Moore M, Samara-Kuko E, Athanasopoulos T, Dickson G, Chai YC, Tedesco FS[#], Chuah MK[#], VandenDriessche T^{#,*}. *Genetic correction of Duchenne muscular dystrophy iPSC-derived inducible myogenic cells using piggyBac transposons encoding full-length dystrophin*.

[#]These authors share joint senior authorship; *Corresponding author.

4.2. Genetic correction of DMD HIDEMs by *piggyBac* transposons expressing full-length dystrophin and transplantation in dystrophic mice

4.2.1. Generation and characterization of DMD patient-specific HIDEMs

Human iPSC-derived mesoangioblast-like cells (HIDEMs) utilized in this study were kindly provided by our collaborator in this study Dr. Tedesco from the University College of London (London, United Kingdom). DMD HIDEMs were obtained from iPSCs of a patient carrying a deletion of exons 4-43 in the dystrophin gene, as described in (Maffioletti et al., 2015; Tedesco et al., 2012; Kazuki et al., 2010). HIDEMs from a healthy donor (HD; (Maffioletti et al., 2015; Tedesco et al., 2012)) were used as control, where indicated.

Briefly, DMD iPSCs were disaggregated to a single cell suspension and induced to differentiate into expandable cells resembling human MABs using a procedure, which entails four stages with different culture densities, media and surface coating. This was achieved without requiring the generation of embryoid bodies or prospective cell isolation. Human iPSC differentiation with this protocol yielded relatively homogeneous MAB-like cells populations. Cell characterization by flow cytometry was performed to ensure that the desired cell population was obtained. Specifically, the markers assessed were the following: CD13, CD31, CD44, CD45, CD49b, CD56, CD146, alkaline phosphatase (AP) and stage-specific embryonic marker 4 (SSEA4). In brief, CD146 (a perivascular marker *in vivo*), CD13, CD44 and CD49b expression were highly expressed in normal or DMD patient-specific HIDEs (above 50%). CD56 (myoblast marker), CD45 (pan-hematopoietic marker) and CD31 (endothelial cell marker) were very low or negative. SSEA4, a pluripotency-associated marker, was either negative or lowly expressed. Expression of the quintessential pluripotency marker OCT4, NANOG, SOX2 and KLF4 in HIDEs was either very low or absent.

The DMD HIDEs (or normal healthy donor HIDEs as control) were subsequently induced to differentiate into multinucleated skeletal myotubes following transduction with a tamoxifen-inducible MyoD lentiviral (MyoD-ER(T) LV) vector that triggers and synchronizes the differentiation of the entire culture. Following induction with tamoxifen, the HIDE-derived myotubes expressed *de novo* the terminal myogenic differentiation marker myosin heavy chain (MyHC) as shown by immunofluorescence staining. We have also incidentally observed the formation of sarcomeric striations and spontaneous twitching of myotubes derived from HIDEs after 8 days in myogenic differentiation medium (Supplementary video 1 in Maffioletti et al., 2015).

We have shown that *PB* transposons could efficiently transfer the full-length dystrophin coding DNA sequence (*CDS*, size: 11.1 kb) and correct dystrophic MABs when co-transfected with the hyperactive *PB* (*hyPB*) transposase (see

above – Chapter 4.1; (Loperfido et al., 2015b)). In contrast to MABs that have a limited proliferation potential, DMD HIDEMs has a greater expansion potential and constitute a suitable alternative target for genetic modification with this *PB* transposon system, given their ability to undergo relatively robust and synchronous myogenic differentiation.

4.2.2. Stable GFP expression after *PB* transposition in DMD HIDEM and DMD HIDEM^{MYOD} cells

To engineer the DMD HIDEMs with the *PB* transposons, we explored two alternative protocols. For the first approach, DMD HIDEMs were first transfected with the *PB* transposon components and subsequently transduced with the tamoxifen-regulated MyoD-ER(T) LV vectors, followed by the tamoxifen-mediated induction of myogenic differentiation (Figure 12A). Alternatively, DMD HIDEMs were first transduced with the MyoD-ER(T) LV vectors (designated as DMD HIDEM^{MYOD} cells) and subsequently transfected with the *PB* transposon components, followed by the tamoxifen-mediated induction of myogenic differentiation (Figure 12B).

DMD HIDEMs were first co-transfected with the *hyPB* transposase and a small size transposon coding for GFP (designated as *PB-Pgk-GFP*; transposon size: 5.4 kb). Two different concentrations were used in order to determine the optimal conditions of transfection (0.32 pmol transposase DNA: 0.87 pmol transposon DNA and 0.64 pmol transposase DNA: 1.74 pmol transposon DNA) based on our previous results obtained in *bona fide* MABs transfected with the *PB* transposon (see above – Chapter 4.1; (Loperfido et al., 2015b)). At 8 days post-electroporation (post-EP), 9% of GFP+ cells were detected when the lowest transposase: transposon concentration was used, whereas the percentage of GFP+ cells increased to 20% at the highest transposase: transposon concentration. The transfected cells were enriched for GFP expression by fluorescence-activated cell sorting and showed a stable GFP expression for at

least 45 days post-EP (i.e. 38 days post-sorting) in 97% and 99% of the transfected DMD HIDEMs. (Figure 13A).

Similar results were obtained when we transfected DMD HIDEMs that were already transduced with the MyoD-ER(T) LV vectors prior to transfection with the transposon and transposase constructs, named DMD HIDEM^{MYOD} cells. Sustained GFP expression could be achieved upon transfection of the *PB-Pgk-GFP* transposon with the *hyPB* expression construct in DMD HIDEM^{MYOD} cells. In particular, stable GFP expression could be detected for at least 45 days post-EP in 93% and 95% of the sorted DMD HIDEM^{MYOD} cells respectively when low and high concentrations were used (Figure 13A). When the DMD HIDEM or DMD HIDEM^{MYOD} cells were transfected with the *PB-Pgk-GFP* transposon and an empty expression construct that did not encode for any transposase, sustained GFP expression was not detectable.

Both protocols enabled efficient myogenic differentiation of the DMD HIDEM or DMD HIDEM^{MYOD} cells upon co-transfection with the *hyPB* transposase and the small size transposon coding for GFP and followed by the tamoxifen-mediated induction, consistent with the co-localized expression of MyHC and the transgene GFP encoded by the *PB* transposons (Figure 13B).

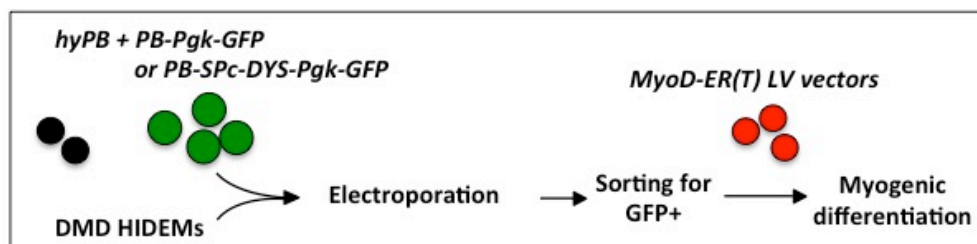
Subsequently, we co-transfected DMD HIDEMs with the *hyPB* transposase and a large *PB* transposon encoding a full-length human dystrophin coding DNA sequence (*CDS*, size: 11.1 kb) and a GFP reporter gene (designated as *PB-SPc-DYS-Pgk-GFP*; transposon size: 17 kb) (see above – Chapter 4.1; (Loperfido et al., 2015b)). The same molar ratios were employed, as in the previous experiment (i.e. 0.32 pmol transposase DNA: 0.87 pmol transposon DNA and 0.64 pmol transposase DNA: 1.74 pmol transposon DNA). At 8 days post-EP, the percentage of GFP+ cells in the unsorted samples was respectively 1.5% and 2.5% upon usage of low and high DNA plasmid concentrations. The transfected cells were enriched for GFP expression by fluorescence-activated cell sorting and the GFP expression was monitored at different time-points post-EP by live imaging using fluorescence microscopy (Figure 14). At 45 days post-

EP (i.e. 38 days post-sorting), the percentage of the GFP+ cells was 86% and 90% of the DMD HIDEMs transfected with low and high plasmid concentrations, respectively.

Similarly, we co-transfected the DMD HIDEM^{MYOD} cells with the large size *PB-SPc-DYS-Pgk-GFP* transposon along with the *hyPB* transposase. This resulted in 79% and 77% of GFP+ DMD HIDEM^{MYOD} cells at 45 days post-EP (Figure 14). As negative controls, untransfected cells and DMD HIDEMs co-transfected with an empty expression plasmid devoid of transposase and the *PB-SPc-DYS-Pgk-GFP* transposon did not show any stable GFP expression (Figure 14).

Collectively, these results indicate that transposition mediated by the *hyPB* transposase is a prerequisite to enable stable GFP expression in the transfected DMD HIDEM or DMD HIDEM^{MYOD} cells. The highest concentration of *PB* transposon components gave the highest percentage in GFP+ of DMD HIDEM or DMD HIDEM^{MYOD} cells. These could be easily enriched for the reporter marker via cell sorting. We therefore continued our investigation on the cells transposed with the highest concentration of *PB* transposons.

A



B

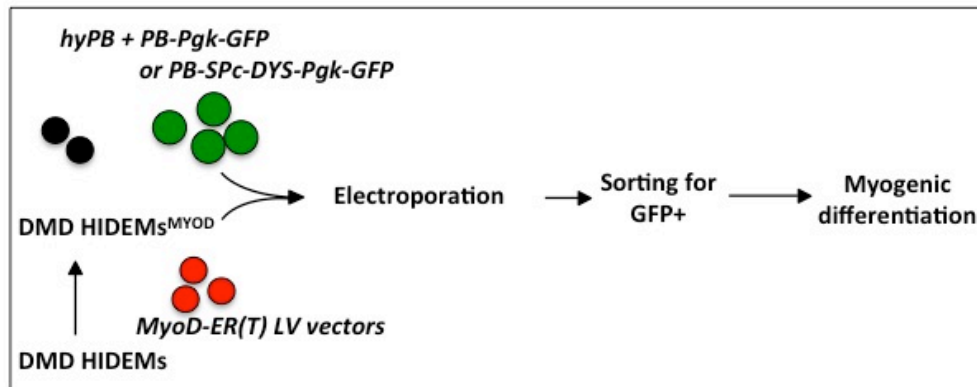


Figure 12. Schematic representation of the two protocols used in this study to obtain stable transposition in HIDEms. (A) A first approach used in this study for genetic correction of DMD HIDEms. DMD HIDEms with deletion of exons 4–43 in the dystrophin gene were electroporated with hyPB transposase and PB-Pgk-GFP or PB-SPc-DYS-Pgk-GFP transposons. Subsequently, they were enriched for the GFP expression by fluorescence-activated cell sorting. In vitro myogenic differentiation was induced upon transduction with lentiviral vectors coding for the tamoxifen-inducible MyoD-ER(T) (MyoD-ER(T) LV vectors), followed by tamoxifen exposure. The expression of the GFP and/or the full-length human dystrophin was investigated in genetically corrected DMD HIDEms upon myogenic differentiation in vitro. (B) A second approach to genetically correct DMD HIDEms previously transduced with MyoD-ER(T) LV vectors and named DMD HIDE^{MYOD} cells. These were electroporated with hyPB transposase and PB-Pgk-GFP or PB-SPc-DYS-Pgk-GFP transposons. Transfected cells were enriched for the GFP expression by fluorescence-activated cell sorting and exposed to tamoxifen in order to induce the myogenic differentiation. The expression of the GFP and/or the full-length human dystrophin was investigated in genetically corrected DMD HIDE^{MYOD} cells upon myogenic differentiation in vitro.

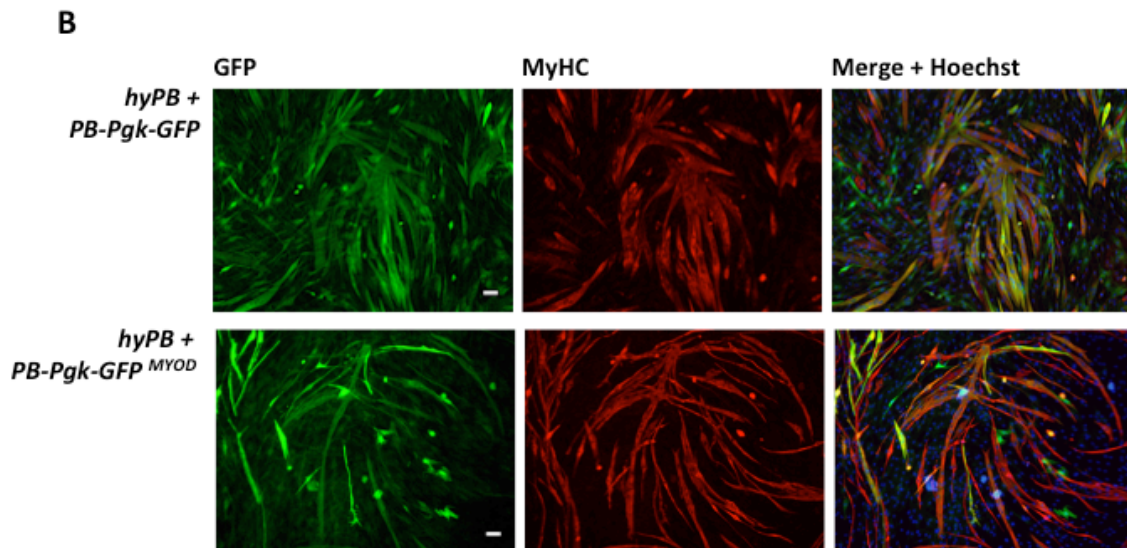
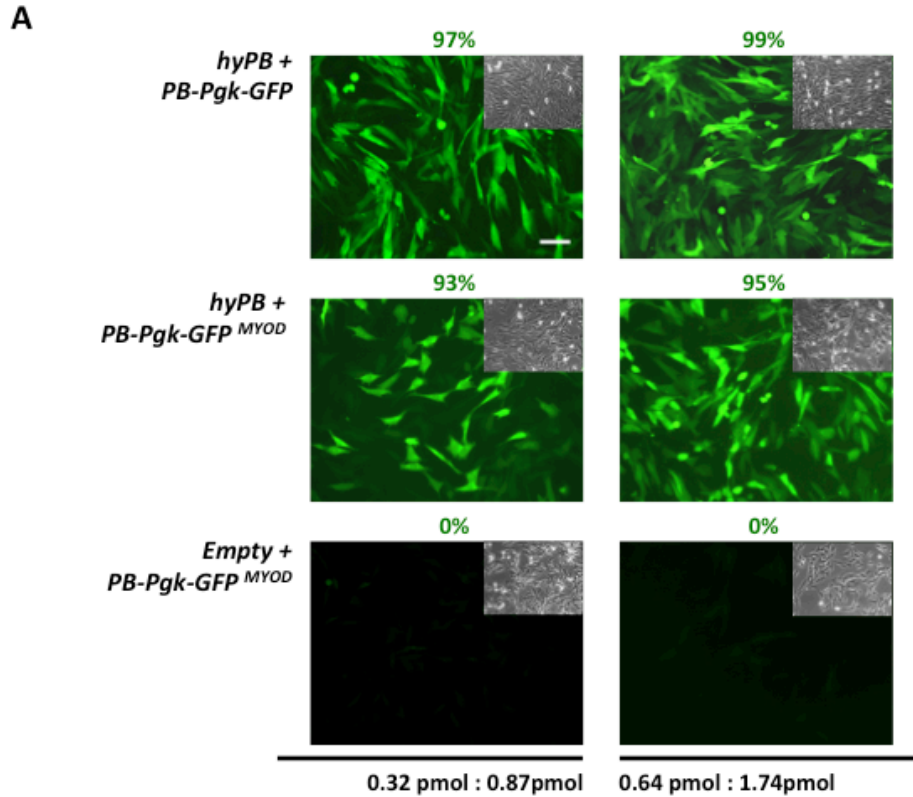


Figure 13. Stable GFP expression after transposition of the small size transposon *PB-Pgk-GFP*. (A) Live cell imaging of DMD HIDEM and DMD HIDEM^{MYOD} cells transfected with *hyPB* and the small size transposon *PB-Pgk-GFP*. Pictures acquired at 45 days post-EP by fluorescence microscopy show the stable expression of the GFP reporter in DMD HIDEM and DMD HIDEM^{MYOD} cells at the concentration of 0.32 pmol transposase DNA: 0.87 pmol transposon DNA and 0.64 pmol transposase DNA: 1.74

pmol transposon DNA. As negative controls, cells transfected with the empty plasmid and PB-Pgk-GFP transposons are also shown. Above the pictures, the percentage of GFP+ cells acquired by the fluorescence-activated cell sorter is reported. Scale bar 75 μm . (B) Immunofluorescence assay of DMD HIDEM and DMD HIDEM^{MYOD} cells transfected with hyPB + PB-Pgk-GFP at the high concentration of 0.64 pmol transposase DNA: 1.74 pmol transposon DNA, and differentiated upon over-expression of tamoxifen-inducible Myo-ER(T). Differentiated cells are positive for GFP (in green) and MyHC (in red) in both the protocols used. Scale bar 100 μm .

A

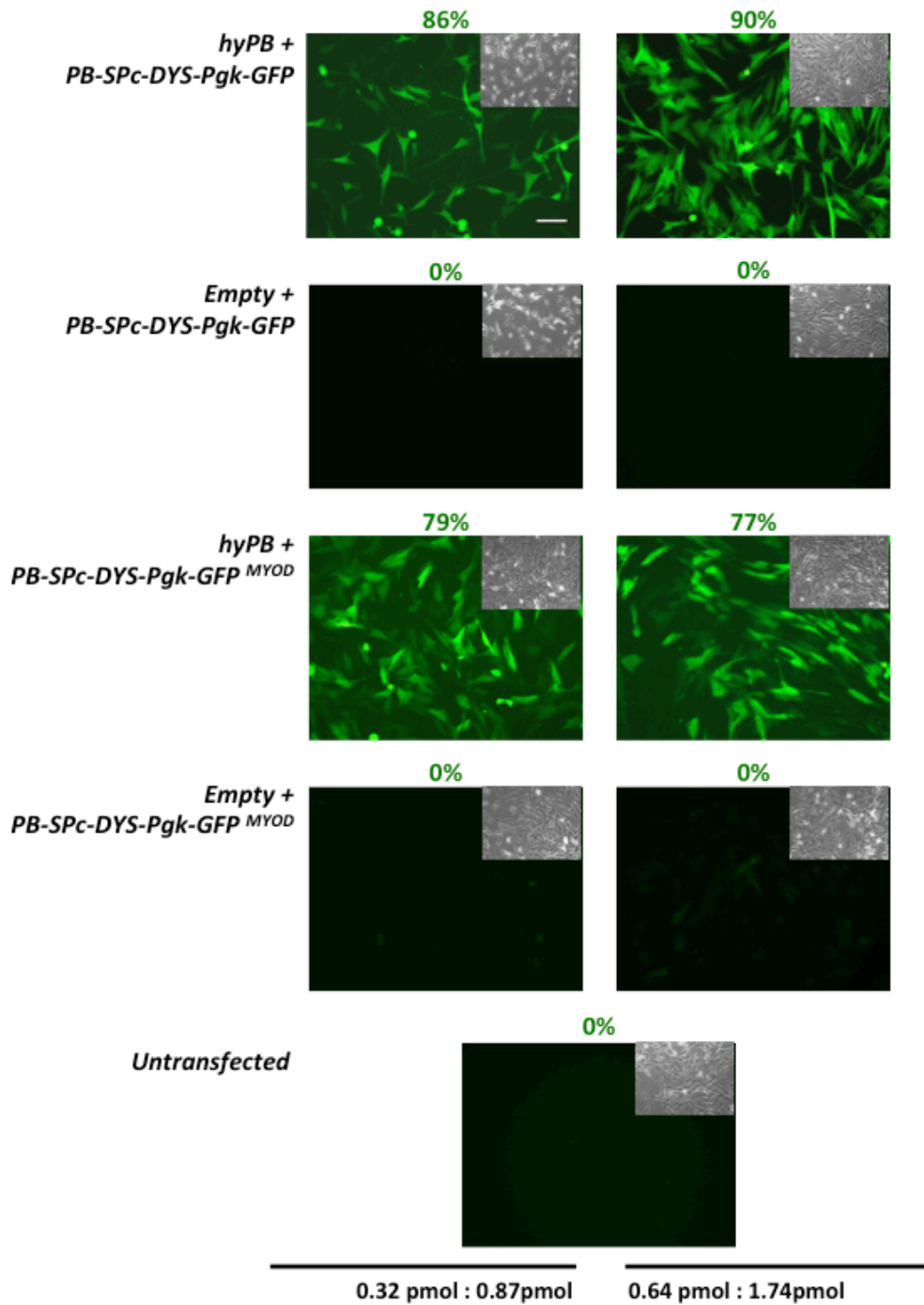


Figure 14. Stable GFP expression after transposition of the large size transposon PB-SPc-DYS-Pgk-GFP. Live cell imaging of DMD HIDE M and DMD HIDE M^{MYOD} cells transfected with hyPB and the large size transposon PB-SPc-DYS-Pgk-GFP. Pictures acquired at 45 days post-EP by fluorescence microscopy show the stable expression of

the GFP reporter in DMD HIDEM and DMD HIDEM^{MYOD} cells at the concentration of 0.32 pmol transposase DNA: 0.87 pmol transposon DNA and 0.64 pmol transposase DNA: 1.74 pmol transposon DNA. As negative controls, cells transfected with the empty plasmid and PB-Pgk-GFP transposons and untransfected cells are also shown. Above the pictures, the percentage of GFP+ cells acquired by the fluorescence-activated cell sorter is reported. Scale bar 75 μ m.

4.2.3. Correction of DMD HIDEM or DMD HIDEM^{MYOD} cells mediated by PB transposons coding for full-length human dystrophin CDS

As described above, according to one protocol DMD HIDEMs transfected with the PB transposons were subsequently transduced with the tamoxifen-regulated MyoD-ER (T) LV vectors followed by the tamoxifen-mediated induction of myogenic differentiation (Figure 12). Alternatively, the DMD HIDEM^{MYO} cells, that were first transduced with the MyoD-ER(T) LV vector and subsequently transfected with the PB transposons, were also subjected to tamoxifen to induce myogenic differentiation.

Transcription levels of the full-length human dystrophin were detected by quantitative reverse transcriptase PCR (qRT-PCR) in DMD HIDEMs transfected with *hyPB* and *PB-SPc-DYS-Pgk-GFP*, either in a proliferative state or in terminally differentiated myotubes (Figure 15A). Similarly, the expression of the GFP mRNA was confirmed by qRT-PCR in DMD HIDEMs transfected with *hyPB* and *PB-SPc-DYS-Pgk-GFP* or the small size transposon *PB-Pgk-GFP*. In contrast, dystrophin and GFP transcripts were not detected in cells derived from the control DMD HIDEMs that were either non-transfected or transfected with the transposons without *hyPB* transposase (Figure 15A). This again provided independent confirmation that *hyPB* transposase-mediated transposition was required for stable GFP and dystrophin gene expression.

To ascertain the full-length size of the human dystrophin transcript encoded by the PB transposons, an RT-PCR was performed to amplify three different regions corresponding to the N-terminal, the central and the C-terminal sequences of the full-length dystrophin transcript, as described in (Loperfido et al., 2015b). The three corresponding PCR bands were detected in the differentiated DMD HIDEM

or DMD HIDEM^{MYOD} cells where the transposon *PB-SPc-DYS-Pgk-GFP* integrated upon co-transfection with *hyPB* transposase confirming the presence of the full-length dystrophin transcript (Figure 15B, S4). In contrast, these bands were absent in untreated cells or when an empty transposase plasmid was used. Consistent with the expression results at the transcriptional level, expression of the full-length human dystrophin protein (427 kDa) was detected by Western blot analysis in differentiated DMD HIDEM cells genetically corrected with the *hyPB* transposase and *PB-SPc-DYS-Pgk-GFP* transposon, upon myogenic differentiation *in vitro* (Figure 15C). In contrast, the dystrophin protein could not be detected in differentiated cells derived from untransfected DMD HIDEMs or in differentiated DMD HIDEMs that were co-transfected with *PB-SPc-DYS-Pgk-GFP* and an empty expression plasmid without transposase. Normal skeletal muscle cells differentiated into myotubes *in vitro* were used as positive control. These data were confirmed by using the immunofluorescence assay where the expression of the full-length human dystrophin protein co-localized with the expression of GFP and myosin in multinucleated myotubes of genetically corrected DMD HIDEMs (Figure 15D). Similarly, GFP protein expression was detected in differentiated DMD HIDEMs transfected with the *hyPB* transposase and small size *PB-Pgk-GFP* transposon (Figure 13B). Dystrophin and GFP were not detectable in the control cells (i.e. in the absence of transposase in transfected cells or in untransfected cells), indicating that transposition is required for the stable and prolonged gene expression into the target cells.

Collectively, these results demonstrate that it is possible to genetically correct DMD patient-specific iPSC-derived myogenic cells using a *PB* transposon system encoding the full-length human dystrophin.

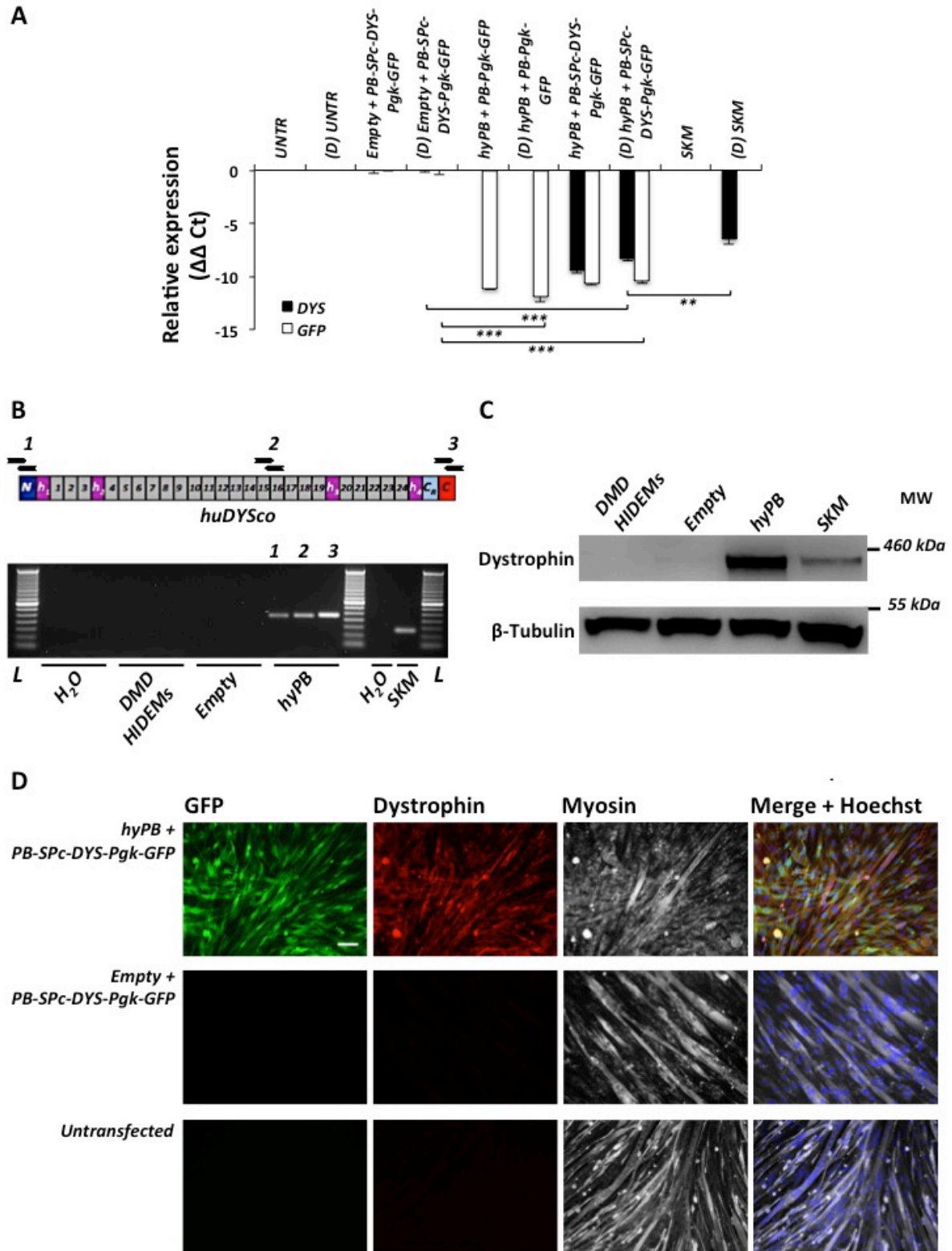


Figure 15. PB-mediated genetic correction of DMD HIDEMs. (A) Bar graph depicting the transcription levels of the full-length human dystrophin (black bars) and GFP (white bars) detected by qRT-PCR analysis in DMD HIDEMs transfected with hyPB and PB-

SPc-DYS-Pgk-GFP or *PB-Pgk-GFP*, when in proliferation or in differentiated myotubes (D: differentiated sample; UNTR: untransfected DMD HIDEs; SKM: skeletal muscle cells). The transcription levels were not detected in untransfected cells or when the empty plasmid devoid of any transposase was used. Data were normalized to the GAPDH housekeeping gene. Shown is mean \pm SEM, n=3 technical repeats, of one experiment, representative of 3 biological repeats; two-tailed unpaired Student's t-test ($***P \leq 0.001$; $**P \leq 0.01$). **(B)** RT-PCR showing expression of full-length human dystrophin transcript in differentiated DMD HIDEs that had undergone transposition after co-transfection with *hyPB* and *PB-SPc-DYS-Pgk-GFP*. Three different primer pairs were used that recognize respectively (1) the N-terminal, (2) a central region and (3) the C-terminal sequences, yielding amplicons of 221 bp, 222 bp and 228 bp, respectively. A schematic representation of the PCR primers relative to the different regions of the dystrophin transcript is depicted above the picture. Negative controls included differentiated untreated DMD HIDEs and differentiated DMD HIDEs co-transfected with the *PB-SPc-DYS-Pgk-GFP* transposon and an empty expression plasmid without transposase (designated as Empty). Normal skeletal muscle (SKM) cells differentiated in myotubes were used as a positive control; the primer pairs *DYS* listed in Table 5 have been used for this sample. L: 50 bp ladder. **(C)** Western blot analysis showing the expression of the full-length human dystrophin protein (427 kDa) in DMD HIDEs genetically corrected with *hyPB* + *PB-SPc-DYS-Pgk-GFP* and upon myogenic differentiation *in vitro*. The full-length human dystrophin protein was confirmed in normal skeletal muscle (SKM) cells differentiated in myotubes *in vitro*. As negative controls, differentiated untransfected DMD HIDEs or co-transfected with the *PB-SPc-DYS-Pgk-GFP* transposon and an empty expression plasmid without transposase (designated as Empty) were included. β -Tubulin (50 kDa) was used to normalize the amount of loaded proteins (MW: molecular weight). **(D)** Immunofluorescence assay depicting the co-localized expression of GFP (in green), full-length dystrophin (in red) and myosin (in white) in DMD HIDEs genetically corrected with *hyPB* + *PB-SPc-DYS-Pgk-GFP* and differentiated in multinucleated myotubes upon over-expression of tamoxifen-inducible *MyoD-ER(T)*. Expression of GFP and dystrophin was absent in differentiated DMD HIDEs co-transfected with the empty plasmid and in differentiated untransfected DMD HIDEs. Scale bar 75 μ m.

4.2.4. Transplantation of genetically corrected DMD HIDEM^{MYOD} cells in scid/mdx mice and safety

Transplantation of genetically corrected DMD HIDEM^{MYOD} cells was performed intramuscularly in scid/mdx mice as previously described (Gerli et al., 2014). This animal model of DMD lacks functional B and T lymphocytes, thus allowing the evaluation of engraftment and regenerative potential of DMD genetically corrected cells in dystrophic mice avoiding a possible immune rejection against xenogeneic and manipulated cells. Scid/mdx mice were pretreated with intraperitoneal injections of tamoxifen during the three days prior to- and post-transplantation, once a day. This would allow the transplanted cells, previously transduced with the tamoxifen-inducible MyoD(ER) cassette, to be exposed to levels of tamoxifen necessary to activate and synchronize their myogenic differentiation *in vivo* (Gerli et al., 2014; Tedesco et al., 2012). The genetically corrected DMD HIDEM^{MYOD} cells were as well pretreated with tamoxifen for 24 hours and injected in the *tibialis anterior* (or *gastrocnemius*) muscles of the scid/mdx mice. As positive controls, HIDEMs generated from healthy donors transduced with MyoD-ER(T) LV vectors were also transplanted. Muscles injected with PBS were used as negative controls.

Transplanted and control muscles were harvested at 1 week and 3 weeks after the injection and processed. Cell engraftment and differentiation were then assessed by immunofluorescence assay on the transplanted muscles. An antibody against Lamin A/C was used to detect grafted human cell nuclei, while a combination of two antibodies against respectively the central domain and C-terminal region of the dystrophin were used to detect donor-derived restoration of the protein absent in the dystrophic mice. An antibody against laminin was employed to visualize the overall structure of the muscle. The genetically corrected DMD HIDEM^{MYOD} cells engrafted in the host muscles and were able to express the full-length human dystrophin mediated by the *PB* transposon into the recipient skeletal muscle fibers, one week after the transplantation (Figure 16A, 16B). Accordingly, the healthy donor HIDEMs were also detected in the injected

muscles and were able to express the human dystrophin, correctly localized on the myofiber membrane (Figure 16A).

In order to assess the safety of the manipulated cells for *in vivo* applications, a tumor formation assay was performed. DMD HIDEMs co-transfected with *hyPB* transposase and *PB-SPc-DYS-Pgk-GFP* transposon (n= 8) or *PB-Pgk-GFP* transposon (n= 8) and transduced with MyoD-ER(T) LV vectors were injected subcutaneously in immunodeficient nude mice. As controls, untransfected DMD HIDEMs with and without MyoD-ER(T) LV vector transduction (n= 4 and n= 2, respectively) were utilized. HeLa cells, a tumorigenic cell line, were injected as a positive control (n= 2). After 4 months, no tumors developed in nude mice transplanted with the different HIDEM cell lines (n= 22). In contrast, tumor formation was observed in the nude mice transplanted with HeLa cells after 1 month (Figure 17). This is consistent with previous reports demonstrating the non-tumorigenic nature of the HIDEMs (Tedesco et al., 2012) and the safety of *PB* transposons as delivery tools for gene therapy (Di Matteo et al., 2014b).

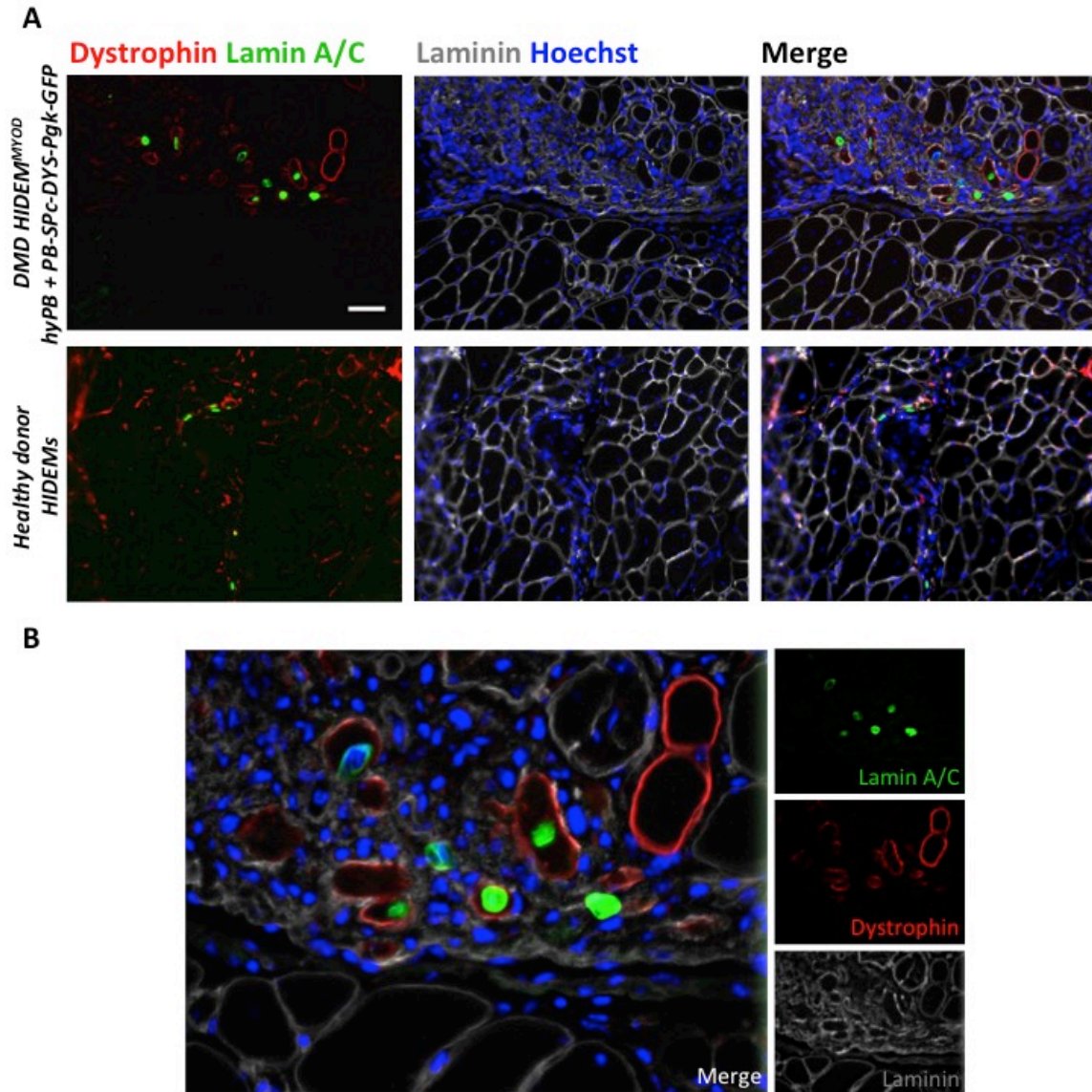


Figure 16. PB-mediated full-length dystrophin expression in scid/mdx mice upon transplantation of genetically corrected DMD *HIDEM*^{MYOD} cells. (A) Immunofluorescence staining of a section of tibialis anterior muscle of scid/mdx mice (upper panel) after intramuscular injection of 1×10^6 DMD *HIDEM*^{MYOD} cells genetically corrected with hyPB and PB-SPc-DYS-Pgk-GFP. The muscle showed the engraftment of the cells as revealed by a cluster of myofibers positive for the dystrophin (in red) containing donor human cell nuclei positive for lamin A/C (in green) a week after the intramuscular transplantation. Revertant fibers from scid/mdx mice can also be identified by the expression of the dystrophin and the absence of lamin A/C positive nuclei. Laminin (in grey) was used to visualize the overall structure of the muscle. The nuclei were stained with Hoechst. As positive control, healthy donor *HIDEMs* engrafted in a

gastrocnemius muscle of *scid/mdx* mice were also showed (lower panel). Scale bar 75 μm . **(B)** Higher magnification of the immunofluorescence staining in (A).

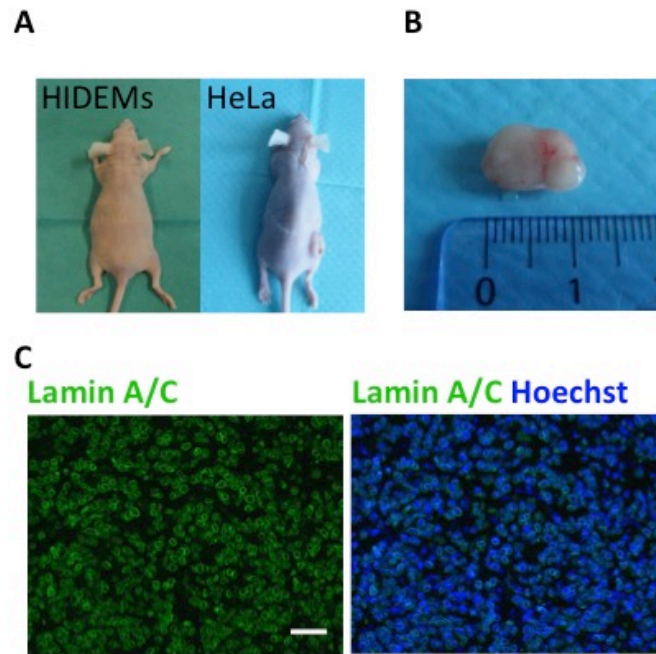


Figure 17. Tumor formation assay. **(A)** Pictures of nude mice transplanted subcutaneously respectively with DMD HIDEM^{MYOD} cells genetically corrected with hyPB + PB-SPc-DYS-Pgk-GFP (left mouse) and HeLa cells (right mouse). They were sacrificed respectively at 4 months and 1 month after the injection. Only nude mice injected with HeLa cells developed tumors. **(B)** Picture of a tumor developed from HeLa cells and harvested at necropsy. **(C)** Immunofluorescence staining for lamin A/C confirmed the human origin of the tumor from HeLa cells. Scale bar 75 μm .

Chapter 5

5. General conclusion

In this study, we have demonstrated that the hyperactive *piggyBac* (*PB*) transposon technology could be used to obtain stable expression of a therapeutically relevant, large-sized transgene such as the full-length human dystrophin coding DNA sequence (*CDS*). Myogenic stem/progenitor cells derived from a dystrophic large animal model for Duchenne muscular dystrophy (DMD) or generated from DMD patient-specific induced pluripotent stem cells (iPSCs) could be genetically corrected upon stable integration of the *PB* transposons into their genome. The expression of the full-length human dystrophin was successfully detected upon myogenic differentiation *in vitro* and transplantation in immunodeficient dystrophic mice *in vivo*. To our knowledge, this is the first report that ascertains the use of *PB* transposons coding for the full-length human dystrophin enabling genetic correction of dystrophic mesoangioblasts or DMD patient-specific iPSC-derived myogenic cells. It is particularly encouraging that genetically corrected DMD HIDEMs were able to express the therapeutic protein upon transplantation *in vivo* in immunodeficient dystrophic mice, without discernable adverse events. This establishes proof-of-concept and may ultimately pave the way towards a new non-viral gene therapy approach to treat DMD patients. This approach offers the possibility to express a functional copy of full-length dystrophin while regenerating new skeletal muscle. At variance with other methods, this approach could potentially be applied to all the different mutations observed in DMD patients and extended to other forms of muscular dystrophies. Further pre-clinical *in vivo* studies in large animal models are needed to ultimately justify a possible use of *PB* transposons expressing full-length human dystrophin in clinical trials for DMD.

Chapter 6

6. Discussion

Recent studies aimed to explore the use of transposons to investigate therapeutic strategies in muscular dystrophies, but these were limited to the use of reporter or marker genes (Ley et al., 2014; Muses et al., 2011a; Quattrocelli et al., 2011; Belay et al., 2010), truncated versions of either dystrophin or utrophin (Filareto et al., 2015, 2013; Muses et al., 2011b) or conditionally immortalized muscle cell-derived cell-lines (Muses et al., 2011a, 2011b) that cannot be clinically deployed. To our knowledge, this is the first report that establishes the use of transposons coding for the full-length human dystrophin enabling genetic correction of dystrophic primary cells or derived from dystrophic iPSCs.

The main advantage of *PB* transposons is that they efficiently integrate their cargo into the target cell genome. This property enables robust stable gene expression in both human and mouse cells, *ex vivo* or *in vivo* (reviewed in (Di Matteo et al., 2012; VandenDriessche et al., 2009); (Di Matteo et al., 2014a; Matsui et al., 2014; Doherty et al., 2012; Yusa et al., 2011; Nakazawa et al., 2009; Ding et al., 2005)). This attribute is particularly relevant for stable genetic modification of stem/progenitor cells and pluripotent stem cells given their intrinsic self-renewal and differentiation potential (Belay et al., 2011). As we observed in this study, *PB* transposons can integrate and yield sustained dystrophin expression in dystrophic MABs isolated from the Golden Retriever muscular dystrophy dog and mesoangioblast-like cells derived from DMD patient-specific iPSCs (HIDEMs) upon their myogenic differentiation.

In contrast, in the absence of any transposase-expressing construct, transgene expression lasted only for short term. This indicates that *bona fide* transposition was a prerequisite for robust dystrophin expression in dystrophic MABs and HIDEMs. It is known that transfection of conventional plasmids results in a very low stable integration frequency (typically 1 stable integrant per 10^5 transfected

cells) (Izsvák et al., 2009; VandenDriessche et al., 2009), consequently hampering its potential clinical applications.

The efficiency of *PB* transposon-mediated delivery of the full-length human dystrophin *CDS* compares favorably with alternative approaches that allowed the production of the wild-type full-length dystrophin protein, such as the human artificial chromosome (HAC; (Tedesco, 2015; Kouprina et al., 2014)). This vector is recognized as an endogenous chromosome within the host cells and is stably maintained throughout subsequent cell divisions obviating the need for genomic integration. The entire human dystrophin genomic locus (2.4 Mb), including the native promoter and regulatory elements, has been accommodated into the HAC (Hoshiya et al., 2009) and transferred in dystrophic mesoangioblasts isolated from *mdx* mice and in DMD patient-specific iPSCs (Tedesco et al., 2011; Kazuki et al., 2010). This approach resulted in full-length human dystrophin expression in the genetically corrected cells. However, the generation of such a relatively complex vector like HAC, together with the low efficiency of microcell-mediated chromosome transfer (MMCT; approximately 1.2×10^{-5}) required to introduce HACs into the target cells, may limit the application of this technology only to clonogenic stem/progenitor cells with high proliferation potential. On the other hand, the use of *PB* transposons is at least 10^4 -fold more efficient than MMCT and may ease the manufacturing constraints compared to MMCT or viral vectors, ultimately facilitating ultimate clinical translation of the *PB* transposon vectors.

Another advantage of the *PB* transposons is that they enabled stable delivery of the full-length human dystrophin *CDS* together with a reporter marker (insert size: 13.7 kb). This exceeds the packaging capacity of γ -retroviral and lentiviral vectors (< 10 kb) and AAV vectors (~5 kb). Consequently, this obviates concerns associated with the use of truncated dystrophins that may not replicate all of the necessary functions of its wild-type counterpart (Sampaolesi et al., 2006). Moreover, expression of full-length human dystrophin is broadly applicable to all patients suffering from DMD, regardless of the underlying genetic defect in the dystrophin locus. This is in contrast with other approaches that are restricted in

their application to correcting specific mutations of the gene, such as exon-skipping strategies or the use of engineered nucleases, although advances in these fields to target multiple mutations are under investigation (Ousterout et al., 2015b; Echigoya and Yokota, 2014). The ability of *PB* transposons to deliver such a relatively large cargo is consistent with previous reports indicating that *PB* transposons can mediate the transfer of large genetic cargos up to 100 kb (Li et al., 2011; Ding et al., 2005). The availability of *PB* transposons encoding either full-length or truncated dystrophin *CDS* characterized in this study may pave the way towards future comprehensive structure-function and comparative studies. Indeed, the present study has broader implications for the use of other hyperactive transposon systems, such as *Sleeping Beauty* for gene therapy of DMD (Muses et al., 2011b; Grabundzija et al., 2010; Huang et al., 2010).

In the present study, we have used nucleofection technology, an electroporation-based transfection method that allows to transfer the DNA plasmids directly into the nuclei and the cytoplasm of both dividing and non-dividing the cells *in vitro* (Izsvák et al., 2009; Hollis et al., 2006). This technique overcomes the limitations related to other transfection methods that rely on nuclear import of plasmid DNA in non-dividing cells (Al-Dosari and Gao, 2009; Midoux et al., 2009). The transfection efficiency of *hyPB* transposase and the large size *PB* transposon in DMD HIDEs was within the range of what could be obtained in dystrophic MABs. Nevertheless, large-size DNA plasmids adversely impact on the transfection efficiency (Sharma et al., 2013). In accordance with these previous findings, we showed that the use of large transgenes (i.e. full-length human dystrophin *CDS*) as opposed to smaller transgenes (i.e. truncated MD1 and MD2 human microdystrophin *CDS*, GFP transgene) adversely impacts on the transfection efficiency in MABs and HIDEs. This may be due, at least in part, to the intrinsic property of the DNA plasmids such as the presence of unmethylated CpG motifs in the backbone sequences that might impair cell viability, possibly involving Toll-like receptor (TLR) pathways (Reyes-Sandoval and Ertl, 2004; Krieg et al., 1995). Indeed, plasmids with a low content in CpG motifs confer

long-term gene expression with less toxicity (Hyde et al., 2008; Yew et al., 2001). Alternatively, transfection efficiency may also have been affected by impaired nuclear import of plasmid DNA due to reduced cytosolic mobility of large size plasmid DNA (Lukacs et al., 2000).

We demonstrated that the use of the hyperactive *PB* transposase (Yusa et al., 2011) compared to the non-hyperactive *mPB* transposase (Cadiñanos and Bradley, 2007) can boost the efficiency and stable expression of large-size transposons. After nucleofection, the surviving transfected cells could be easily enriched by FACS sorting yielding more than 50% GRMD MABs and 80 to 90% DMD HIDEs that had undergone stable transposition, as confirmed from the presence of *PB* transposon copies integrated in the genome of in these cells. Nevertheless, it may be worthwhile to further explore alternative strategies to augment the overall transfection efficiency, viability and expression of the therapeutic gene. This could potentially be achieved by using a minicircle-based transposon system, devoid of any bacterial backbone sequence, as recently validated for *Sleeping Beauty* (Sharma et al., 2013). Consequently, this would reduce the plasmid size, lower CpG content, increase transfection efficiency and decrease DNA toxicity. Alternatively, more potent muscle-specific promoters in combination with enhancers could be used to drive expression of the full-length dystrophin *CDS* (Jonuschies et al., 2014; Rincon et al., 2014; De Bleser et al., 2007).

The therapeutic relevance of MABs, even after prolonged *in vitro* culture, has been highlighted in many previous studies (Domi et al., 2015; Tedesco et al., 2011; Díaz-Manera et al., 2010; Sampaolesi et al., 2006; Palumbo et al., 2004; Sampaolesi et al., 2003). Their intrinsic capability to cross the wall vessels when injected intra-arterially and to contribute to the muscle regeneration in animal models has represented a substantial advantage over other muscle stem cells (i.e. myoblasts) (Dellavalle et al., 2007). We have confirmed the characteristic phenotype of the MABs used in our study based on the expression of adult dog

MAB markers and their ability to undergo myogenic differentiation *in vitro*. As reported in the literature (Sampaolesi et al., 2006), adult dog MABs have a myogenic potential that is activated upon fusion with myoblasts or after exposure to MyoD. Accordingly, in our study genetically corrected GRMD mesoangioblasts were transduced to express the tamoxifen-inducible MyoDER(T) and undergo myogenic differentiation at late passage *in vitro* (i.e. passage P15-18).

According to previous and recent studies on human MABs, a high proliferation rate has been observed for approximately 20 population doublings, with a doubling time of approximately 36 h (Cossu et al., 2015; Dellavalle et al., 2007) without compromising their stem cell properties. Though the initial transfection efficiency in GRMD MABs was about 3%, we could rapidly enrich for those cells that had undergone stable transposition by FACS sorting, thus avoiding protracted cell culture.

Dystrophin levels corresponding to 30% of the levels normally found in healthy individuals and in animal models are sufficient to prevent muscular dystrophy (Neri et al., 2007; Wells et al., 1995). In accordance with these data, pre-clinical studies based on the use of MABs have shown a therapeutic effect in dystrophic mice and dogs with dystrophin expression ranging 5 to 30% of normal levels (Tedesco et al., 2011; Sampaolesi et al., 2006). This has been achieved by injecting 1×10^6 cells/muscle in the mouse and 5×10^7 cells/kg in the dog model. Considering treatment of pediatric subjects with less advanced muscle disease and more likely to benefit from this cell therapy, this would translate into a total cell dose of 75×10^7 MABs in a 15 kg patient although the possibility of repeated injection to reach efficacy still needs to be investigated. Up to 2×10^9 human MABs can readily be obtained after *in vitro* expansion of initial cells isolated from a single muscle biopsy (100–200 mg) (Cossu et al., 2015; Dellavalle et al., 2007). Based on our current results, we estimated that 9×10^8 stably transfected GRMD MABs expressing dystrophin after *PB*-mediated transposition could be obtained 35 days post-transfection of 3×10^6 cells. Consequently, the required dose to treat pediatric DMD patients is within reach. It is encouraging that initially more MABs

outgrew from explants of young DMD patients (Dellavalle et al., 2007) suggesting that the yield of MABs and/or their proliferative capacity may possibly be even higher in younger than in older patients with advanced disease.

Allogeneic MABs have recently been tested in a first-in-human phase I/II clinical trial in DMD patients under immunosuppressive treatment (EudraCT N° 2011-000176-33, (Cossu et al., 2015)). Administration at escalating doses of HLA-matched donor MABs in the limb arteries of the patients was considered relatively safe, which was the primary endpoint of the study. One patient developed an acute thalamic stroke with no clinical consequences but it was unclear whether it correlated with the MAB infusion. Muscle biopsies confirmed the presence of donor DNA in 4/5 patients and expression of donor dystrophin in one patient. Though no functional improvements were observed in the treated patients, functional measures stabilized in 2/3 ambulant patients. The study also provided insights to further improve efficacy by enrolling younger patients with less advanced muscle disease and/or increase the MAB dose. Moreover, the use of gene-modified autologous MABs may further augment the efficacy with the added advantage over allogeneic MABs that immune suppression may not be needed in this case.

Though MABs can be expanded extensively for 20 passages and exhibit a remarkable proliferative potential, their lifespan is nonetheless limited (Tonlrenzi et al., 2007). This likely reflected normal cellular processes that gradually contribute to cellular senescence (Holliday, 2014). In addition, the *PB* transposon technology is potentially amenable to be used in alternative adult myogenic stem cell sources distinct from MABs (Costamagna et al., 2015; Benedetti et al., 2013). Ultimately, the use of iPSC-derived myogenic cells, that have unlimited expansion potential, may represent an attractive alternative, provided they can safely and efficiently be converted into transplantable myogenic cells (reviewed in (Loperfido et al., 2015a)). Therefore, in the present study we have validated the use of *PB* transposon system coding for the full-length dystrophin to genetically

corrected HIDEs, generated from a DMD patient (Tedesco et al., 2012). As previously described in our studies, a stepwise protocol for differentiating pluripotent stem cells towards the mesodermal lineage allowed the generation of the DMD HIDEs (Maffioletti et al., 2015). These cells resemble mesoangioblasts for morphology, surface markers and gene expression profile. Nevertheless, HIDEs show unlimited proliferation capacity in contrast to most primary myogenic cells. Upon tamoxifen-inducible MyoD overexpression, the myogenic differentiation of HIDEs could be accomplished *in vitro* or after transplantation into immune-deficient dystrophic mice *in vivo* (Maffioletti et al., 2015; Gerli et al., 2014; Tedesco et al., 2012). Although a synchronized activation and differentiation has been observed in the whole culture *in vitro*, the analysis of the temporal control of the tamoxifen on the myogenic activation of the HIDEs (or MIDEs) *in vivo* needs further investigation. The use of muscle-specific promoters and enhancer elements could be employed to circumscribe the activation of the tamoxifen-driven myogenic differentiation to the muscle compartment and improve the strategy. Nevertheless, other methods can also be used to provide MyoD for myogenic differentiation, as reviewed in (Loperfido et al., 2015a).

In the current study, DMD HIDEs were transduced with inducible MyoD-ER LV vectors before or after the transfection with the *PB* transposons and myogenic differentiation was subsequently induced by tamoxifen. The ability of the genetically corrected DMD HIDEs to engraft in skeletal muscle and produce the *PB*-mediated full-length human dystrophin upon differentiation *in vivo* was validated in immunodeficient dystrophic scid/mdx mice. Upon tamoxifen administration and intra-muscular cell transplantation, the presence of human cell nuclei and the restoration of the dystrophin expression were detected in the fiber membrane of the transplanted muscles by immunofluorescence staining. These results establish a proof of concept for a gene therapy platform based on the combination of non-viral vectors able to deliver the full-length human dystrophin and transplantable DMD patient-specific iPSC derived myogenic cells.

Nevertheless, previous studies have shown that the engraftment of HIDEs upon intra-muscular injection in immunodeficient dystrophic mouse models is less efficient (i.e. five to six fold less) compared to when mouse counterpart (so called MIDEs, mouse iPSC-derived mesoangioblast-like cells) is employed (Gerli et al., 2014; Tedesco et al., 2012). This reflects the species-specific differences in survival, migration and differentiation that depend largely on the interaction of the transplanted cells with the host microenvironment (Maffioletti et al., 2015). On the other hand, studies based on murine muscle stem/progenitor cells -or their cognate myogenic ESC/iPSC derivatives may not necessarily replicate all of the features of their human counterparts in a clinical setting. Therefore, further *in vivo* studies employing the use of dystrophic mouse models with a more profound immune deficiency than the mild model of mdx (i.e. combined lack of T, B and NK cells; (Arpke et al., 2013; Vallese et al., 2013)) are needed to better investigate the efficiency and efficacy of the xenogenic engraftment of the genetically corrected DMD HIDEs upon intra-muscle and intra-arterial transplantation. The use of an appropriate immunodeficient dystrophic mouse model to test genetically corrected DMD HIDEs would increase the efficiency of engraftment and the stable expression of the therapeutic protein, thus providing valuable information about their application in therapy approaches of muscular dystrophies (Tedesco et al., 2012).

Though genomic integration of *PB* transposons is required for sustained expression in dividing and differentiating stem/progenitor cells, it could raise some concerns related to the risk of insertional oncogenesis by potentially activating oncogenes that are in the vicinity of the integration sites (Biasco et al., 2012). From a recent study, it emerges that *PB* transposons exhibit a random integration pattern in the genome of murine mesoangioblasts suggesting that in these cells they do not preferentially integrate into genes and their regulatory regions (Ley et al., 2014). However, further investigation on larger sampling is needed. This risk of insertional oncogenesis could be even minimized by retargeting *PB*-mediated integration into potential 'safe harbor' loci (Kettlun et al.,

2011; Wilson and George, 2010). However, it is reassuring that the *PB* transposon copy number detected in the present study fell within an acceptable and relatively safe range of genomic integrations per cell (i.e. 0.5-1.7 copies per diploid genome), in accordance with the European medicines agency guidelines (http://www.ema.europa.eu/ema/index.jsp?curl=pages/regulation/general/general_content_000410.jsp&mid=WC0b01ac058002958d).

Notably, in a tumor formation assay we have assessed that DMD HIDEMs manipulated with the *hyPB* transposase and the *PB* transposons, with or without MyoD-ER LV infection, do not generate tumors. This is consistent with other studies that demonstrated the non-tumorigenic nature of HIDEMs (Tedesco et al., 2012). Moreover, the safety profile of the *PB* transposon system as an integrating non-viral system gene delivery tool has been previously validated in tumor-prone mouse models (Di Matteo et al., 2014). More exhaustive safety studies are needed in sensitive model systems to assess the potential risk of insertional oncogenesis using these hyperactive *PB* transposons when used in conjunction with myogenic stem/progenitor cells.

References

- Aartsma-Rus, A., Ginjaar, I.B., and Bushby, K. (2016). The importance of genetic diagnosis for Duchenne muscular dystrophy. *J. Med. Genet.*
- Abujarour, R., Bennett, M., Valamehr, B., Lee, T.T., Robinson, M., Robbins, D., Le, T., Lai, K., and Flynn, P. (2014). Myogenic differentiation of muscular dystrophy-specific induced pluripotent stem cells for use in drug discovery. *Stem Cells Transl. Med.* **3**, 149–160.
- Aiuti, A., Biasco, L., Scaramuzza, S., Ferrua, F., Cicalese, M.P., Baricordi, C., Dionisio, F., Calabria, A., Giannelli, S., Castiello, M.C., et al. (2013). Lentiviral hematopoietic stem cell gene therapy in patients with Wiskott-Aldrich syndrome. *Science* **341**, 1233151.
- Al-Dosari, M.S., and Gao, X. (2009). Nonviral gene delivery: principle, limitations, and recent progress. *AAPS J.* **11**, 671–681.
- Al-Zaidy, S., Rodino-Klapac, L., and Mendell, J.R. (2014). Gene therapy for muscular dystrophy: moving the field forward. *Pediatr. Neurol.* **51**, 607–618.
- Arechavala-Gomez, V., Kinali, M., Feng, L., Guglieri, M., Edge, G., Main, M., Hunt, D., Lehovsky, J., Straub, V., Bushby, K., et al. (2010). Revertant fibres and dystrophin traces in Duchenne muscular dystrophy: implication for clinical trials. *Neuromuscul Disord.* **20**, 295–301.
- Arpke, R.W., Darabi, R., Mader, T.L., Zhang, Y., Toyama, A., Lonetree, C.-L., Nash, N., Lowe, D.A., Perlingeiro, R.C.R., and Kyba, M. (2013). A new immuno-, dystrophin-deficient model, the NSG-mdx(4Cv) mouse, provides evidence for functional improvement following allogeneic satellite cell transplantation. *Stem Cells Dayt. Ohio* **31**, 1611–1620.
- Athanasopoulos, T., Foster, H., Foster, K., and Dickson, G. (2011). Codon optimization of the microdystrophin gene for Duchene muscular dystrophy gene therapy. *Methods Mol. Biol. Clifton NJ* **709**, 21–37.
- Bachrach, E., Li, S., Perez, A.L., Schienda, J., Liadaki, K., Volinski, J., Flint, A., Chamberlain, J., and Kunkel, L.M. (2004). Systemic delivery of human microdystrophin to regenerating mouse dystrophic muscle by muscle progenitor cells. *Proc. Natl. Acad. Sci. U. S. A.* **101**, 3581–3586.
- Barton, E.R., Morris, L., Musaro, A., Rosenthal, N., and Sweeney, H.L. (2002). Muscle-specific expression of insulin-like growth factor I counters muscle decline in mdx mice. *J. Cell Biol.* **157**, 137–148.
- Barton-Davis, E.R., Cordier, L., Shoturma, D.I., Leland, S.E., and Sweeney, H.L. (1999). Aminoglycoside antibiotics restore dystrophin function to skeletal muscles of mdx mice. *J. Clin. Invest.* **104**, 375–381.
- Baus, J., Liu, L., Heggstad, A.D., Sanz, S., and Fletcher, B.S. (2005). Hyperactive transposase mutants of the Sleeping Beauty transposon. *Mol. Ther.* **12**, 1148–1156.

Belay, E., Mátrai, J., Acosta-Sanchez, A., Ma, L., Quattrocelli, M., Mátés, L., Sancho-Bru, P., Geraerts, M., Yan, B., Vermeesch, J., et al. (2010). Novel hyperactive transposons for genetic modification of induced pluripotent and adult stem cells: a nonviral paradigm for coaxed differentiation. *Stem Cells Dayt. Ohio* 28, 1760–1771.

Belay, E., Dastidar, S., VandenDriessche, T., and Chuah, M.K.L. (2011). Transposon-mediated gene transfer into adult and induced pluripotent stem cells. *Curr. Gene Ther.* 11, 406–413.

Benchaouir, R., and Goyenvalle, A. (2012). Splicing modulation mediated by small nuclear RNAs as therapeutic approaches for muscular dystrophies. *Curr. Gene Ther.* 12, 179–191.

Benedetti, S., Hoshiya, H., and Tedesco, F.S. (2013). Repair or replace? Exploiting novel gene and cell therapy strategies for muscular dystrophies. *FEBS J.* 280, 4263–4280.

Béroud, C., Tuffery-Giraud, S., Matsuo, M., Hamroun, D., Humbertclaude, V., Monnier, N., Moizard, M.-P., Voelckel, M.-A., Calemard, L.M., Boisseau, P., et al. (2007). Multiexon skipping leading to an artificial DMD protein lacking amino acids from exons 45 through 55 could rescue up to 63% of patients with Duchenne muscular dystrophy. *Hum. Mutat.* 28, 196–202.

Berry, C., Hannenhalli, S., Leipzig, J., and Bushman, F.D. (2006). Selection of target sites for mobile DNA integration in the human genome. *PLoS Comput. Biol.* 2, e157.

Biasco, L., Baricordi, C., and Aiuti, A. (2012). Retroviral integrations in gene therapy trials. *Mol. Ther.* 20, 709–716.

Biémont, C. (2009). Are transposable elements simply silenced or are they under house arrest? *Trends Genet. TIG* 25, 333–334.

Biffi, A., Montini, E., Lorioli, L., Cesani, M., Fumagalli, F., Plati, T., Baldoli, C., Martino, S., Calabria, A., Canale, S., et al. (2013). Lentiviral hematopoietic stem cell gene therapy benefits metachromatic leukodystrophy. *Science* 341, 1233158.

Bladen, C.L., Salgado, D., Monges, S., Foncuberta, M.E., Kekou, K., Kosma, K., Dawkins, H., Lamont, L., Roy, A.J., Chamova, T., et al. (2015). The TREAT-NMD DMD Global Database: analysis of more than 7,000 Duchenne muscular dystrophy mutations. *Hum. Mutat.* 36, 395–402.

Blake, D.J., Weir, A., Newey, S.E., and Davies, K.E. (2002). Function and genetics of dystrophin and dystrophin-related proteins in muscle. *Physiol. Rev.* 82, 291–329.

Boisgerault, F., and Mingozzi, F. (2015). The Skeletal Muscle Environment and Its Role in Immunity and Tolerance to AAV Vector-Mediated Gene Transfer. *Curr. Gene Ther.* 15, 381–394.

Bowers, W.J., Mastrangelo, M.A., Howard, D.F., Southerland, H.A., Maguire-Zeiss, K.A., and Federoff, H.J. (2006). Neuronal precursor-restricted transduction via in utero CNS

gene delivery of a novel bipartite HSV amplicon/transposase hybrid vector. *Mol. Ther.* **13**, 580–588.

Bowles, D.E., McPhee, S.W.J., Li, C., Gray, S.J., Samulski, J.J., Camp, A.S., Li, J., Wang, B., Monahan, P.E., Rabinowitz, J.E., et al. (2012). Phase 1 gene therapy for Duchenne muscular dystrophy using a translational optimized AAV vector. *Mol. Ther.* **20**, 443–455.

Brunelli, S., Sciorati, C., D'Antona, G., Innocenzi, A., Covarello, D., Galvez, B.G., Perrotta, C., Monopoli, A., Sanvito, F., Bottinelli, R., et al. (2007). Nitric oxide release combined with nonsteroidal antiinflammatory activity prevents muscular dystrophy pathology and enhances stem cell therapy. *Proc. Natl. Acad. Sci. U. S. A.* **104**, 264–269.

Brunetti-Pierri, N., Palmer, D.J., Beaudet, A.L., Carey, K.D., Finegold, M., and Ng, P. (2004). Acute toxicity after high-dose systemic injection of helper-dependent adenoviral vectors into nonhuman primates. *Hum. Gene Ther.* **15**, 35–46.

Burnight, E.R., Staber, J.M., Korsakov, P., Li, X., Brett, B.T., Scheetz, T.E., Craig, N.L., and McCray, P.B. (2012). A Hyperactive Transposase Promotes Persistent Gene Transfer of a piggyBac DNA Transposon. *Mol. Ther. Nucleic Acids* **1**, e50.

Bushby, K., Finkel, R., Birnkrant, D.J., Case, L.E., Clemens, P.R., Cripe, L., Kaul, A., Kinnett, K., McDonald, C., Pandya, S., et al. (2010a). Diagnosis and management of Duchenne muscular dystrophy, part 1: diagnosis, and pharmacological and psychosocial management. *Lancet Neurol.* **9**, 77–93.

Bushby, K., Finkel, R., Birnkrant, D.J., Case, L.E., Clemens, P.R., Cripe, L., Kaul, A., Kinnett, K., McDonald, C., Pandya, S., et al. (2010b). Diagnosis and management of Duchenne muscular dystrophy, part 2: implementation of multidisciplinary care. *Lancet Neurol.* **9**, 177–189.

Bushby, K., Finkel, R., Wong, B., Barohn, R., Campbell, C., Comi, G.P., Connolly, A.M., Day, J.W., Flanigan, K.M., Goemans, N., et al. (2014). Ataluren treatment of patients with nonsense mutation dystrophinopathy. *Muscle Nerve* **50**, 477–487.

Buyse, G.M., Voit, T., Schara, U., Straathof, C.S.M., D'Angelo, M.G., Bernert, G., Cuisset, J.-M., Finkel, R.S., Goemans, N., McDonald, C.M., et al. (2015). Efficacy of idebenone on respiratory function in patients with Duchenne muscular dystrophy not using glucocorticoids (DELOS): a double-blind randomised placebo-controlled phase 3 trial. *Lancet Lond. Engl.* **385**, 1748–1757.

Cadiñanos, J., and Bradley, A. (2007). Generation of an inducible and optimized piggyBac transposon system. *Nucleic Acids Res.* **35**, e87.

Cai, Y., Bak, R.O., Krogh, L.B., Staunstrup, N.H., Moldt, B., Corydon, T.J., Schrøder, L.D., and Mikkelsen, J.G. (2014). DNA transposition by protein transduction of the piggyBac transposase from lentiviral Gag precursors. *Nucleic Acids Res.* **42**, e28.

Cary, L.C., Goebel, M., Corsaro, B.G., Wang, H.G., Rosen, E., and Fraser, M.J. (1989). Transposon mutagenesis of baculoviruses: analysis of *Trichoplusia ni* transposon IFP2 insertions within the FP-locus of nuclear polyhedrosis viruses. *Virology* **172**, 156–169.

Cassano, M., Dellavalle, A., Tedesco, F.S., Quattrocchi, M., Crippa, S., Ronzoni, F., Salvade, A., Berardi, E., Torrente, Y., Cossu, G., et al. (2011). Alpha sarcoglycan is required for FGF-dependent myogenic progenitor cell proliferation in vitro and in vivo. *Dev. Camb. Engl.* *138*, 4523–4533.

Cavazzana-Calvo, M., Payen, E., Negre, O., Wang, G., Hehir, K., Fusil, F., Down, J., Denaro, M., Brady, T., Westerman, K., et al. (2010). Transfusion independence and HMGA2 activation after gene therapy of human β -thalassaemia. *Nature* *467*, 318–322.

Chamberlain, J.S., Metzger, J., Reyes, M., Townsend, D., and Faulkner, J.A. (2007). Dystrophin-deficient mdx mice display a reduced life span and are susceptible to spontaneous rhabdomyosarcoma. *FASEB J. Off. Publ. Fed. Am. Soc. Exp. Biol.* *21*, 2195–2204.

Chen, S., Shimoda, M., Chen, J., Matsumoto, S., and Grayburn, P.A. (2012). Ectopic transgenic expression of NKX2.2 induces differentiation of adult pancreatic progenitors and mediates islet regeneration. *Cell Cycle Georget. Tex* *11*, 1544–1553.

Cooper, B.J., Winand, N.J., Stedman, H., Valentine, B.A., Hoffman, E.P., Kunkel, L.M., Scott, M.O., Fischbeck, K.H., Kornegay, J.N., and Avery, R.J. (1988). The homologue of the Duchenne locus is defective in X-linked muscular dystrophy of dogs. *Nature* *334*, 154–156.

Cossu, G., and Bianco, P. (2003). Mesoangioblasts--vascular progenitors for extravascular mesodermal tissues. *Curr. Opin. Genet. Dev.* *13*, 537–542.

Cossu, G., Previtali, S.C., Napolitano, S., Cicalese, M.P., Tedesco, F.S., Nicastro, F., Noviello, M., Roostalu, U., Natali Sora, M.G., Scarlato, M., et al. (2015). Intra-arterial transplantation of HLA-matched donor mesoangioblasts in Duchenne muscular dystrophy. *EMBO Mol. Med.*

Costamagna, D., Berardi, E., Ceccarelli, G., and Sampaolesi, M. (2015). Adult Stem Cells and Skeletal Muscle Regeneration. *Curr. Gene Ther.*

Cui, Z., Geurts, A.M., Liu, G., Kaufman, C.D., and Hackett, P.B. (2002). Structure-function analysis of the inverted terminal repeats of the sleeping beauty transposon. *J. Mol. Biol.* *318*, 1221–1235.

De Bleser, P., Hooghe, B., Vlieghe, D., and van Roy, F. (2007). A distance difference matrix approach to identifying transcription factors that regulate differential gene expression. *Genome Biol.* *8*, R83.

Decary, S., Hamida, C.B., Mouly, V., Barbet, J.P., Hentati, F., and Butler-Browne, G.S. (2000). Shorter telomeres in dystrophic muscle consistent with extensive regeneration in young children. *Neuromuscul Disord.* *10*, 113–120.

Dellavalle, A., Sampaolesi, M., Tonlorenzi, R., Tagliafico, E., Sacchetti, B., Perani, L., Innocenzi, A., Galvez, B.G., Messina, G., Morosetti, R., et al. (2007). Pericytes of human skeletal muscle are myogenic precursors distinct from satellite cells. *Nat. Cell Biol.* *9*, 255–267.

Dellavalle, A., Maroli, G., Covarello, D., Azzoni, E., Innocenzi, A., Perani, L., Antonini, S., Sambasivan, R., Brunelli, S., Tajbakhsh, S., et al. (2011). Pericytes resident in postnatal skeletal muscle differentiate into muscle fibres and generate satellite cells. *Nat. Commun.* 2, 499.

Denti, M.A., Rosa, A., D'Antona, G., Sthandier, O., De Angelis, F.G., Nicoletti, C., Allocca, M., Pansarasa, O., Parente, V., Musarò, A., et al. (2006). Body-wide gene therapy of Duchenne muscular dystrophy in the mdx mouse model. *Proc. Natl. Acad. Sci. U. S. A.* 103, 3758–3763.

Díaz-Manera, J., Touvier, T., Dellavalle, A., Tonlorenzi, R., Tedesco, F.S., Messina, G., Meregalli, M., Navarro, C., Perani, L., Bonfanti, C., et al. (2010). Partial dysferlin reconstitution by adult murine mesoangioblasts is sufficient for full functional recovery in a murine model of dysferlinopathy. *Cell Death Dis.* 1, e61.

Di Matteo, M., Belay, E., Chuah, M.K., and Vandendriessche, T. (2012). Recent developments in transposon-mediated gene therapy. *Expert Opin. Biol. Ther.* 12, 841–858.

Di Matteo, M., Samara-Kuko, E., Ward, N.J., Waddington, S.N., McVey, J.H., Chuah, M.K.L., and Vandendriessche, T. (2014a). Hyperactive piggyBac transposons for sustained and robust liver-targeted gene therapy. *Mol. Ther.* 22, 1614–1624.

Di Matteo, M., Samara-Kuko, E., Ward, N.J., Waddington, S.N., McVey, J.H., Chuah, M.K.L., and Vandendriessche, T. (2014b). Hyperactive piggyBac transposons for sustained and robust liver-targeted gene therapy. *Mol. Ther.* 22, 1614–1624.

Ding, S., Wu, X., Li, G., Han, M., Zhuang, Y., and Xu, T. (2005). Efficient transposition of the piggyBac (PB) transposon in mammalian cells and mice. *Cell* 122, 473–483.

Doherty, J.E., Huye, L.E., Yusa, K., Zhou, L., Craig, N.L., and Wilson, M.H. (2012). Hyperactive piggyBac gene transfer in human cells and in vivo. *Hum. Gene Ther.* 23, 311–320.

Domi, T., Porrello, E., Velardo, D., Capotondo, A., Biffi, A., Tonlorenzi, R., Amadio, S., Ambrosi, A., Miyagoe-Suzuki, Y., Takeda, S., Ichi, et al. (2015). Mesoangioblast delivery of miniagrin ameliorates murine model of merosin-deficient congenital muscular dystrophy type 1A. *Skelet. Muscle* 5, 30.

Dominici, M., Le Blanc, K., Mueller, I., Slaper-Cortenbach, I., Marini, F., Krause, D., Deans, R., Keating, A., Prockop, D., and Horwitz, E. (2006). Minimal criteria for defining multipotent mesenchymal stromal cells. The International Society for Cellular Therapy position statement. *Cytotherapy* 8, 315–317.

Duan, D. (2015). Duchenne muscular dystrophy gene therapy in the canine model. *Hum. Gene Ther. Clin. Dev.* 26, 57–69.

Dumont, N.A., Wang, Y.X., von Maltzahn, J., Pasut, A., Bentzinger, C.F., Brun, C.E., and Rudnicki, M.A. (2015). Dystrophin expression in muscle stem cells regulates their polarity and asymmetric division. *Nat. Med.* 21, 1455–1463.

Echigoya, Y., and Yokota, T. (2014). Skipping multiple exons of dystrophin transcripts using cocktail antisense oligonucleotides. *Nucleic Acid Ther.* 24, 57–68.

Emery, A.E. (1993). Duchenne muscular dystrophy--Meryon's disease. *Neuromuscul Disord.* 3, 263–266.

Emery, A.E.H. (2002). The muscular dystrophies. *Lancet* 359, 687–695.

English, K., and Mahon, B.P. (2011). Allogeneic mesenchymal stem cells: agents of immune modulation. *J. Cell. Biochem.* 112, 1963–1968.

English, K., Tonlorenzi, R., Cossu, G., and Wood, K.J. (2013). Mesoangioblasts suppress T cell proliferation through IDO and PGE-2-dependent pathways. *Stem Cells Dev.* 22, 512–523.

Ervasti, J.M. (2007). Dystrophin, its interactions with other proteins, and implications for muscular dystrophy. *Biochim. Biophys. Acta* 1772, 108–117.

Escobar, H., Schöwel, V., Spuler, S., Marg, A., and Izsvák, Z. (2016). Full-length Dysferlin Transfer by the Hyperactive Sleeping Beauty Transposase Restores Dysferlin-deficient Muscle. *Mol. Ther. Nucleic Acids* 5, e277.

Farini, A., Meregalli, M., Belicchi, M., Battistelli, M., Parolini, D., D'Antona, G., Gavina, M., Ottoboni, L., Constantin, G., Bottinelli, R., et al. (2007). T and B lymphocyte depletion has a marked effect on the fibrosis of dystrophic skeletal muscles in the scid/mdx mouse. *J. Pathol.* 213, 229–238.

Filareto, A., Parker, S., Darabi, R., Borges, L., Iacovino, M., Schaaf, T., Mayerhofer, T., Chamberlain, J.S., Ervasti, J.M., Mclvor, R.S., et al. (2013). An ex vivo gene therapy approach to treat muscular dystrophy using inducible pluripotent stem cells. *Nat. Commun.* 4, 1549.

Filareto, A., Rinaldi, F., Arpke, R.W., Darabi, R., Belanto, J.J., Toso, E.A., Miller, A.Z., Ervasti, J.M., Mclvor, R.S., Kyba, M., et al. (2015). Pax3-induced expansion enables the genetic correction of dystrophic satellite cells. *Skelet. Muscle* 5, 36.

Finkel, R.S., Flanigan, K.M., Wong, B., Bönnemann, C., Sampson, J., Sweeney, H.L., Reha, A., Northcutt, V.J., Elfring, G., Barth, J., et al. (2013). Phase 2a study of ataluren-mediated dystrophin production in patients with nonsense mutation Duchenne muscular dystrophy. *PloS One* 8, e81302.

Foster, H., Sharp, P.S., Athanasopoulos, T., Trollet, C., Graham, I.R., Foster, K., Wells, D.J., and Dickson, G. (2008). Codon and mRNA sequence optimization of microdystrophin transgenes improves expression and physiological outcome in dystrophic mdx mice following AAV2/8 gene transfer. *Mol. Ther.* 16, 1825–1832.

Fraser, M.J., Smith, G.E., and Summers, M.D. (1983). Acquisition of Host Cell DNA Sequences by Baculoviruses: Relationship Between Host DNA Insertions and FP Mutants of *Autographa californica* and *Galleria mellonella* Nuclear Polyhedrosis Viruses. *J. Virol.* 47, 287–300.

Fraser, M.J., Brusca, J.S., Smith, G.E., and Summers, M.D. (1985). Transposon-mediated mutagenesis of a baculovirus. *Virology* 145, 356–361.

Fraser, M.J., Cary, L., Boonvisudhi, K., and Wang, H.G. (1995). Assay for movement of Lepidopteran transposon IFP2 in insect cells using a baculovirus genome as a target DNA. *Virology* 211, 397–407.

Fraser, M.J., Ciszczon, T., Elick, T., and Bauser, C. (1996). Precise excision of TTAA-specific lepidopteran transposons piggyBac (IFP2) and tagalong (TFP3) from the baculovirus genome in cell lines from two species of Lepidoptera. *Insect Mol. Biol.* 5, 141–151.

Galla, M., Schambach, A., Falk, C.S., Maetzig, T., Kuehle, J., Lange, K., Zychlinski, D., Heinz, N., Brugman, M.H., Göhring, G., et al. (2011). Avoiding cytotoxicity of transposases by dose-controlled mRNA delivery. *Nucleic Acids Res.* 39, 7147–7160.

Galli, D., Innocenzi, A., Staszewsky, L., Zanetta, L., Sampaolesi, M., Bai, A., Martinoli, E., Carlo, E., Balconi, G., Fiordaliso, F., et al. (2005). Mesoangioblasts, vessel-associated multipotent stem cells, repair the infarcted heart by multiple cellular mechanisms: a comparison with bone marrow progenitors, fibroblasts, and endothelial cells. *Arterioscler. Thromb. Vasc. Biol.* 25, 692–697.

Galvan, D.L., Nakazawa, Y., Kaja, A., Kettlun, C., Cooper, L.J.N., Rooney, C.M., and Wilson, M.H. (2009). Genome-wide mapping of PiggyBac transposon integrations in primary human T cells. *J. Immunother. Hagerstown Md* 1997 32, 837–844.

Gargioli, C., Coletta, M., De Grandis, F., Cannata, S.M., and Cossu, G. (2008). PIGF-MMP-9-expressing cells restore microcirculation and efficacy of cell therapy in aged dystrophic muscle. *Nat. Med.* 14, 973–978.

Gerli, M.F.M., Maffioletti, S.M., Millet, Q., and Tedesco, F.S. (2014). Transplantation of induced pluripotent stem cell-derived mesoangioblast-like myogenic progenitors in mouse models of muscle regeneration. *J. Vis. Exp. JoVE* e50532.

Geurts, A.M., Yang, Y., Clark, K.J., Liu, G., Cui, Z., Dupuy, A.J., Bell, J.B., Largaespada, D.A., and Hackett, P.B. (2003). Gene transfer into genomes of human cells by the sleeping beauty transposon system. *Mol. Ther.* 8, 108–117.

Goyenvalle, A., Vulin, A., Fougères, F., Leturcq, F., Kaplan, J.-C., Garcia, L., and Danos, O. (2004). Rescue of dystrophic muscle through U7 snRNA-mediated exon skipping. *Science* 306, 1796–1799.

Goyenvalle, A., Babbs, A., Wright, J., Wilkins, V., Powell, D., Garcia, L., and Davies, K.E. (2012a). Rescue of severely affected dystrophin/utrophin-deficient mice through scAAV-U7snRNA-mediated exon skipping. *Hum. Mol. Genet.* 21, 2559–2571.

Goyenvalle, A., Wright, J., Babbs, A., Wilkins, V., Garcia, L., and Davies, K.E. (2012b). Engineering multiple U7snRNA constructs to induce single and multiexon-skipping for Duchenne muscular dystrophy. *Mol. Ther.* 20, 1212–1221.

Grabundzija, I., Irgang, M., Mátés, L., Belay, E., Matrai, J., Gogol-Döring, A., Kawakami, K., Chen, W., Ruiz, P., Chuah, M.K.L., et al. (2010). Comparative analysis of transposable element vector systems in human cells. *Mol. Ther.* *18*, 1200–1209.

Grabundzija, I., Wang, J., Sebe, A., Erdei, Z., Kajdi, R., Devaraj, A., Steinemann, D., Szuhai, K., Stein, U., Cantz, T., et al. (2013). Sleeping Beauty transposon-based system for cellular reprogramming and targeted gene insertion in induced pluripotent stem cells. *Nucleic Acids Res.* *41*, 1829–1847.

Gregorevic, P., Blankinship, M.J., Allen, J.M., Crawford, R.W., Meuse, L., Miller, D.G., Russell, D.W., and Chamberlain, J.S. (2004). Systemic delivery of genes to striated muscles using adeno-associated viral vectors. *Nat. Med.* *10*, 828–834.

Gregorevic, P., Allen, J.M., Minami, E., Blankinship, M.J., Haraguchi, M., Meuse, L., Finn, E., Adams, M.E., Froehner, S.C., Murry, C.E., et al. (2006). rAAV6-microdystrophin preserves muscle function and extends lifespan in severely dystrophic mice. *Nat. Med.* *12*, 787–789.

Guse, K., Suzuki, M., Sule, G., Bertin, T.K., Tynismaa, H., Ahola-Erkkilä, S., Palmer, D., Suomalainen, A., Ng, P., Cerullo, V., et al. (2012). Capsid-modified adenoviral vectors for improved muscle-directed gene therapy. *Hum. Gene Ther.* *23*, 1065–1070.

Hacein-Bey-Abina, S., Pai, S.-Y., Gaspar, H.B., Armant, M., Berry, C.C., Blanche, S., Bleesing, J., Blondeau, J., de Boer, H., Buckland, K.F., et al. (2014). A modified γ -retrovirus vector for X-linked severe combined immunodeficiency. *N. Engl. J. Med.* *371*, 1407–1417.

Hacein-Bey Abina, S., Gaspar, H.B., Blondeau, J., Caccavelli, L., Charrier, S., Buckland, K., Picard, C., Six, E., Himoudi, N., Gilmour, K., et al. (2015). Outcomes following gene therapy in patients with severe Wiskott-Aldrich syndrome. *JAMA* *313*, 1550–1563.

Hackett, C.S., Geurts, A.M., and Hackett, P.B. (2007). Predicting preferential DNA vector insertion sites: implications for functional genomics and gene therapy. *Genome Biol.* *8 Suppl 1*, S12.

Hackett, P.B., Largaespada, D.A., and Cooper, L.J.N. (2010). A transposon and transposase system for human application. *Mol. Ther.* *18*, 674–683.

Hackett, P.B., Aronovich, E.L., Hunter, D., Urness, M., Bell, J.B., Kass, S.J., Cooper, L.J.N., and Mclvor, S. (2011). Efficacy and safety of Sleeping Beauty transposon-mediated gene transfer in preclinical animal studies. *Curr. Gene Ther.* *11*, 341–349.

Hackett, P.B., Largaespada, D.A., Switzer, K.C., and Cooper, L.J.N. (2013). Evaluating risks of insertional mutagenesis by DNA transposons in gene therapy. *Transl. Res. J. Lab. Clin. Med.* *161*, 265–283.

Hausl, M.A., Zhang, W., Mütter, N., Rauschhuber, C., Franck, H.G., Merricks, E.P., Nichols, T.C., Kay, M.A., and Ehrhardt, A. (2010). Hyperactive sleeping beauty transposase enables persistent phenotypic correction in mice and a canine model for hemophilia B. *Mol. Ther.* *18*, 1896–1906.

Hegge, J.O., Wooddell, C.I., Zhang, G., Hagstrom, J.E., Braun, S., Huss, T., Sebestyén, M.G., Emborg, M.E., and Wolff, J.A. (2010). Evaluation of hydrodynamic limb vein injections in nonhuman primates. *Hum. Gene Ther.* *21*, 829–842.

Helderman-van den Enden, A.T.J.M., Straathof, C.S.M., Aartsma-Rus, A., den Dunnen, J.T., Verbist, B.M., Bakker, E., Verschuuren, J.J.G.M., and Ginjaar, H.B. (2010). Becker muscular dystrophy patients with deletions around exon 51; a promising outlook for exon skipping therapy in Duchenne patients. *Neuromuscul Disord.* *20*, 251–254.

Herweijer, H., and Wolff, J.A. (2007). Gene therapy progress and prospects: hydrodynamic gene delivery. *Gene Ther.* *14*, 99–107.

Hoffman, E.P., Brown, R.H., and Kunkel, L.M. (1987). Dystrophin: the protein product of the Duchenne muscular dystrophy locus. *Cell* *51*, 919–928.

Holliday, R. (2014). The commitment of human cells to senescence. *Interdiscip. Top. Gerontol.* *39*, 1–7.

Hollis, R.P., Nightingale, S.J., Wang, X., Pepper, K.A., Yu, X.-J., Barsky, L., Crooks, G.M., and Kohn, D.B. (2006). Stable gene transfer to human CD34(+) hematopoietic cells using the Sleeping Beauty transposon. *Exp. Hematol.* *34*, 1333–1343.

Hoshiya, H., Kazuki, Y., Abe, S., Takiguchi, M., Kajitani, N., Watanabe, Y., Yoshino, T., Shirayoshi, Y., Higaki, K., Messina, G., et al. (2009). A highly stable and nonintegrated human artificial chromosome (HAC) containing the 2.4 Mb entire human dystrophin gene. *Mol. Ther.* *17*, 309–317.

Howe, S.J., Mansour, M.R., Schwarzwaelder, K., Bartholomae, C., Hubank, M., Kempster, H., Brugman, M.H., Pike-Overzet, K., Chatters, S.J., de Ridder, D., et al. (2008). Insertional mutagenesis combined with acquired somatic mutations causes leukemogenesis following gene therapy of SCID-X1 patients. *J. Clin. Invest.* *118*, 3143–3150.

Huang, X., Guo, H., Tammana, S., Jung, Y.-C., Mellgren, E., Bassi, P., Cao, Q., Tu, Z.J., Kim, Y.C., Ekker, S.C., et al. (2010). Gene transfer efficiency and genome-wide integration profiling of Sleeping Beauty, Tol2, and piggyBac transposons in human primary T cells. *Mol. Ther.* *18*, 1803–1813.

Huye, L.E., Nakazawa, Y., Patel, M.P., Yvon, E., Sun, J., Savoldo, B., Wilson, M.H., Dotti, G., and Rooney, C.M. (2011). Combining mTor inhibitors with rapamycin-resistant T cells: a two-pronged approach to tumor elimination. *Mol. Ther.* *19*, 2239–2248.

Hyde, S.C., Pringle, I.A., Abdullah, S., Lawton, A.E., Davies, L.A., Varathalingam, A., Nunez-Alonso, G., Green, A.-M., Bazzani, R.P., Sumner-Jones, S.G., et al. (2008). CpG-free plasmids confer reduced inflammation and sustained pulmonary gene expression. *Nat. Biotechnol.* *26*, 549–551.

Ivics, Z., and Izsvák, Z. (2006). Transposons for gene therapy! *Curr. Gene Ther.* *6*, 593–607.

- Ivics, Z., and Izsvák, Z. (2011). Nonviral gene delivery with the sleeping beauty transposon system. *Hum. Gene Ther.* 22, 1043–1051.
- Ivics, Z., Izsvák, Z., Minter, A., and Hackett, P.B. (1996). Identification of functional domains and evolution of Tc1-like transposable elements. *Proc. Natl. Acad. Sci. U. S. A.* 93, 5008–5013.
- Ivics, Z., Hackett, P.B., Plasterk, R.H., and Izsvák, Z. (1997). Molecular reconstruction of Sleeping Beauty, a Tc1-like transposon from fish, and its transposition in human cells. *Cell* 91, 501–510.
- Ivics, Z., Garrels, W., Mátés, L., Yau, T.Y., Bashir, S., Zidek, V., Landa, V., Geurts, A., Pravenec, M., Rülcke, T., et al. (2014a). Germline transgenesis in pigs by cytoplasmic microinjection of Sleeping Beauty transposons. *Nat. Protoc.* 9, 810–827.
- Ivics, Z., Hiripi, L., Hoffmann, O.I., Mátés, L., Yau, T.Y., Bashir, S., Zidek, V., Landa, V., Geurts, A., Pravenec, M., et al. (2014b). Germline transgenesis in rabbits by pronuclear microinjection of Sleeping Beauty transposons. *Nat. Protoc.* 9, 794–809.
- Ivics, Z., Mátés, L., Yau, T.Y., Landa, V., Zidek, V., Bashir, S., Hoffmann, O.I., Hiripi, L., Garrels, W., Kues, W.A., et al. (2014c). Germline transgenesis in rodents by pronuclear microinjection of Sleeping Beauty transposons. *Nat. Protoc.* 9, 773–793.
- Izsvák, Z., Khare, D., Behlke, J., Heinemann, U., Plasterk, R.H., and Ivics, Z. (2002). Involvement of a bifunctional, paired-like DNA-binding domain and a transpositional enhancer in Sleeping Beauty transposition. *J. Biol. Chem.* 277, 34581–34588.
- Izsvák, Z., Chuah, M.K.L., Vandendriessche, T., and Ivics, Z. (2009). Efficient stable gene transfer into human cells by the Sleeping Beauty transposon vectors. *Methods San Diego Calif* 49, 287–297.
- Izsvák, Z., Hackett, P.B., Cooper, L.J.N., and Ivics, Z. (2010). Translating Sleeping Beauty transposition into cellular therapies: victories and challenges. *BioEssays News Rev. Mol. Cell. Dev. Biol.* 32, 756–767.
- Jin, Z., Maiti, S., Huls, H., Singh, H., Olivares, S., Mátés, L., Izsvák, Z., Ivics, Z., Lee, D.A., Champlin, R.E., et al. (2011). The hyperactive Sleeping Beauty transposase SB100X improves the genetic modification of T cells to express a chimeric antigen receptor. *Gene Ther.* 18, 849–856.
- Jonuschies, J., Antoniou, M., Waddington, S., Boldrin, L., Muntoni, F., Thrasher, A., and Morgan, J. (2014). The human desmin promoter drives robust gene expression for skeletal muscle stem cell-mediated gene therapy. *Curr. Gene Ther.* 14, 276–288.
- Karsi, A., Moav, B., Hackett, P., and Liu, Z. (2001). Effects of insert size on transposition efficiency of the sleeping beauty transposon in mouse cells. *Mar. Biotechnol. N. Y.* N 3, 241–245.
- Kastelein, J.J.P., Ross, C.J.D., and Hayden, M.R. (2013). From mutation identification to therapy: discovery and origins of the first approved gene therapy in the Western world. *Hum. Gene Ther.* 24, 472–478.

- Kawano, R., Ishizaki, M., Maeda, Y., Uchida, Y., Kimura, E., and Uchino, M. (2008). Transduction of full-length dystrophin to multiple skeletal muscles improves motor performance and life span in utrophin/dystrophin double knockout mice. *Mol. Ther.* *16*, 825–831.
- Kawecka, K., Theodoulides, M., Hasoglu, Y., Jarmin, S., Kymalainen, H., Le-Heron, A., Popplewell, L., Malerba, A., Dickson, G., and Athanasopoulos, T. (2015). Adeno-Associated Virus (AAV) Mediated Dystrophin Gene Transfer Studies and Exon Skipping Strategies for Duchenne Muscular Dystrophy (DMD). *Curr. Gene Ther.* *15*, 395–415.
- Kazuki, Y., and Oshimura, M. (2011). Human artificial chromosomes for gene delivery and the development of animal models. *Mol. Ther.* *19*, 1591–1601.
- Kazuki, Y., Hiratsuka, M., Takiguchi, M., Osaki, M., Kajitani, N., Hoshiya, H., Hiramatsu, K., Yoshino, T., Kazuki, K., Ishihara, C., et al. (2010). Complete genetic correction of ipsc cells from Duchenne muscular dystrophy. *Mol. Ther.* *18*, 386–393.
- Kebriaei, P., Huls, H., Jena, B., Munsell, M., Jackson, R., Lee, D.A., Hackett, P.B., Rondon, G., Shpall, E., Champlin, R.E., et al. (2012). Infusing CD19-directed T cells to augment disease control in patients undergoing autologous hematopoietic stem-cell transplantation for advanced B-lymphoid malignancies. *Hum. Gene Ther.* *23*, 444–450.
- Keith, J.H., Schaeper, C.A., Fraser, T.S., and Fraser, M.J. (2008). Mutational analysis of highly conserved aspartate residues essential to the catalytic core of the piggyBac transposase. *BMC Mol. Biol.* *9*, 73.
- Kettlun, C., Galvan, D.L., George, A.L., Kaja, A., and Wilson, M.H. (2011). Manipulating piggyBac transposon chromosomal integration site selection in human cells. *Mol. Ther.* *19*, 1636–1644.
- Kimura, E., Li, S., Gregorevic, P., Fall, B.M., and Chamberlain, J.S. (2010). Dystrophin delivery to muscles of mdx mice using lentiviral vectors leads to myogenic progenitor targeting and stable gene expression. *Mol. Ther.* *18*, 206–213.
- Klein, C.J., Covert, D.D., Bulman, D.E., Ray, P.N., Mendell, J.R., and Burghes, A.H. (1992). Somatic reversion/suppression in Duchenne muscular dystrophy (DMD): evidence supporting a frame-restoring mechanism in rare dystrophin-positive fibers. *Am. J. Hum. Genet.* *50*, 950–959.
- Kole, R., and Krieg, A.M. (2015). Exon skipping therapy for Duchenne muscular dystrophy. *Adv. Drug Deliv. Rev.* *87*, 104–107.
- Koo, T., Okada, T., Athanasopoulos, T., Foster, H., Takeda, S., Ichi, and Dickson, G. (2011a). Long-term functional adeno-associated virus-microdystrophin expression in the dystrophic CXMDj dog. *J. Gene Med.* *13*, 497–506.
- Koo, T., Malerba, A., Athanasopoulos, T., Trollet, C., Boldrin, L., Ferry, A., Popplewell, L., Foster, H., Foster, K., and Dickson, G. (2011b). Delivery of AAV2/9-microdystrophin genes incorporating helix 1 of the coiled-coil motif in the C-terminal domain of dystrophin improves muscle pathology and restores the level of α 1-syntrophin and α -dystrobrevin in skeletal muscles of mdx mice. *Hum. Gene Ther.* *22*, 1379–1388.

- Koonin, E.V., and Krupovic, M. (2015). Evolution of adaptive immunity from transposable elements combined with innate immune systems. *Nat. Rev. Genet.* *16*, 184–192.
- Koppanati, B.M., Li, J., Reay, D.P., Wang, B., Daood, M., Zheng, H., Xiao, X., Watchko, J.F., and Clemens, P.R. (2010). Improvement of the mdx mouse dystrophic phenotype by systemic in utero AAV8 delivery of a minidystrophin gene. *Gene Ther.* *17*, 1355–1362.
- Kornegay, J.N., Li, J., Bogan, J.R., Bogan, D.J., Chen, C., Zheng, H., Wang, B., Qiao, C., Howard, J.F., and Xiao, X. (2010). Widespread muscle expression of an AAV9 human mini-dystrophin vector after intravenous injection in neonatal dystrophin-deficient dogs. *Mol. Ther.* *18*, 1501–1508.
- Kouprina, N., Tomilin, A.N., Masumoto, H., Earnshaw, W.C., and Larionov, V. (2014). Human artificial chromosome-based gene delivery vectors for biomedicine and biotechnology. *Expert Opin. Drug Deliv.* *11*, 517–535.
- Kren, B.T., Unger, G.M., Sjeklocha, L., Trossen, A.A., Korman, V., Diethelm-Okita, B.M., Reding, M.T., and Steer, C.J. (2009). Nanocapsule-delivered Sleeping Beauty mediates therapeutic Factor VIII expression in liver sinusoidal endothelial cells of hemophilia A mice. *J. Clin. Invest.*
- Krieg, A.M., Yi, A.K., Matson, S., Waldschmidt, T.J., Bishop, G.A., Teasdale, R., Koretzky, G.A., and Klinman, D.M. (1995). CpG motifs in bacterial DNA trigger direct B-cell activation. *Nature* *374*, 546–549.
- Kuang, S., Kuroda, K., Le Grand, F., and Rudnicki, M.A. (2007). Asymmetric self-renewal and commitment of satellite stem cells in muscle. *Cell* *129*, 999–1010.
- Kuang, S., Gillespie, M.A., and Rudnicki, M.A. (2008). Niche regulation of muscle satellite cell self-renewal and differentiation. *Cell Stem Cell* *2*, 22–31.
- Kudryashova, E., Kramerova, I., and Spencer, M.J. (2012). Satellite cell senescence underlies myopathy in a mouse model of limb-girdle muscular dystrophy 2H. *J. Clin. Invest.* *122*, 1764–1776.
- Kymäläinen, H., Appelt, J.U., Giordano, F.A., Davies, A.F., Ogilvie, C.M., Ahmed, S.G., Laufs, S., Schmidt, M., Bode, J., Yáñez-Muñoz, R.J., et al. (2014). Long-term episomal transgene expression from mitotically stable integration-deficient lentiviral vectors. *Hum. Gene Ther.* *25*, 428–442.
- Lacoste, A., Berenshteyn, F., and Brivanlou, A.H. (2009). An efficient and reversible transposable system for gene delivery and lineage-specific differentiation in human embryonic stem cells. *Cell Stem Cell* *5*, 332–342.
- Le Grand, F., Jones, A.E., Seale, V., Scimè, A., and Rudnicki, M.A. (2009). Wnt7a activates the planar cell polarity pathway to drive the symmetric expansion of satellite stem cells. *Cell Stem Cell* *4*, 535–547.
- Le Guiner, C., Montus, M., Servais, L., Cherel, Y., Francois, V., Thibaud, J.-L., Wary, C., Matot, B., Larcher, T., Guigand, L., et al. (2014). Forelimb Treatment in a Large Cohort

of Dystrophic Dogs Supports Delivery of a Recombinant AAV for Exon Skipping in Duchenne Patients. *Mol. Ther.* 22, 1923–1935.

Ley, D., Van Zwieten, R., Puttini, S., Iyer, P., Cochard, A., and Mermoud, N. (2014). A PiggyBac-mediated approach for muscle gene transfer or cell therapy. *Stem Cell Res.* 13, 390–403.

Li, H.L., Fujimoto, N., Sasakawa, N., Shirai, S., Ohkame, T., Sakuma, T., Tanaka, M., Amano, N., Watanabe, A., Sakurai, H., et al. (2015). Precise correction of the dystrophin gene in duchenne muscular dystrophy patient induced pluripotent stem cells by TALEN and CRISPR-Cas9. *Stem Cell Rep.* 4, 143–154.

Li, M.A., Turner, D.J., Ning, Z., Yusa, K., Liang, Q., Eckert, S., Rad, L., Fitzgerald, T.W., Craig, N.L., and Bradley, A. (2011). Mobilization of giant piggyBac transposons in the mouse genome. *Nucleic Acids Res.* 39, e148.

Li, O., English, K., Tonlorenzi, R., Cossu, G., Saverio Tedesco, F., and Wood, K.J. (2013). Human iPSC-derived mesoangioblasts, like their tissue-derived counterparts, suppress T cell proliferation through IDO- and PGE-2-dependent pathways. *F1000Research* 2, 24.

Li, S., Kimura, E., Fall, B.M., Reyes, M., Angello, J.C., Welikson, R., Hauschka, S.D., and Chamberlain, J.S. (2005a). Stable transduction of myogenic cells with lentiviral vectors expressing a minidystrophin. *Gene Ther.* 12, 1099–1108.

Li, X., Eastman, E.M., Schwartz, R.J., and Draghia-Akli, R. (1999). Synthetic muscle promoters: activities exceeding naturally occurring regulatory sequences. *Nat. Biotechnol.* 17, 241–245.

Li, X., Lobo, N., Bauser, C.A., and Fraser, M.J. (2001). The minimum internal and external sequence requirements for transposition of the eukaryotic transformation vector piggyBac. *Mol. Genet. Genomics* 266, 190–198.

Li, X., Harrell, R.A., Handler, A.M., Beam, T., Hennessy, K., and Fraser, M.J. (2005b). piggyBac internal sequences are necessary for efficient transformation of target genomes. *Insect Mol. Biol.* 14, 17–30.

Livak, K.J., and Schmittgen, T.D. (2001). Analysis of relative gene expression data using real-time quantitative PCR and the 2(-Delta Delta C(T)) Method. *Methods San Diego Calif* 25, 402–408.

Lohe, A.R., and Hartl, D.L. (1996). Autoregulation of mariner transposase activity by overproduction and dominant-negative complementation. *Mol. Biol. Evol.* 13, 549–555.

Long, C., McAnally, J.R., Shelton, J.M., Mireault, A.A., Bassel-Duby, R., and Olson, E.N. (2014). Prevention of muscular dystrophy in mice by CRISPR/Cas9-mediated editing of germline DNA. *Science* 345, 1184–1188.

Long, C., Amoasii, L., Mireault, A.A., McAnally, J.R., Li, H., Sanchez-Ortiz, E., Bhattacharyya, S., Shelton, J.M., Bassel-Duby, R., and Olson, E.N. (2015). Postnatal

genome editing partially restores dystrophin expression in a mouse model of muscular dystrophy. *Science* 351, 400-3.

Loperfido, M., Steele-Stallard, H.B., Tedesco, F.S., and VandenDriessche, T. (2015a). Pluripotent Stem Cells for Gene Therapy of Degenerative Muscle Diseases. *Curr. Gene Ther.*

Loperfido, M., Jarmin, S., Dastidar, S., Di Matteo, M., Perini, I., Moore, M., Nair, N., Samara-Kuko, E., Athanasopoulos, T., Tedesco, F.S., et al. (2015b). piggyBac transposons expressing full-length human dystrophin enable genetic correction of dystrophic mesoangioblasts. *Nucleic Acids Res.*

Lu, Q.-L., Cirak, S., and Partridge, T. (2014). What Can We Learn From Clinical Trials of Exon Skipping for DMD? *Mol. Ther. Nucleic Acids* 3, e152.

Lukacs, G.L., Haggie, P., Seksek, O., Lechardeur, D., Freedman, N., and Verkman, A.S. (2000). Size-dependent DNA mobility in cytoplasm and nucleus. *J. Biol. Chem.* 275, 1625–1629.

Maffioletti, S.M., Noviello, M., English, K., and Tedesco, F.S. (2014). Stem cell transplantation for muscular dystrophy: the challenge of immune response. *BioMed Res. Int.* 2014, 964010.

Maffioletti, S.M., Gerli, M.F.M., Ragazzi, M., Dastidar, S., Benedetti, S., Loperfido, M., VandenDriessche, T., Chuah, M.K., and Tedesco, F.S. (2015). Efficient derivation and inducible differentiation of expandable skeletal myogenic cells from human ES and patient-specific iPS cells. *Nat. Protoc.* 10, 941–958.

Maggio, I., Stefanucci, L., Janssen, J.M., Liu, J., Chen, X., Mouly, V., and Gonçalves, M.A.F.V. (2016). Selection-free gene repair after adenoviral vector transduction of designer nucleases: rescue of dystrophin synthesis in DMD muscle cell populations. *Nucleic Acids Res.* 44, 1449–1470.

Malik, V., Rodino-Klapac, L.R., Viollet, L., Wall, C., King, W., Al-Dahhak, R., Lewis, S., Shilling, C.J., Kota, J., Serrano-Munuera, C., et al. (2010). Gentamicin-induced readthrough of stop codons in Duchenne muscular dystrophy. *Ann. Neurol.* 67, 771–780.

Mann, C.J., Perdiguero, E., Kharraz, Y., Aguilar, S., Pessina, P., Serrano, A.L., and Muñoz-Cánoves, P. (2011). Aberrant repair and fibrosis development in skeletal muscle. *Skelet. Muscle* 1, 21.

Manuri, P.V.R., Wilson, M.H., Maiti, S.N., Mi, T., Singh, H., Olivares, S., Dawson, M.J., Huls, H., Lee, D.A., Rao, P.H., et al. (2010). piggyBac transposon/transposase system to generate CD19-specific T cells for the treatment of B-lineage malignancies. *Hum. Gene Ther.* 21, 427–437.

Marg, A., Escobar, H., Gloy, S., Kufeld, M., Zacher, J., Spuler, A., Birchmeier, C., Izsvák, Z., and Spuler, S. (2014). Human satellite cells have regenerative capacity and are genetically manipulable. *J. Clin. Invest.* 124, 4257–4265.

- Mátés, L., Izsvák, Z., and Ivics, Z. (2007). Technology transfer from worms and flies to vertebrates: transposition-based genome manipulations and their future perspectives. *Genome Biol.* 8 Suppl 1, S1.
- Mátés, L., Chuah, M.K.L., Belay, E., Jerchow, B., Manoj, N., Acosta-Sanchez, A., Grzela, D.P., Schmitt, A., Becker, K., Matrai, J., et al. (2009). Molecular evolution of a novel hyperactive Sleeping Beauty transposase enables robust stable gene transfer in vertebrates. *Nat. Genet.* 41, 753–761.
- Matsui, H., Fujimoto, N., Sasakawa, N., Ohinata, Y., Shima, M., Yamanaka, S., Sugimoto, M., and Hotta, A. (2014). Delivery of full-length factor VIII using a piggyBac transposon vector to correct a mouse model of hemophilia A. *PLoS One* 9, e104957.
- Mauro, A. (1961). Satellite cell of skeletal muscle fibers. *J. Biophys. Biochem. Cytol.* 9, 493–495.
- McClintock, B. (1950). The origin and behavior of mutable loci in maize. *Proc. Natl. Acad. Sci. U. S. A.* 36, 344–355.
- McDonald, C.M., Henricson, E.K., Han, J.J., Abresch, R.T., Nicorici, A., Atkinson, L., Elfving, G.L., Reha, A., and Miller, L.L. (2010). The 6-minute walk test in Duchenne/Becker muscular dystrophy: longitudinal observations. *Muscle Nerve* 42, 966–974.
- McGreevy, J.W., Hakim, C.H., McIntosh, M.A., and Duan, D. (2015). Animal models of Duchenne muscular dystrophy: from basic mechanisms to gene therapy. *Dis. Model. Mech.* 8, 195–213.
- Meir, Y.-J.J., and Wu, S.C.-Y. (2011). Transposon-based vector systems for gene therapy clinical trials: challenges and considerations. *Chang Gung Med. J.* 34, 565–579.
- Meir, Y.-J.J., Weirauch, M.T., Yang, H.-S., Chung, P.-C., Yu, R.K., and Wu, S.C.-Y. (2011). Genome-wide target profiling of piggyBac and Tol2 in HEK 293: pros and cons for gene discovery and gene therapy. *BMC Biotechnol.* 11, 28.
- Meir, Y.-J.J., Lin, A., Huang, M.-F., Lin, J.-R., Weirauch, M.T., Chou, H.-C., Lin, S.-J.A., and Wu, S.C.-Y. (2013). A versatile, highly efficient, and potentially safer piggyBac transposon system for mammalian genome manipulations. *FASEB J. Off. Publ. Fed. Am. Soc. Exp. Biol.* 27, 4429–4443.
- Mendell, J.R., and Lloyd-Puryear, M. (2013). Report of MDA muscle disease symposium on newborn screening for Duchenne muscular dystrophy. *Muscle Nerve* 48, 21–26.
- Mendell, J.R., Campbell, K., Rodino-Klapac, L., Sahenk, Z., Shilling, C., Lewis, S., Bowles, D., Gray, S., Li, C., Galloway, G., et al. (2010). Dystrophin immunity in Duchenne’s muscular dystrophy. *N. Engl. J. Med.* 363, 1429–1437.
- Mendell, J.R., Goemans, N., Lowes, L.P., Alfano, L.N., Berry, K., Shao, J., Kaye, E.M., Mercuri, E., and Eteplirsén Study Group and Telethon Foundation DMD Italian Network (2016). Longitudinal effect of eteplirsén versus historical control on ambulation in Duchenne muscular dystrophy. *Ann. Neurol.* 79, 257–271.

Meng, J., Counsell, J.R., Reza, M., Laval, S.H., Danos, O., Thrasher, A., Lochmüller, H., Muntoni, F., and Morgan, J.E. (2016). Autologous skeletal muscle derived cells expressing a novel functional dystrophin provide a potential therapy for Duchenne Muscular Dystrophy. *Sci. Rep.* 6, 19750.

Mercuri, E., and Muntoni, F. (2013). Muscular dystrophies. *Lancet Lond. Engl.* 381, 845–860.

Mercuri, E., and Muntoni, F. (2015). Efficacy of idebenone in Duchenne muscular dystrophy. *Lancet Lond. Engl.* 385, 1704–1706.

Meregalli, M., Navarro, C., Sitzia, C., Farini, A., Montani, E., Wein, N., Razini, P., Beley, C., Cassinelli, L., Parolini, D., et al. (2013). Full-length dysferlin expression driven by engineered human dystrophic blood derived CD133+ stem cells. *FEBS J.* 280, 6045–6060.

Midoux, P., Pichon, C., Yaouanc, J.-J., and Jaffrès, P.-A. (2009). Chemical vectors for gene delivery: a current review on polymers, peptides and lipids containing histidine or imidazole as nucleic acids carriers. *Br. J. Pharmacol.* 157, 166–178.

Minasi, M.G., Riminucci, M., De Angelis, L., Borello, U., Berarducci, B., Innocenzi, A., Caprioli, A., Sirabella, D., Baiocchi, M., De Maria, R., et al. (2002). The meso-angioblast: a multipotent, self-renewing cell that originates from the dorsal aorta and differentiates into most mesodermal tissues. *Dev. Camb. Engl.* 129, 2773–2783.

Mingozzi, F., Meulenberg, J.J., Hui, D.J., Basner-Tschakarjan, E., Hasbrouck, N.C., Edmonson, S.A., Hutnick, N.A., Betts, M.R., Kastelein, J.J., Stroes, E.S., et al. (2009). AAV-1-mediated gene transfer to skeletal muscle in humans results in dose-dependent activation of capsid-specific T cells. *Blood* 114, 2077–2086.

Mitra, R., Fain-Thornton, J., and Craig, N.L. (2008). piggyBac can bypass DNA synthesis during cut and paste transposition. *EMBO J.* 27, 1097–1109.

Moldt, B., Miskey, C., Staunstrup, N.H., Gogol-Döring, A., Bak, R.O., Sharma, N., Mátés, L., Izsvák, Z., Chen, W., Ivics, Z., et al. (2011). Comparative genomic integration profiling of Sleeping Beauty transposons mobilized with high efficacy from integrase-defective lentiviral vectors in primary human cells. *Mol. Ther.* 19, 1499–1510.

Muses, S., Morgan, J.E., and Wells, D.J. (2011a). A new extensively characterised conditionally immortal muscle cell-line for investigating therapeutic strategies in muscular dystrophies. *PLoS One* 6, e24826.

Muses, S., Morgan, J.E., and Wells, D.J. (2011b). Restoration of dystrophin expression using the Sleeping Beauty transposon. *PLoS Curr.* 3, RRN1296.

Nakazawa, Y., Huye, L.E., Dotti, G., Foster, A.E., Vera, J.F., Manuri, P.R., June, C.H., Rooney, C.M., and Wilson, M.H. (2009). Optimization of the PiggyBac transposon system for the sustained genetic modification of human T lymphocytes. *J. Immunother. Hagerstown Md* 1997 32, 826–836.

- Nakazawa, Y., Huye, L.E., Salsman, V.S., Leen, A.M., Ahmed, N., Rollins, L., Dotti, G., Gottschalk, S.M., Wilson, M.H., and Rooney, C.M. (2011). PiggyBac-mediated cancer immunotherapy using EBV-specific cytotoxic T-cells expressing HER2-specific chimeric antigen receptor. *Mol. Ther.* *19*, 2133–2143.
- Nathwani, A.C., Reiss, U.M., Tuddenham, E.G.D., Rosales, C., Chowdhary, P., McIntosh, J., Della Peruta, M., Lheriteau, E., Patel, N., Raj, D., et al. (2014). Long-term safety and efficacy of factor IX gene therapy in hemophilia B. *N. Engl. J. Med.* *371*, 1994–2004.
- Negróni, E., Vallese, D., Vilquin, J.-T., Butler-Browne, G., Mouly, V., and Trollet, C. (2011). Current advances in cell therapy strategies for muscular dystrophies. *Expert Opin. Biol. Ther.* *11*, 157–176.
- Nelson, C.E., Hakim, C.H., Ousterout, D.G., Thakore, P.I., Moreb, E.A., Rivera, R.M.C., Madhavan, S., Pan, X., Ran, F.A., Yan, W.X., et al. (2015). In vivo genome editing improves muscle function in a mouse model of Duchenne muscular dystrophy. *Science* *351*, 403-7.
- Nelson, M.D., Rader, F., Tang, X., Tavyev, J., Nelson, S.F., Miceli, M.C., Elashoff, R.M., Sweeney, H.L., and Victor, R.G. (2014). PDE5 inhibition alleviates functional muscle ischemia in boys with Duchenne muscular dystrophy. *Neurology* *82*, 2085–2091.
- Neri, M., Torelli, S., Brown, S., Ugo, I., Sabatelli, P., Merlini, L., Spitali, P., Rimessi, P., Gualandi, F., Sewry, C., et al. (2007). Dystrophin levels as low as 30% are sufficient to avoid muscular dystrophy in the human. *Neuromuscul Disord.* *17*, 913–918.
- Noviello, M., Tedesco, F.S., Bondanza, A., Tonlorenzi, R., Rosaria Carbone, M., Gerli, M.F.M., Markt, S., Napolitano, S., Cicalese, M.P., Ciceri, F., et al. (2014). Inflammation converts human mesoangioblasts into targets of alloreactive immune responses: implications for allogeneic cell therapy of DMD. *Mol. Ther.* *22*, 1342–1352.
- Ohshima, S., Shin, J.-H., Yuasa, K., Nishiyama, A., Kira, J., Okada, T., and Takeda, S. (2009). Transduction efficiency and immune response associated with the administration of AAV8 vector into dog skeletal muscle. *Mol. Ther.* *17*, 73–80.
- Ousterout, D.G., Perez-Pinera, P., Thakore, P.I., Kabadi, A.M., Brown, M.T., Qin, X., Fedrigo, O., Mouly, V., Tremblay, J.P., and Gersbach, C.A. (2013). Reading frame correction by targeted genome editing restores dystrophin expression in cells from Duchenne muscular dystrophy patients. *Mol. Ther.* *21*, 1718–1726.
- Ousterout, D.G., Kabadi, A.M., Thakore, P.I., Perez-Pinera, P., Brown, M.T., Majoros, W.H., Reddy, T.E., and Gersbach, C.A. (2015a). Correction of dystrophin expression in cells from Duchenne muscular dystrophy patients through genomic excision of exon 51 by zinc finger nucleases. *Mol. Ther.* *23*, 523–532.
- Ousterout, D.G., Kabadi, A.M., Thakore, P.I., Majoros, W.H., Reddy, T.E., and Gersbach, C.A. (2015b). Multiplex CRISPR/Cas9-based genome editing for correction of dystrophin mutations that cause Duchenne muscular dystrophy. *Nat. Commun.* *6*, 6244.
- Owens, J.B., Urschitz, J., Stoytchev, I., Dang, N.C., Stoytcheva, Z., Belcaid, M., Maragathavally, K.J., Coates, C.J., Segal, D.J., and Moisyadi, S. (2012). Chimeric

piggyBac transposases for genomic targeting in human cells. *Nucleic Acids Res.* *40*, 6978–6991.

Owens, J.B., Mauro, D., Stoytchev, I., Bhakta, M.S., Kim, M.-S., Segal, D.J., and Moisyadi, S. (2013). Transcription activator like effector (TALE)-directed piggyBac transposition in human cells. *Nucleic Acids Res.* *41*, 9197–9207.

Palumbo, R., Sampaolesi, M., De Marchis, F., Tonlorenzi, R., Colombetti, S., Mondino, A., Cossu, G., and Bianchi, M.E. (2004). Extracellular HMGB1, a signal of tissue damage, induces mesoangioblast migration and proliferation. *J. Cell Biol.* *164*, 441–449.

Parent, A. (2005). Duchenne De Boulogne: a pioneer in neurology and medical photography. *Can. J. Neurol. Sci. J. Can. Sci. Neurol.* *32*, 369–377.

Partridge, T.A., Morgan, J.E., Coulton, G.R., Hoffman, E.P., and Kunkel, L.M. (1989). Conversion of mdx myofibres from dystrophin-negative to -positive by injection of normal myoblasts. *Nature* *337*, 176–179.

Périé, S., Trollet, C., Mouly, V., Vanneaux, V., Mamchaoui, K., Bouazza, B., Marolleau, J.P., Laforêt, P., Chapon, F., Eymard, B., et al. (2014). Autologous myoblast transplantation for oculopharyngeal muscular dystrophy: a phase I/IIa clinical study. *Mol. Ther.* *22*, 219–225.

Petrof, B.J., Shrager, J.B., Stedman, H.H., Kelly, A.M., and Sweeney, H.L. (1993). Dystrophin protects the sarcolemma from stresses developed during muscle contraction. *Proc. Natl. Acad. Sci. U. S. A.* *90*, 3710–3714.

Plasterk, R.H., Izsvák, Z., and Ivics, Z. (1999). Resident aliens: the Tc1/mariner superfamily of transposable elements. *Trends Genet. TIG* *15*, 326–332.

Podetz-Pedersen, K.M., Bell, J.B., Steele, T.W.J., Wilber, A., Shier, W.T., Belur, L.R., Mclvor, R.S., and Hackett, P.B. (2010). Gene Expression in Lung and Liver After Intravenous Infusion of Polyethylenimine Complexes of *Sleeping Beauty* Transposons. *Hum. Gene Ther.* *21*, 210–220.

Popplewell, L., Koo, T., Leclerc, X., Duclert, A., Mamchaoui, K., Gouble, A., Mouly, V., Voit, T., Pâques, F., Cédronne, F., et al. (2013). Gene correction of a duchenne muscular dystrophy mutation by meganuclease-enhanced exon knock-in. *Hum. Gene Ther.* *24*, 692–701.

Prakash, V., Moore, M., and Yáñez-Muñoz, R.J. (2016). Current progress in therapeutic gene editing for monogenic diseases. *Mol. Ther.*

Quattrocelli, M., Palazzolo, G., Floris, G., Schöffski, P., Anastasia, L., Orlacchio, A., Vandendriessche, T., Chuah, M.K.L., Cossu, G., Verfaillie, C., et al. (2011). Intrinsic cell memory reinforces myogenic commitment of pericyte-derived iPSCs. *J. Pathol.* *223*, 593–603.

Relaix, F., and Zammit, P.S. (2012). Satellite cells are essential for skeletal muscle regeneration: the cell on the edge returns centre stage. *Dev. Camb. Engl.* *139*, 2845–2856.

Reyes-Sandoval, A., and Ertl, H.C.J. (2004). CpG methylation of a plasmid vector results in extended transgene product expression by circumventing induction of immune responses. *Mol. Ther.* *9*, 249–261.

Rincon, M.Y., Sarcar, S., Danso-Abeam, D., Keyaerts, M., Matrai, J., Samara-Kuko, E., Acosta-Sanchez, A., Athanasopoulos, T., Dickson, G., Lahoutte, T., et al. (2014). Genome-wide Computational Analysis Reveals Cardiomyocyte-specific Transcriptional Cis-regulatory Motifs That Enable Efficient Cardiac Gene Therapy. *Mol. Ther.*

Rocheteau, P., Gayraud-Morel, B., Siegl-Cachedenier, I., Blasco, M.A., and Tajbakhsh, S. (2012). A subpopulation of adult skeletal muscle stem cells retains all template DNA strands after cell division. *Cell* *148*, 112–125.

Rodino-Klapac, L.R., Montgomery, C.L., Bremer, W.G., Shontz, K.M., Malik, V., Davis, N., Sprinkle, S., Campbell, K.J., Sahenk, Z., Clark, K.R., et al. (2010). Persistent expression of FLAG-tagged micro dystrophin in nonhuman primates following intramuscular and vascular delivery. *Mol. Ther.* *18*, 109–117.

Romero, N.B., Braun, S., Benveniste, O., Leturcq, F., Hogrel, J.-Y., Morris, G.E., Barois, A., Eymard, B., Payan, C., Ortega, V., et al. (2004). Phase I study of dystrophin plasmid-based gene therapy in Duchenne/Becker muscular dystrophy. *Hum. Gene Ther.* *15*, 1065–1076.

Ross, J.J., Hong, Z., Willenbring, B., Zeng, L., Isenberg, B., Lee, E.H., Reyes, M., Keirstead, S.A., Weir, E.K., Tranquillo, R.T., et al. (2006). Cytokine-induced differentiation of multipotent adult progenitor cells into functional smooth muscle cells. *J. Clin. Invest.* *116*, 3139–3149.

Rudnicki, M.A., Le Grand, F., McKinnell, I., and Kuang, S. (2008). The molecular regulation of muscle stem cell function. *Cold Spring Harb. Symp. Quant. Biol.* *73*, 323–331.

Sacco, A., Mourkioti, F., Tran, R., Choi, J., Llewellyn, M., Kraft, P., Shkreli, M., Delp, S., Pomerantz, J.H., Artandi, S.E., et al. (2010). Short telomeres and stem cell exhaustion model Duchenne muscular dystrophy in mdx/mTR mice. *Cell* *143*, 1059–1071.

Saito, S., Nakazawa, Y., Sueki, A., Matsuda, K., Tanaka, M., Yanagisawa, R., Maeda, Y., Sato, Y., Okabe, S., Inukai, T., et al. (2014). Anti-leukemic potency of piggyBac-mediated CD19-specific T cells against refractory Philadelphia chromosome-positive acute lymphoblastic leukemia. *Cytotherapy* *16*, 1257–1269.

Salva, M.Z., Himeda, C.L., Tai, P.W., Nishiuchi, E., Gregorevic, P., Allen, J.M., Finn, E.E., Nguyen, Q.G., Blankinship, M.J., Meuse, L., et al. (2007). Design of tissue-specific regulatory cassettes for high-level rAAV-mediated expression in skeletal and cardiac muscle. *Mol. Ther.* *15*, 320–329.

Sampaolesi, M., Torrente, Y., Innocenzi, A., Tonlorenzi, R., D'Antona, G., Pellegrino, M.A., Barresi, R., Bresolin, N., De Angelis, M.G.C., Campbell, K.P., et al. (2003). Cell therapy of alpha-sarcoglycan null dystrophic mice through intra-arterial delivery of mesoangioblasts. *Science* *301*, 487–492.

- Sampaolesi, M., Biressi, S., Tonlorenzi, R., Innocenzi, A., Draghici, E., Cusella de Angelis, M.G., and Cossu, G. (2005). Cell therapy of primary myopathies. *Arch. Ital. Biol.* **143**, 235–242.
- Sampaolesi, M., Blot, S., D'Antona, G., Granger, N., Tonlorenzi, R., Innocenzi, A., Mognol, P., Thibaud, J.-L., Galvez, B.G., Barthélémy, I., et al. (2006). Mesoangioblast stem cells ameliorate muscle function in dystrophic dogs. *Nature* **444**, 574–579.
- Scherer, W.F., Syverton, J.T., and Gey, G.O. (1953). Studies on the propagation in vitro of poliomyelitis viruses. IV. Viral multiplication in a stable strain of human malignant epithelial cells (strain HeLa) derived from an epidermoid carcinoma of the cervix. *J. Exp. Med.* **97**, 695–710.
- Schrepfer, S., Deuse, T., Reichenspurner, H., Fischbein, M.P., Robbins, R.C., and Pelletier, M.P. (2007). Stem cell transplantation: the lung barrier. *Transplant. Proc.* **39**, 573–576.
- Serra, F., Quarta, M., Canato, M., Toniolo, L., De Arcangelis, V., Trotta, A., Spath, L., Monaco, L., Reggiani, C., and Naro, F. (2012). Inflammation in muscular dystrophy and the beneficial effects of non-steroidal anti-inflammatory drugs. *Muscle Nerve* **46**, 773–784.
- Sharma, N., Cai, Y., Bak, R.O., Jakobsen, M.R., Schrøder, L.D., and Mikkelsen, J.G. (2013). Efficient sleeping beauty DNA transposition from DNA minicircles. *Mol. Ther. Nucleic Acids* **2**, e74.
- Sharma, R.R., Pollock, K., Hubel, A., and McKenna, D. (2014). Mesenchymal stem or stromal cells: a review of clinical applications and manufacturing practices. *Transfusion (Paris)* **54**, 1418–1437.
- Shin, J.-H., Yue, Y., Smith, B., and Duan, D. (2012). Humoral immunity to AAV-6, 8, and 9 in normal and dystrophic dogs. *Hum. Gene Ther.* **23**, 287–294.
- Shin, J.-H., Pan, X., Hakim, C.H., Yang, H.T., Yue, Y., Zhang, K., Terjung, R.L., and Duan, D. (2013). Microdystrophin ameliorates muscular dystrophy in the canine model of duchenne muscular dystrophy. *Mol. Ther.* **21**, 750–757.
- Shinin, V., Gayraud-Morel, B., Gomès, D., and Tajbakhsh, S. (2006). Asymmetric division and cosegregation of template DNA strands in adult muscle satellite cells. *Nat. Cell Biol.* **8**, 677–687.
- Shoji, E., Sakurai, H., Nishino, T., Nakahata, T., Heike, T., Awaya, T., Fujii, N., Manabe, Y., Matsuo, M., and Sehara-Fujisawa, A. (2015). Early pathogenesis of Duchenne muscular dystrophy modelled in patient-derived human induced pluripotent stem cells. *Sci. Rep.* **5**, 12831.
- Sicinski, P., Geng, Y., Ryder-Cook, A.S., Barnard, E.A., Darlison, M.G., and Barnard, P.J. (1989). The molecular basis of muscular dystrophy in the mdx mouse: a point mutation. *Science* **244**, 1578–1580.

- de Silva, S., Lotta, L.T., Burris, C.A., and Bowers, W.J. (2010). Virion-associated cofactor high-mobility group DNA-binding protein-1 facilitates transposition from the herpes simplex virus/Sleeping Beauty amplicon vector platform. *Hum. Gene Ther.* *21*, 1615–1622.
- Skipper, K.A., Andersen, P.R., Sharma, N., and Mikkelsen, J.G. (2013). DNA transposon-based gene vehicles - scenes from an evolutionary drive. *J. Biomed. Sci.* *20*, 92.
- Skuk, D., and Tremblay, J.P. (2011). Intramuscular cell transplantation as a potential treatment of myopathies: clinical and preclinical relevant data. *Expert Opin. Biol. Ther.* *11*, 359–374.
- Skuk, D., Goulet, M., Roy, B., Piette, V., Côté, C.H., Chapdelaine, P., Hogrel, J.-Y., Paradis, M., Bouchard, J.-P., Sylvain, M., et al. (2007). First test of a “high-density injection” protocol for myogenic cell transplantation throughout large volumes of muscles in a Duchenne muscular dystrophy patient: eighteen months follow-up. *Neuromuscul Disord.* *17*, 38–46.
- Staunstrup, N.H., Moldt, B., Mátés, L., Villesen, P., Jakobsen, M., Ivics, Z., Izsvák, Z., and Mikkelsen, J.G. (2009). Hybrid lentivirus-transposon vectors with a random integration profile in human cells. *Mol. Ther.* *17*, 1205–1214.
- Stein, S., Ott, M.G., Schultze-Strasser, S., Jauch, A., Burwinkel, B., Kinner, A., Schmidt, M., Krämer, A., Schwäble, J., Glimm, H., et al. (2010). Genomic instability and myelodysplasia with monosomy 7 consequent to EVI1 activation after gene therapy for chronic granulomatous disease. *Nat. Med.* *16*, 198–204.
- Swierczek, M., Izsvák, Z., and Ivics, Z. (2012). The Sleeping Beauty transposon system for clinical applications. *Expert Opin. Biol. Ther.* *12*, 139–153.
- Tabebordbar, M., Zhu, K., Cheng, J.K.W., Chew, W.L., Widrick, J.J., Yan, W.X., Maesner, C., Wu, E.Y., Xiao, R., Ran, F.A., et al. (2015). In vivo gene editing in dystrophic mouse muscle and muscle stem cells. *Science* *351*, 407-11.
- Tanaka, A., Woltjen, K., Miyake, K., Hotta, A., Ikeya, M., Yamamoto, T., Nishino, T., Shoji, E., Sehara-Fujisawa, A., Manabe, Y., et al. (2013). Efficient and reproducible myogenic differentiation from human iPS cells: prospects for modeling Miyoshi Myopathy in vitro. *PloS One* *8*, e61540.
- Tedesco, F.S. (2015). Human artificial chromosomes for Duchenne muscular dystrophy and beyond: challenges and hopes. *Chromosome Res. Int. J. Mol. Supramol. Evol. Asp. Chromosome Biol.* *23*, 135–141.
- Tedesco, F.S., and Cossu, G. (2012). Stem cell therapies for muscle disorders. *Curr. Opin. Neurol.* *25*, 597–603.
- Tedesco, F.S., Hoshiya, H., D’Antona, G., Gerli, M.F.M., Messina, G., Antonini, S., Tonlorenzi, R., Benedetti, S., Berghella, L., Torrente, Y., et al. (2011). Stem cell-mediated transfer of a human artificial chromosome ameliorates muscular dystrophy. *Sci. Transl. Med.* *3*, 96ra78.

Tedesco, F.S., Gerli, M.F.M., Perani, L., Benedetti, S., Ungaro, F., Cassano, M., Antonini, S., Tagliafico, E., Artusi, V., Longa, E., et al. (2012). Transplantation of genetically corrected human iPSC-derived progenitors in mice with limb-girdle muscular dystrophy. *Sci. Transl. Med.* 4, 140ra89.

Tinsley, J.M., and Davies, K.E. (1993). Utrophin: a potential replacement for dystrophin? *Neuromuscul Disord.* 3, 537–539.

Tinsley, J., Robinson, N., and Davies, K.E. (2015). Safety, tolerability, and pharmacokinetics of SMT C1100, a 2-arylbenzoxazole utrophin modulator, following single- and multiple-dose administration to healthy male adult volunteers. *J. Clin. Pharmacol.* 55, 698–707.

Tinsley, J.M., Fairclough, R.J., Storer, R., Wilkes, F.J., Potter, A.C., Squire, S.E., Powell, D.S., Cozzoli, A., Capogrosso, R.F., Lambert, A., et al. (2011). Daily treatment with SMT C1100, a novel small molecule utrophin upregulator, dramatically reduces the dystrophic symptoms in the mdx mouse. *PLoS One* 6, e19189.

Tonlorenzi, R., Dellavalle, A., Schnapp, E., Cossu, G., and Sampaolesi, M. (2007). Isolation and characterization of mesoangioblasts from mouse, dog, and human tissues. *Curr. Protoc. Stem Cell Biol.* Chapter 2, Unit 2B.1.

Torrente, Y., Belicchi, M., Marchesi, C., D'Antona, G., Cogiamanian, F., Pisati, F., Gavina, M., Giordano, R., Tonlorenzi, R., Fagiolari, G., et al. (2007). Autologous transplantation of muscle-derived CD133+ stem cells in Duchenne muscle patients. *Cell Transplant.* 16, 563–577.

Turchiano, G., Latella, M.C., Gogol-Döring, A., Cattoglio, C., Mavilio, F., Izsvák, Z., Ivics, Z., and Recchia, A. (2014). Genomic analysis of Sleeping Beauty transposon integration in human somatic cells. *PLoS One* 9, e112712.

Vallese, D., Negroni, E., Duguez, S., Ferry, A., Trollet, C., Aamiri, A., Vosshenrich, C.A.J., Füchtbauer, E.-M., Di Santo, J.P., Vitiello, L., et al. (2013). The Rag2^{-/-}Il2rb^{-/-}Dmd^{-/-} mouse: a novel dystrophic and immunodeficient model to assess innovating therapeutic strategies for muscular dystrophies. *Mol. Ther.* 21, 1950–1957.

VandenDriessche, T., and Chuah, M.K. (2016). CRISPR/Cas9 Flexes Its Muscles: In Vivo Somatic Gene Editing for Muscular Dystrophy. *Mol. Ther.* 24, 414–416.

VandenDriessche, T., Ivics, Z., Izsvák, Z., and Chuah, M.K.L. (2009). Emerging potential of transposons for gene therapy and generation of induced pluripotent stem cells. *Blood* 114, 1461–1468.

Vargas, J., Gusella, G.L., Najfeld, V., Klotman, M.E., and Cara, A. (2004). Novel integrase-defective lentiviral episomal vectors for gene transfer. *Hum. Gene Ther.* 15, 361–372.

Vigdal, T.J., Kaufman, C.D., Izsvák, Z., Voytas, D.F., and Ivics, Z. (2002). Common physical properties of DNA affecting target site selection of sleeping beauty and other Tc1/mariner transposable elements. *J. Mol. Biol.* 323, 441–452.

Vink, C.A., Gaspar, H.B., Gabriel, R., Schmidt, M., Mclvor, R.S., Thrasher, A.J., and Qasim, W. (2009). Sleeping beauty transposition from nonintegrating lentivirus. *Mol. Ther.* *17*, 1197–1204.

Voigt, K., Izsvák, Z., and Ivics, Z. (2008). Targeted gene insertion for molecular medicine. *J. Mol. Med. Berl. Ger.* *86*, 1205–1219.

Voit, T., Topaloglu, H., Straub, V., Muntoni, F., Deconinck, N., Campion, G., De Kimpe, S.J., Eagle, M., Guglieri, M., Hood, S., et al. (2014). Safety and efficacy of drisapersen for the treatment of Duchenne muscular dystrophy (DEMAND II): an exploratory, randomised, placebo-controlled phase 2 study. *Lancet Neurol.* *13*, 987–996.

Vulin, A., Barthélémy, I., Goyenvalle, A., Thibaud, J.-L., Beley, C., Griffith, G., Bouchaoui, R., le Hir, M., Unterfinger, Y., Lorain, S., et al. (2012). Muscle function recovery in golden retriever muscular dystrophy after AAV1-U7 exon skipping. *Mol. Ther.* *20*, 2120–2133.

Wagner, K.R., Fleckenstein, J.L., Amato, A.A., Barohn, R.J., Bushby, K., Escolar, D.M., Flanigan, K.M., Pestronk, A., Tawil, R., Wolfe, G.I., et al. (2008). A phase I/II trial of MYO-029 in adult subjects with muscular dystrophy. *Ann. Neurol.* *63*, 561–571.

Walisko, O., Izsvák, Z., Szabó, K., Kaufman, C.D., Herold, S., and Ivics, Z. (2006). Sleeping Beauty transposase modulates cell-cycle progression through interaction with Miz-1. *Proc. Natl. Acad. Sci. U. S. A.* *103*, 4062–4067.

Wang, B., Li, J., Fu, F.H., and Xiao, X. (2009). Systemic human minidystrophin gene transfer improves functions and life span of dystrophin and dystrophin/utrophin-deficient mice. *J. Orthop. Res. Off. Publ. Orthop. Res. Soc.* *27*, 421–426.

Wang, Z., Zhu, T., Qiao, C., Zhou, L., Wang, B., Zhang, J., Chen, C., Li, J., and Xiao, X. (2005). Adeno-associated virus serotype 8 efficiently delivers genes to muscle and heart. *Nat. Biotechnol.* *23*, 321–328.

Wang, Z., Allen, J.M., Riddell, S.R., Gregorevic, P., Storb, R., Tapscott, S.J., Chamberlain, J.S., and Kuhr, C.S. (2007a). Immunity to adeno-associated virus-mediated gene transfer in a random-bred canine model of Duchenne muscular dystrophy. *Hum. Gene Ther.* *18*, 18–26.

Wang, Z., Kuhr, C.S., Allen, J.M., Blankinship, M., Gregorevic, P., Chamberlain, J.S., Tapscott, S.J., and Storb, R. (2007b). Sustained AAV-mediated dystrophin expression in a canine model of Duchenne muscular dystrophy with a brief course of immunosuppression. *Mol. Ther.* *15*, 1160–1166.

Welch, E.M., Barton, E.R., Zhuo, J., Tomizawa, Y., Friesen, W.J., Trifillis, P., Paushkin, S., Patel, M., Trotta, C.R., Hwang, S., et al. (2007). PTC124 targets genetic disorders caused by nonsense mutations. *Nature* *447*, 87–91.

Wells, D.J., Wells, K.E., Asante, E.A., Turner, G., Sunada, Y., Campbell, K.P., Walsh, F.S., and Dickson, G. (1995). Expression of human full-length and minidystrophin in transgenic mdx mice: implications for gene therapy of Duchenne muscular dystrophy. *Hum. Mol. Genet.* *4*, 1245–1250.

Wen, S., Zhang, H., Li, Y., Wang, N., Zhang, W., Yang, K., Wu, N., Chen, X., Deng, F., Liao, Z., et al. (2014). Characterization of constitutive promoters for piggyBac transposon-mediated stable transgene expression in mesenchymal stem cells (MSCs). *PLoS One* 9, e94397.

Williams, D.A. (2008). Sleeping beauty vector system moves toward human trials in the United States. *Mol. Ther.* 16, 1515–1516.

Wilson, J.M. (2009). Lessons learned from the gene therapy trial for ornithine transcarbamylase deficiency. *Mol. Genet. Metab.* 96, 151–157.

Wilson, M.H., and George, A.L. (2010). Designing and testing chimeric zinc finger transposases. *Methods Mol. Biol. Clifton NJ* 649, 353–363.

Wilson, M.H., Coates, C.J., and George, A.L. (2007). PiggyBac transposon-mediated gene transfer in human cells. *Mol. Ther.* 15, 139–145.

Woodard, L.E., and Wilson, M.H. (2015). piggyBac-ing models and new therapeutic strategies. *Trends Biotechnol.* 33, 525–533.

Wooddell, C.I., Hegge, J.O., Zhang, G., Sebestyén, M.G., Noble, M., Griffin, J.B., Pfannes, L.V., Herweijer, H., Hagstrom, J.E., Braun, S., et al. (2011). Dose response in rodents and nonhuman primates after hydrodynamic limb vein delivery of naked plasmid DNA. *Hum. Gene Ther.* 22, 889–903.

Xu, L., Park, K.H., Zhao, L., Xu, J., El Refaey, M., Gao, Y., Zhu, H., Ma, J., and Han, R. (2015). CRISPR-mediated Genome Editing Restores Dystrophin Expression and Function in mdx Mice. *Mol. Ther.*

Xue, X., Huang, X., Nodland, S.E., Mátés, L., Ma, L., Izsvák, Z., Ivics, Z., LeBien, T.W., McIvor, R.S., Wagner, J.E., et al. (2009). Stable gene transfer and expression in cord blood-derived CD34+ hematopoietic stem and progenitor cells by a hyperactive Sleeping Beauty transposon system. *Blood* 114, 1319–1330.

Yaffe, D., and Saxel, O. (1977). Serial passaging and differentiation of myogenic cells isolated from dystrophic mouse muscle. *Nature* 270, 725–727.

Yant, S.R., Meuse, L., Chiu, W., Ivics, Z., Izsvák, Z., and Kay, M.A. (2000). Somatic integration and long-term transgene expression in normal and haemophilic mice using a DNA transposon system. *Nat. Genet.* 25, 35–41.

Yant, S.R., Ehrhardt, A., Mikkelsen, J.G., Meuse, L., Pham, T., and Kay, M.A. (2002). Transposition from a gutless adeno-transposon vector stabilizes transgene expression in vivo. *Nat. Biotechnol.* 20, 999–1005.

Yant, S.R., Park, J., Huang, Y., Mikkelsen, J.G., and Kay, M.A. (2004). Mutational analysis of the N-terminal DNA-binding domain of sleeping beauty transposase: critical residues for DNA binding and hyperactivity in mammalian cells. *Mol. Cell. Biol.* 24, 9239–9247.

- Yant, S.R., Wu, X., Huang, Y., Garrison, B., Burgess, S.M., and Kay, M.A. (2005). High-resolution genome-wide mapping of transposon integration in mammals. *Mol. Cell. Biol.* *25*, 2085–2094.
- Yasuno, T., Osafune, K., Sakurai, H., Asaka, I., Tanaka, A., Yamaguchi, S., Yamada, K., Hitomi, H., Arai, S., Kurose, Y., et al. (2014). Functional analysis of iPSC-derived myocytes from a patient with carnitine palmitoyltransferase II deficiency. *Biochem. Biophys. Res. Commun.* *448*, 175–181.
- Yew, N.S., Przybylska, M., Ziegler, R.J., Liu, D., and Cheng, S.H. (2001). High and sustained transgene expression in vivo from plasmid vectors containing a hybrid ubiquitin promoter. *Mol. Ther.* *4*, 75–82.
- Yuasa, K., Yoshimura, M., Urasawa, N., Ohshima, S., Howell, J.M., Nakamura, A., Hijikata, T., Miyagoe-Suzuki, Y., and Takeda, S. (2007). Injection of a recombinant AAV serotype 2 into canine skeletal muscles evokes strong immune responses against transgene products. *Gene Ther.* *14*, 1249–1260.
- Yue, Y., Pan, X., Hakim, C.H., Kodippili, K., Zhang, K., Shin, J.-H., Yang, H.T., McDonald, T., and Duan, D. (2015). Safe and bodywide muscle transduction in young adult Duchenne muscular dystrophy dogs with adeno-associated virus. *Hum. Mol. Genet.* *24*, 5880–5890.
- Yukihara, M., Ito, K., Tanoue, O., Goto, K., Matsushita, T., Matsumoto, Y., Masuda, M., Kimura, S., and Ueoka, R. (2011). Effective drug delivery system for duchenne muscular dystrophy using hybrid liposomes including gentamicin along with reduced toxicity. *Biol. Pharm. Bull.* *34*, 712–716.
- Yusa, K., Zhou, L., Li, M.A., Bradley, A., and Craig, N.L. (2011). A hyperactive piggyBac transposase for mammalian applications. *Proc. Natl. Acad. Sci. U. S. A.* *108*, 1531–1536.
- Zaiss, A.-K., Liu, Q., Bowen, G.P., Wong, N.C.W., Bartlett, J.S., and Muruve, D.A. (2002). Differential activation of innate immune responses by adenovirus and adeno-associated virus vectors. *J. Virol.* *76*, 4580–4590.
- Zammit, P.S., Relaix, F., Nagata, Y., Ruiz, A.P., Collins, C.A., Partridge, T.A., and Beauchamp, J.R. (2006). Pax7 and myogenic progression in skeletal muscle satellite cells. *J. Cell Sci.* *119*, 1824–1832.
- Zayed, H., Izsvák, Z., Khare, D., Heinemann, U., and Ivics, Z. (2003). The DNA-bending protein HMGB1 is a cellular cofactor of Sleeping Beauty transposition. *Nucleic Acids Res.* *31*, 2313–2322.
- Zayed, H., Izsvák, Z., Walisko, O., and Ivics, Z. (2004). Development of hyperactive sleeping beauty transposon vectors by mutational analysis. *Mol. Ther.* *9*, 292–304.
- Zhang, G., Wooddell, C.I., Hegge, J.O., Griffin, J.B., Huss, T., Braun, S., and Wolff, J.A. (2010). Functional efficacy of dystrophin expression from plasmids delivered to mdx mice by hydrodynamic limb vein injection. *Hum. Gene Ther.* *21*, 221–237.

Zhao, C., Farruggio, A.P., Bjornson, C.R.R., Chavez, C.L., Geisinger, J.M., Neal, T.L., Karow, M., and Calos, M.P. (2014). Recombinase-mediated reprogramming and dystrophin gene addition in mdx mouse induced pluripotent stem cells. *PLoS One* 9, e96279.

Zoltick, P.W., Chirmule, N., Schnell, M.A., Gao, G.P., Hughes, J.V., and Wilson, J.M. (2001). Biology of E1-deleted adenovirus vectors in nonhuman primate muscle. *J. Virol.* 75, 5222–5229.

Appendix

Figure S1. Isolation and characterization of GRMD MABs. (A) A phase contrast image of a muscle biopsy of a GRMD dog during the outgrowth of adherent cells with some small, round and refractile poor adherent cells (Scale bar 100 μ m). (B) Alkaline phosphatase (AP) immunoenzymatic staining performed on GRMD cells at passage 5 (P5) to detect AP⁺ adult pericyte-derived stem/progenitor cells (Scale bar 100 μ m). (C) FACS analysis on GRMD cells at P5 showing the surface marker profile CD44⁺, CD34⁻, CD45⁻ typical of adult MABs. (D) Bar graphs depicting the decreased transcript levels of markers such as PAX7, MYF5, CD56, desmin and the presence of NG2 and PDGFR β detected by semi-quantitative RT-PCR. Shown are means \pm SEM triplicate semi-quantitative RT-PCR analysis performed for a biological replicate; two-tailed unpaired Student's t-test (***p \leq 0.001; **p \leq 0.01; ns: not significant). (E) Pictures of electrophoresis on 2% agarose gel of amplicons from (D). (F) The multilineage mesodermal differentiation potential of the isolated GRMD MABs was assessed by *in vitro* differentiation assays into skeletal muscle and (G) smooth muscle. (Scale bar 100 μ m). Bulk: cell population directly derived from the GRMD muscle biopsy; P5: GRMD cells at passage 5; P10: GRMD cells at passage 10; L1: 100 bp ladder; L2: 1 Kb ladder; S- α Actinin: Sarcomeric- α actinin; MyHC: Myosin heavy chain; α -SMA: α -Smooth muscle actin.

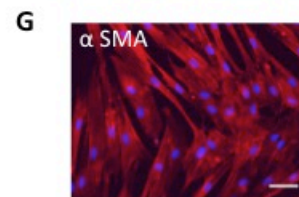
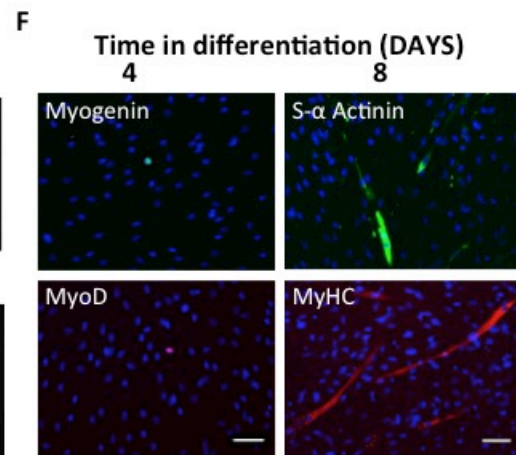
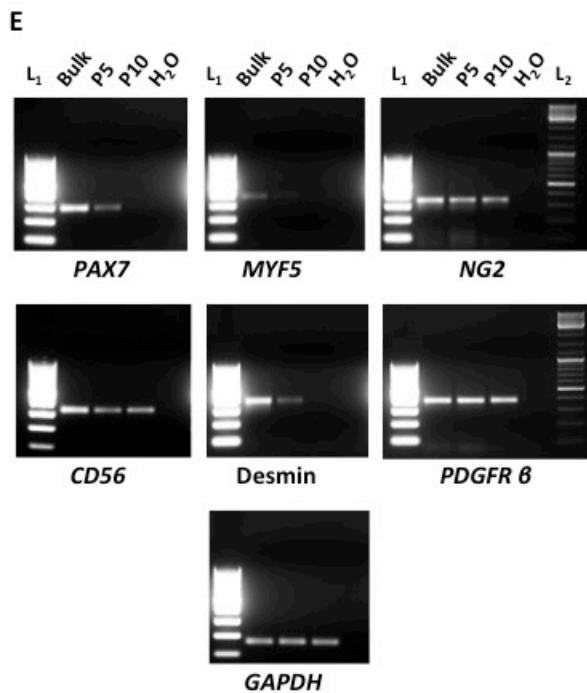
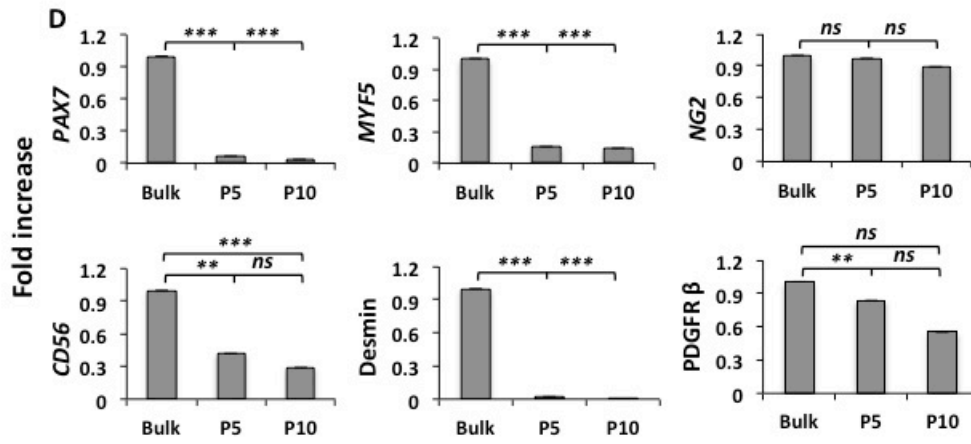
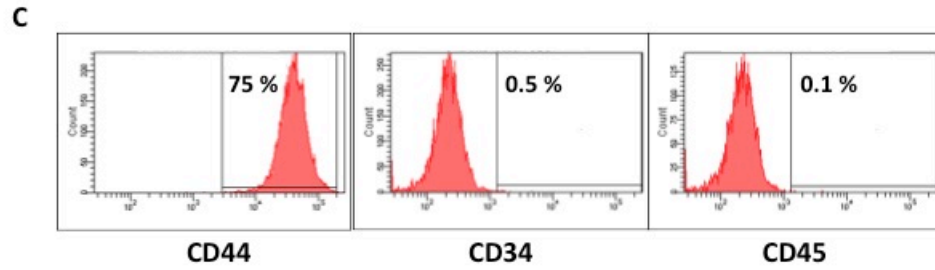
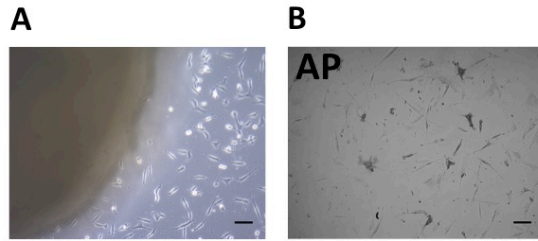


Figure S2. Optimization of the transfection protocol for GRMD MABs. The bar graphs represent the percentage of GFP+ of GRMD MABs and the viability at 72h post-EP when the large size PB-SPc-DYS-Pgk-GFP transposon has been used to transfect GRMD MABs together with the hyPB transposase. The empty plasmid has been used as control. The use of low dose of plasmids (ratio of 0.32 pmol transposase DNA: 0.87 pmol transposon DNA) led to a lower but not statistically significant percentage of GFP+ cells when compared to the higher dose of plasmid (0.63 pmol transposase DNA: 1.74 pmol transposon DNA). On the other hand, it consistently increases the viability of transfected cells thus providing an optimized condition for electroporation of the large size PB-SPc-DYS-Pgk-GFP transposon into GRMD MABs. Results were presented as mean±SEM of three independent biological replicates; two-tailed unpaired Student's t-test (** $p \leq 0.001$; * $p \leq 0.05$; ns: not significant).

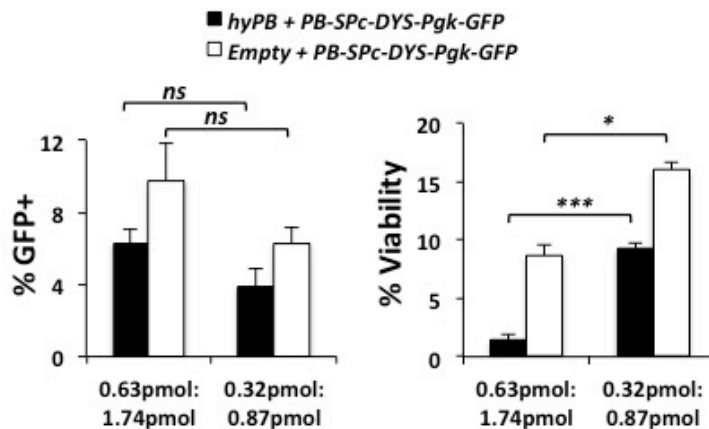


Figure S3. Immunostaining on differentiated GRMD MABs transposed with *hyPB + PB-Pgk-GFP*. At 21 days post-EP, GRMD MABs transposed with *hyPB + PB-Pgk-GFP* were induced to differentiate in skeletal muscle *in vitro*, upon *MyoD-ER(T)* overexpression and 6 days in conditioning medium. The *PB*-transposon mediated *GFP* expression was detected by IF, together with the *MyHC* expression in multinucleated myotubes. In contrast, the control GRMD MABs co-transfected with the empty plasmid that does not encode any transposase and the same transposon did not show any *GFP* expression. The nuclei were stained with *Hoechst* (Scale bar 100 μm).

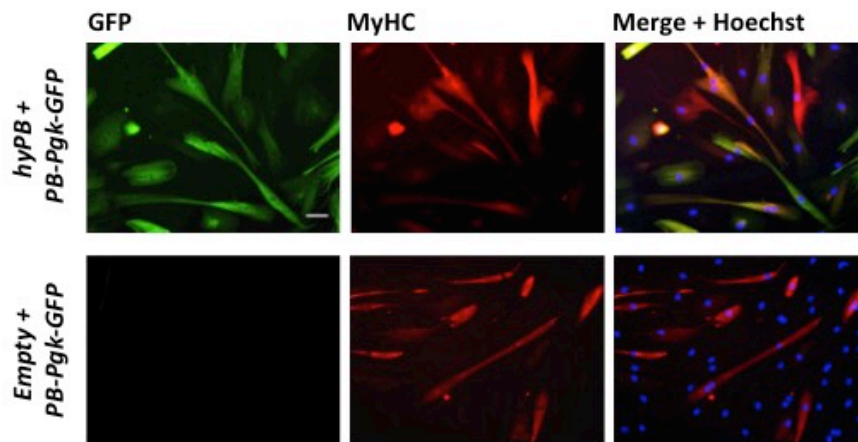
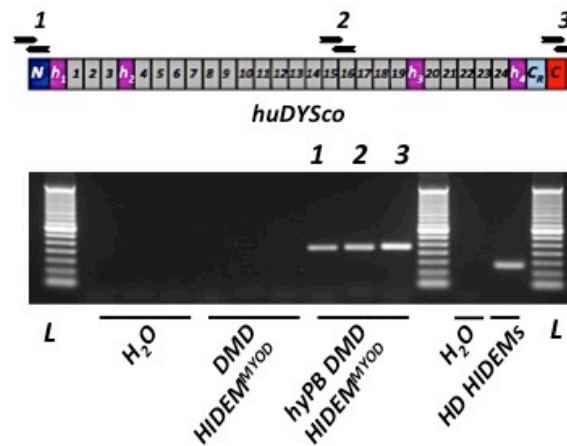


Figure S4. RT-PCR on full-length human dystrophin transcript in genetically corrected DMD HIDEM^{MYOD} cells. Picture of an RT-PCR performed on differentiated DMD HIDEM^{MYOD} cells that had undergone transposition after co-transfection with hyPB and PB-SPc-DYS-Pgk-GFP. Three different primer pairs were used that recognize respectively (1) the N-terminal, (2) a central region and (3) the C-terminal sequences of the full-length human dystrophin transcript, yielding amplicons of 221 bp, 222 bp and 228 bp respectively. A schematic representation of the PCR primers relative to the different regions of the dystrophin transcript is depicted above the picture. As negative control, differentiated untreated DMD HIDEM^{MYOD} cells were used. HIDEM^{MYOD} cells from a healthy donor (HD) and differentiated in myotubes were employed as a positive control; the primer pairs *DYS* listed in Table 5 have been used for this sample. L: 50 bp ladder.



Curriculum vitae

I. Education

September 2010 - April 2016

PhD in Biomedical Sciences (KUL) and Medical Sciences (VUB)

Joint PhD program: University of Leuven, KUL, Belgium / Free University of Brussels, VUB, Belgium. Thesis topic: "Development of a transposon-based stem cell-gene therapy for Duchenne muscular dystrophy."

Supervisors: Prof. Thierry VandenDriessche (KUL), Prof. Marinee K. Chuah (VUB)

Co-supervisor: Prof. Maurilio Sampaolesi (KUL)

May 2013 – November 2014

Visiting Research Scientist

University College of London, UCL, United Kingdom. Project topic: "Genetic correction of induced pluripotent stem cell-derived myogenic progenitors from DMD patients using piggyBac transposons expressing full-length dystrophin and transplantation in dystrophic mice."

Supervisor: Dr. Francesco Saverio Tedesco

September 2006 - March 2009

Master of Science in Medical Biotechnology

University of Pavia, Italy. Thesis topic: "Gene Therapy for the Wiskott-Aldrich syndrome: optimization of the transduction protocol and integration analysis of the lentiviral vector."

Final mark: 110/110 maxima cum laude

Supervisors: Prof. Anna Villa, Prof. Maurilio Sampaolesi

September 2003 - July 2006

Bachelor of Science in Biotechnology - Medical Course

University of Pavia, Italy. Thesis topic: "Complete sequencing of three samples of Sardinian mitochondrial DNA and the U5b3 haplogroup definition."

Final mark: 110/110 maxima cum laude

Supervisor: Prof. Antonio Torroni

II. Employment history

October 2009 – August 2010

Postgraduate Researcher

University of Leuven, KUL, Belgium. Project topic: “Validation of the use of meganucleases generated by Collectis to target “safe harbor” sites in human cell genome.”

Managers: Prof. Thierry VandenDriessche, Prof. Marinee K. Chuah

May 2009 – September 2009

Postgraduate Researcher

University of Leuven, KUL, Belgium. Project topic: “miRNA Lentiviral Vector Integration and Gene Targeting Efficacy in Cardiac Progenitors.”

Manager: Prof. Maurilio Sampaolesi

III. Fundings

As a PhD student, I have been awarded several personal fellowships and grants: FWO PhD fellowship (2010-2014), FWO research project grant (2010-2014), FWO travel grant (March 2014 - September 2014), WFWG grant (2015), EMBO travel grant (2015). As a postgraduate research fellow, I have been awarded a personal fellowship from the University of Pavia, Italy (May 2009 - September 2009).

FWO: Flanders Fund for Scientific Research; WFWG: Scientific Fund Willy Gepts.

Publications and scientific communication

***piggyBac* transposons expressing full-length human dystrophin enable genetic correction of dystrophic mesoangioblasts.** Loperfido M, Jarmin S, Dastidar S, Di Matteo M, Perini I, Moore M, Nair N, Samara-Kuko E, Athanasopoulos T, Tedesco FS, Dickson G, Sampaolesi M, VandenDriessche T, Chuah MK. *Nucleic Acids Research* 2016 Jan 29;44(2):744-60. doi: 10.1093/nar/gkv1464. Epub 2015 Dec 17.

Pluripotent Stem Cells for Gene Therapy of Degenerative Muscle Diseases. Loperfido M*, Steele-Stallard HB*, Tedesco FS, VandenDriessche T. *Current Gene Therapy* 2015;15(4):364-80.

* The authors declare joint first authorship.

Efficient derivation and inducible differentiation of expandable skeletal myogenic cells from human ES and patient-specific iPS cells. Maffioletti SM*, Gerli MF*, Ragazzi M, Dastidar S, Benedetti S, Loperfido M, VandenDriessche T, Chuah MK, Tedesco FS. *Nature Protocols* 2015 Jul;10(7):941-58. doi: 10.1038/nprot.2015.057. Epub 2015 Jun 4. (Article awarded as cover story of the issue).

* The authors declare joint first authorship.

Preclinical safety and efficacy of human CD34⁺ cells transduced with lentiviral vector for the treatment of Wiskott-Aldrich syndrome. Scaramuzza S*, Biasco L*, Ripamonti A, Castiello MC, Loperfido M, Draghici E, Hernandez RJ, Benedicenti F, Radrizzani M, Salomoni M, Ranzani M, Bartholomae CC, Vicenzi E, Finocchi A, Bredius R, Bosticardo M, Schmidt M, von Kalle C, Montini E, Biffi A, Roncarolo MG, Naldini L, Villa A, Aiuti A. *Molecular Therapy* 2013 Jan;21(1):175-84. doi: 10.1038/mt.2012.23. Epub 2012 Feb 28.

* The authors declare joint first authorship.

Chromosomal context and epigenetic mechanisms control the efficacy of genome editing by rare-cutting designer endonucleases. Daboussi F, Zaslavskiy M, Poirot L, Loperfido M, Gouble A, Guyot V, Leduc S, Galetto R, Grizot S, Oficjalska D, Perez C, Delacôte F, Dupuy A, Chion-Sotinel I, Le Clerre D, Lebuhotel C, Danos O, Lemaire F, Oussedik K, Cédrone F, Epinat JC, Smith J, Yáñez-Muñoz RJ, Dickson G, Popplewell L,

Koo T, VandenDriessche T, Chuah MK, Duclert A, Duchateau P, Pâques F. Nucleic Acids Research 2012 Jul;40(13):6367-79. Epub 2012 Mar 29.

miRNA Lentiviral Vector Integration and Gene Targeting Efficacy in Cardiac Progenitors. Loperfido M, Crippa S, Sampaolesi M. Journal of Stem Cell Research and Therapy 2012, S9 <http://dx.doi.org/10.4172/2157-7633.S9-003>.

Genetic correction of Duchenne muscular dystrophy iPSC-derived inducible myogenic cells using *piggyBac* transposons encoding full-length dystrophin.

Loperfido M, Dastidar S, Gerli MFM, Ragazzi M, Di Matteo M, Nair N, Jarmin S, Moore M, Samara-Kuko E, Athanasopoulos T, Dickson G, Chai YC, Tedesco FS[#], Chuah MK[#], VandenDriessche T^{#*}. *Submitted*.

Next-generation muscle-directed gene therapy using skeletal-muscle specific transcriptional modules identified by genome-wide computational analysis. Sarcar S, Rincón MY, Evens H, Tipanee J, Keyaerts M, Loperfido M, Berardi E, Samara-Kuko E, in't Veld P, Dickson G, Sampaolesi M, Lahoutte T, De Bleser P, VandenDriessche T, Chuah MK. *Submitted*.

My data have been presented at the following conferences and seminars:

ASGCT – 2016 Washington, USA (Poster presentation)

International congress of Myology – 2016 Lyon, France (Oral presentation)

VUB RGRG PhD day – 2015 Brussels, Belgium (Oral presentation)

EMBO conference – 2015 Manchester, UK (Poster presentation)

KUL Progress report Research Seminar – 2014 Leuven, Belgium (Oral presentation)

VUB RGRG PhD day – 2013 Brussels, Belgium (Oral presentation)

KUL CMVB Research Seminar – 2012 Leuven, Belgium (Oral presentation)

